

Diss. ETH No. 13635

**Anthropogenic and Dynamic Contributions
to Ozone Trends of the Swiss Total Ozone,
Umkehr and Balloon Sounding Series.**

A dissertation submitted to the
SWISS FEDERAL INSTITUTE OF TECHNOLOGY
ZURICH

for the degree of
Doctor of Natural Sciences

presented by
ANDREA K. WEISS
Dipl.-Geophys. TU Karlsruhe
born 28 February 1972 in Dresden
citizen of Germany

accepted on the recommendation of
Prof. T. Peter, examiner
Dr. N. R. P. Harris, co-examiner
Dr. J. Staehelin, co-examiner

2000

Forschen und Wissen - Physik

Andrea K. Weiss

**Anthropogenic and Dynamic Contributions
to Ozone Trends of the Swiss Total Ozone,
Umkehr and Balloon Sounding Series**

Diss. ETH Zürich

**GCA-Verlag
Herdecke 2000**

Die Deutsche Bibliothek – CIP - Einheitsaufnahme

Weiss, Andrea K. :

Anthropogenic and Dynamic Contributions to Ozone Trends of the Swiss
Total Ozone, Umkehr and Balloon Sounding Series / Andrea K. Weiss. –

Als Ms. gedr. – Herdecke : GCA-Verl., 2000

(Forschen und Wissen – Physik)

Zugl: Zürich, Eidgenössische Techn. Hochsch., Diss., 2000

ISBN 3-934389-88-0

Copyright GCA-Verlag, Herdecke 2000

Alle Rechte, auch das des auszugsweisen Nachdruckes, der auszugsweisen oder
vollständigen Wiedergabe, der Speicherung in Datenverarbeitungsanlagen und der
Übersetzung, vorbehalten.

Als Manuskript gedruckt. Printed in Germany.

ISSN 1436-1205

ISBN 3-934389-88-0

GCA-Verlag der GCA mbH, Bahnhofstr. 31, D 58313 Herdecke

Telefon 02330/10520

- Telefax 02330/2207

Internet: www.gca-verlag.de

- eMail: info@gca-verlag.de

Contents

Abstract	1
Zusammenfassung	3
Executive Summary	5
1 Introduction	7
2 Theoretical Background	9
2.1 Ozone in the atmosphere	9
2.1.1 The shape of the ozone profile	9
2.1.2 Ozone variability	12
2.1.3 Anthropogenic ozone destruction	19
2.2 Dynamical principles	22
2.2.1 The meridional circulation	22
2.2.2 Wave origin and fate	24
2.2.3 The polar vortex	25
2.2.4 QBO	26

2.2.5	Solar influence	26
2.2.6	NAO and AO	27
2.2.7	Tropopause	29
2.3	Why ozone profile trend analysis	30
3	Statistical tools	33
3.1	Significance and p-value	33
3.2	Correlation	34
3.3	Linear regression	36
3.4	The commonly used ozone trend model	37
3.5	The new ozone trend model	38
3.6	Cumulative differences for break detection	40
4	Data	43
4.1	Ozone measurement systems	43
4.1.1	Total ozone	44
4.1.2	Umkehr	46
4.1.3	Brewer-Mast soundings	54
4.1.4	SBUV	56
4.1.5	SAGE	56
4.2	Used proxies for natural ozone variability: AOD, QBO, solar activity, NAO/AO and tropopause pressure	58
5	Results of Homogeneity checks	63
5.1	Difference of Payerne soundings and Arosa Umkehr results	63

5.1.1	Clear contradiction in measurements	64
5.1.2	Different trends of soundings and Umkehr	65
5.1.3	Searching for the culprit	67
5.2	Homogeneity checks with the Umkehr series of Arosa	68
5.2.1	Umkehr records and stability tests at Arosa	68
5.2.2	Confirming the results of the standard series	70
5.2.3	N-values of the instruments	70
5.2.4	Implications from the instrumental differences on the retrieved ozone trends	71
5.2.5	Conclusions for the Umkehr series	78
5.3	Using satellites as referees	79
5.3.1	Comparisons with SBUV	79
5.3.2	Comparisons with SAGE II	82
5.4	Conclusions from homogeneity checks	85
6	Total Ozone Trend Analysis	89
6.1	Total ozone and tropopause pressure	90
6.2	Total ozone and NAO	91
6.3	Extended total ozone trend model	93
6.4	Conclusions from total ozone trend analysis	96
7	Ozone Profile Trend Analysis	99
7.1	Searching for the cause of the vertical structure of O ₃ trends	99
7.2	Tropopause pressure and ozone	101

7.3	Natural influences and anthropogenic trends	103
7.3.1	Significance of tropopause pressure with respect to season and height	104
7.3.2	QBO, solar signal and aerosols	111
7.3.3	Resulting ozone profile trends	111
7.4	Discussion and future research	113
7.5	Conclusions from ozone profile trend analysis	115
8	Summary and Conclusions	117
	Acronyms and Abbreviations	121
A	Daily Ozone Variability	123
B	Conversion of units	125
C	Used Software	127
D	www Data Sources	129
	References	131
	Acknowledgments	145
	Curriculum vitae	147

List of Figures

2.1	Ozone profile and Umkehr layers	10
2.2	Total ozone of Arosa	12
2.3	Payerne soundings and tropopause	14
2.4	Extra-tropical pump	23
2.5	SPARC-estimate of ozone profile trends	32
3.1	Cumulative differences of gaussian data	42
4.1	The Dobson spectrophotometer D101 of Arosa	45
4.2	The Umkehr measurement system	47
4.3	Umkehr kernels	50
4.4	Aerosol loading	58
4.5	Solar activity	59
4.6	Quasi-Biennial Oscillation (QBO)	59
4.7	The North Atlantic Oscillation (NAO) index	60
4.8	The Arctic Oscillation (AO) index	61
4.9	Tropopause pressure over Arosa	61

5.1	Difference of Arosa Umkehr and Payerne soundings . . .	64
5.2	Umkehr and sounding trends	66
5.3	Break detection in the difference Umkehr-Payerne . . .	67
5.4	Periods of Umkehr observations at Arosa	69
5.5	Standard Umkehr N-values	72
5.6	D101 N-values	73
5.7	Coincident N-values	74
5.8	Difference in N-values	75
5.9	Difference in ozone layer content	76
5.10	Relative difference in ozone layer content	77
5.11	Break detection with SBUV, soundings, Umkehr — L4 .	81
5.12	Break detection with SBUV, soundings, Umkehr — L5 .	81
5.13	Difference of SAGE and Payerne soundings	83
5.14	Difference of SAGE and Umkehr	84
6.1	How the tropopause pressure influences ozone	91
6.2	Total ozone, tropopause pressure, NAO for Arosa and Reykjavik	92
6.3	Cross correlation map of tropopause pressure and NAO	94
6.4	Arosa total ozone and NAO	95
7.1	Tropopause pressure and ozone in L2	104
7.2	Significance of tropopause pressure	106
7.3	Significances of tropopause pressure, QBO, AOD and so- lar flux	107

7.4	Significance of NAO	109
7.5	Significance of AO	110
7.6	Ozone profile trends with their dynamical contribution removed	112
A.1	Ozone profile variability in nbar	124

Seite Leer /
Blank leaf

List of Tables

2.1	Influences on ozone	15
2.2	Chapman theory	19
2.3	Catalytic gas phase O ₃ destruction	20
5.1	Contradictions attributed to D15, D101, and Payerne soundings	70
6.1	Total ozone trend estimates for Arosa and Reykjavik	97
7.1	Ozone profile trends	113
7.2	Explained variance in the ozone profile	114
A.1	Variability of daily total ozone	123

Abstract

The mechanisms and amounts of ozone profile trends (i.e., height dependent trends in the troposphere and stratosphere), are still under discussion in the ozone community. Here a new trend analysis has been performed with the Swiss long-term total ozone and ozone profile series, giving special considerations to the North Atlantic Oscillation (NAO). This is a climatic pattern governing tropopause pressure over Europe and the Atlantic, which in turn influences the ozone distribution.

The two Swiss ozone profiling techniques used at Arosa and Payerne yield contradicting trend results in the middle stratosphere. This questions the instrumental stability of the series. Stability checks and break detection show a behavior which could be due to numerous badly defined breaks in the Umkehr measurements of Arosa and the balloon soundings of Payerne, or a continuous change possibly of natural origin. Umkehr instrument stability can be confirmed with the supplementary Umkehr instruments at Arosa. Still, it is possible that the whole Umkehr method is subject to drifting. With satellite data from SAGE and SBUV a judgment concerning stability has been attempted but can not yield general conclusions. Confidence in the stability of the Payerne soundings is restored by their ability to resemble dynamically caused ozone changes.

Such dynamical changes have been found to contribute significantly to ozone trends. For the analyzed period (1968-1996) about half of the lower stratospheric trends in winter and spring are to be attributed to dynamics, and about a third of the trend in total ozone over Switzerland. The analysis is expanded to a station in Iceland where the predicted effect of dynamics is an increase of ozone (in contrast to Switzerland

where it is a decrease).

The anthropogenic trends caused by man-made ozone depleting chemicals, were determined with a new statistical stepwise regression model. It accounts for season- and height-dependent natural influences as tropopause pressure, North Atlantic Oscillation (NAO), Arctic Oscillation (AO), Quasi-Biennial Oscillation (QBO), aerosol loading, and solar cycle. The statistically significant influences constitute the particular model applicable for the different parts of the ozone profile which are chosen according to the Umkehr layers.

In conclusion, anthropogenic trends in mid-latitudes of the Northern Hemisphere should be estimated taking into account at least one dynamical proxy. Tropopause pressure is suggested as the most appropriate one. The largest effect occurs in the lower stratosphere in winter and spring.

Zusammenfassung

Die Ursachen und das Ausmass der Ozonprofiltrends (d.h. der höhenabhängigen Langzeitveränderungen in der Troposphäre und Stratosphäre) sind Gegenstand aktueller Forschung. In dieser Arbeit wird eine neue Trendanalyse der schweizerischen Gesamtozonreihe und der Ozonprofilreihen präsentiert. Dabei wird erstmals der Einfluss der Nord-Atlantischen Oszillation (NAO) berücksichtigt. Die NAO ist eine wichtige Klimavariablen, die auch den Tropopausendruck über Europa und dem Atlantik bestimmt, welcher wiederum die Ozonverteilung beeinflusst.

In Arosa und Payerne werden seit Jahrzehnten mit zwei verschiedenen Methoden operationell Ozonprofile über der Schweiz gemessen. Diese Umkehrmessungen und Ballonsondierungen zeigen widersprüchliche Trends in der mittleren Stratosphäre, was ihre instrumentelle Stabilität in Frage stellt.

Statistische Tests zeigen eine Vielzahl von schlecht definierten Brüchen zwischen den Umkehrmessungen von Arosa und den Ballonsondierungen von Payerne. Diese könnten auch eine kontinuierliche Drift zwischen den beiden Messmethoden widerspiegeln, welche möglicherweise atmosphärischen Ursprungs ist. Durch Vergleiche der verschiedenen Messinstrumente von Arosa konnte die Stabilität der Umkehrmessreihe bestätigt werden. Die Möglichkeit, dass die gesamte Umkehrmethode einer Drift unterliegt, bleibt bestehen.

Um die Stabilität der Umkehr und der Ballonsondierungen zu beurteilen, wurden satellitengestützten Messungen (SAGE und SBUV) herangezogen, welche jedoch keine allgemeinen Schlüsse zulassen. Für

die Stabilität der Sondierungen spricht, dass sie dynamisch bedingte Ozonänderungen gut widerspiegeln.

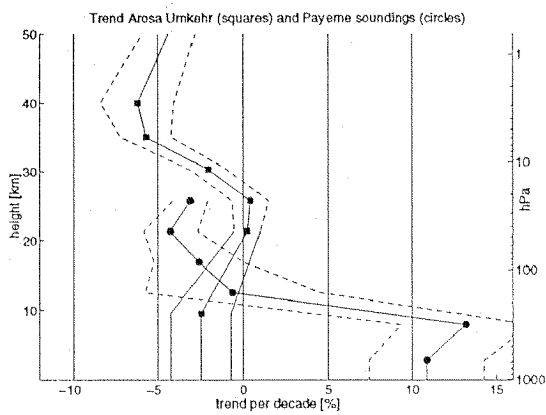
Die Dynamik der Atmosphäre erwies sich als wichtiger Faktor für die Ozontrends. Dynamischen Veränderungen erklären etwa die Hälfte der mit den Sondierungen gemessenen Ozontrends in der unteren Stratosphäre im Winter und Frühling der betrachteten Zeitperiode (1968-1996). Das entspricht etwa einem Drittel des Gesamtozontrends. Dies wurde durch die Trendanalyse der Gesamtozonreihe von Arosa belegt.

Die Trendanalyse wurde auf eine Station in Island ausgedehnt, für welche der umgekehrter Einfluss der NAO theoretisch vorhergesagt wurde. Das Ergebnis bestätigt, dass sich dort das Gesamtozon durch den dynamischen Einfluss erhöhte (im Gegensatz zur Schweiz, wo es sich verringerte).

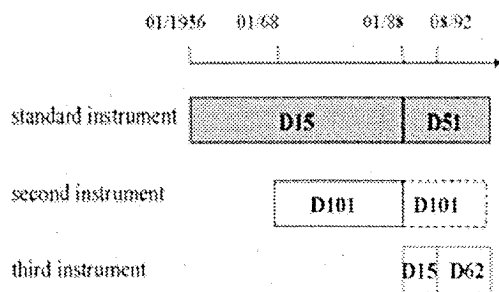
Die anthropogenen Trends (d.h. durch Emissionen ozonzerstörender Substanzen verursacht) wurden mit einem verbesserten schrittweisen Regressionsmodell bestimmt. Die jahreszeitliche Abhängigkeit und die Höhenabhängigkeit der natürlichen Einflüsse auf das Ozon wurden in das Modell einbezogen. Bei diesen natürlichen Einflüssen handelt es sich um den Tropopausendruck, die Nord-Atlantische Oszillation (NAO), die Arktische Oszillation (AO), die Quasi-Biennale Oszillation (QBO), den stratosphärischen Aerosolgehalt und die Sonnenaktivität. Das Ozonprofil wurde entsprechend der Umkehrschichten unterteilt und so eine höhenabhängige Trendanalyse mit den jeweils signifikanten Einflüssen durchgeführt.

Die wichtigste Schlussfolgerung ist, dass zur Bestimmung der anthropogenen Ozontrends in den mittleren Breiten der Nordhemisphäre die Dynamik der Atmosphäre berücksichtigt werden muss. Zur Beschreibung der Dynamik wird der Tropopausendruck als die geeignetste Grösse vorgeschlagen. Die Dynamik beeinflusst die Trends am stärksten in der unteren Stratosphäre im Winter und im Frühling.

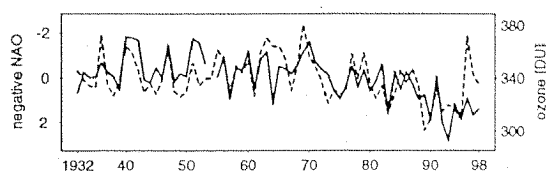
Executive Summary



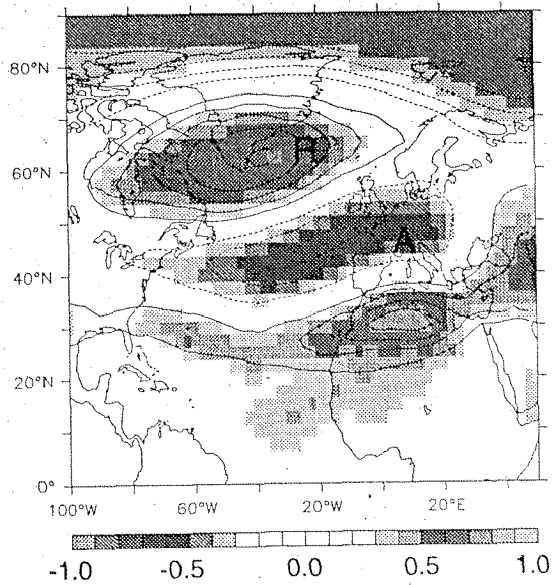
Umkehr measurements of Arosa and balloon soundings of Payerne yield different ozone trends.



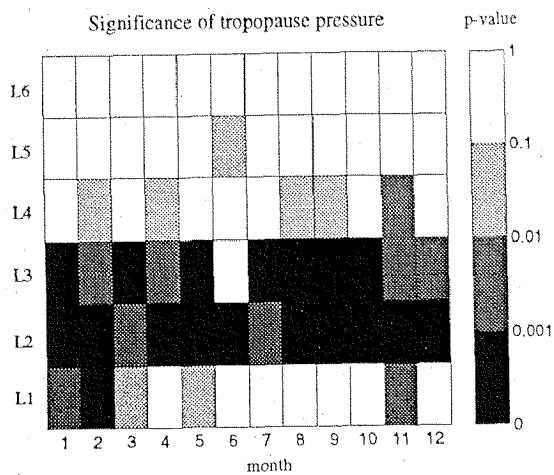
Homogeneity checks confirm the stability of the standard Umkehr instruments.



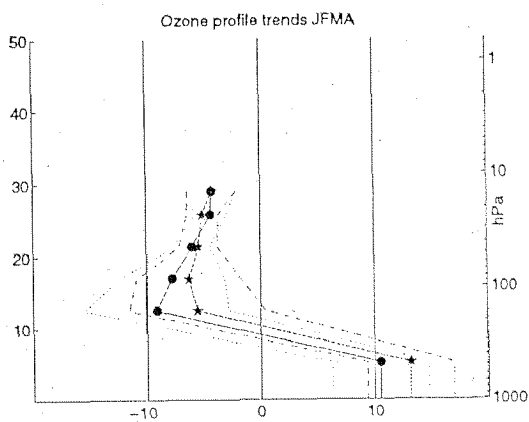
The North Atlantic Oscillation (NAO) index is anticorrelated with the total ozone over Arosa.



The North Atlantic Oscillation (NAO) controls tropopause pressure over Europe and the North Atlantic region.



New estimates for contributions of natural factors to ozone variability were found. Tropopause pressure is highly significant throughout the year in the lower stratosphere.



Dynamics attribute to about half of the winter and spring lower stratospheric ozone trends in Switzerland.

Chapter 1

Introduction

Ozone changes became a matter of public concern because man-made chlorofluorocarbons (CFCs) and other ozone depleting substances are weakening the stratospheric ozone shield. On the other hand, tropospheric ozone is increasing due to pollution by traffic and industry. These changes caused by mankind are called *anthropogenic trends*. The anthropogenic trends, which are reverse in sign in the troposphere and in the stratosphere, and natural effects are summed when investigating *total ozone*, which is the entire amount of ozone in an atmospheric column. It protects the life on Earth from short-wave solar radiation. Dramatic total ozone loss due to CFCs and other ozone depleting substances has been observed at high latitudes in polar spring in the last decades. But also at mid-latitudes total ozone has decreased noticeable, giving concern for public health and agriculture.

The distribution of ozone with height is commonly referred to as the *ozone profile*. Its long-term changes are of general interest for stratospheric chemistry, dynamics and climate research.

Extensive and detailed work has been done to determine and understand the changes in total ozone and in the ozone profile. Observational techniques are described by SPARC (1998) and Staehelin et al. (2000). A recent summary of ozone chemistry is given in Solomon (1999) and scientific knowledge related to ozone problems is recapitulated in WMO (1999). The primary objective of the international efforts is to evaluate

the anthropogenic ozone destruction. To achieve a good estimate for this, instrumental instabilities must be identified and accounted for at the ambitious scale of about one percent per decade. In addition, natural variability has to be understood. Ozone changes not explicable by known natural causes are attributed to anthropogenic ozone destruction. Commonly, a linear regression model is applied to determine the anthropogenic trends. However, the model is imperfect. Major physical understanding seems missing.

In this thesis substantial improvements of the total ozone and ozone profile trend models for mid-latitudes are implemented. An improved analysis technique is developed and physical understanding is extended with new reasoning for inter-decadal ozone variability.

The analysis is based on the Swiss long-term ozone series: the total ozone series of Arosa and two ozone profiling series, namely the Payerne balloon soundings and the Arosa Umkehr measurements. The North Atlantic Oscillation (NAO) and the Arctic Oscillation (AO), which are climatic variables, are introduced to the trend analysis of the Swiss records. NAO and AO have recently been recognized to play a major role in the long-term variability of the stratosphere (Hurrell 1995, Thompson and Wallace 1998). In this thesis they are identified to cause dynamical contributions to the observed long-term ozone changes. Here dynamical changes, the cause of which is yet unknown, are classified as *natural influences* on ozone.

In Chapter 2, the current understanding of ozone abundance and change is briefly summarized, and relevant dynamical processes which are often ignored in literature, are contemplated. The mathematical model is rethought and refined in Chapter 3. The data quality of the different measurement systems is critically discussed in Chapter 4, and homogeneity checks for the Swiss long-term ozone profiling series are applied in Chapter 5. New proxies for ozone trend analysis, the NAO index and tropopause pressure, are shown to be of larger importance than the other parameters commonly used in literature (Chapter 6). A revised ozone profile trend analysis is given in Chapter 7. Chapters 5, 6 and 7 have intermediate conclusions for the reader who wants to glance over the results of this thesis. In Chapter 8, the results and their implications are discussed.

Chapter 2

Theoretical Background

2.1 Ozone in the atmosphere

The current understanding of stratospheric ozone research is briefly summarized. The ozone profile is explained, its variability is described and natural factors are illuminated. A short survey is given on the chemistry of anthropogenic ozone depletion.

2.1.1 The shape of the ozone profile

The sum of all ozone residing in the atmospheric column is called *total ozone*. Its distribution with height is the *ozone profile*. The shape of the ozone profile is connected with the general structure of the atmosphere. The lower part of the atmosphere, in which the weather occurs, is called the *troposphere*. It extends from the ground to the *tropopause*, a transport barrier, which is situated at the height of approximately 8-18 km depending on geographical latitude and season. About 4/5 of the air mass is tropospheric. Aloft, in the *stratosphere*, the temperature rises with altitude. The stratosphere extends to the stratopause, and only 0.1% of air resides above. The steadily rising temperature causes the *stratification* of air, the stable layering in the stratosphere. The stratospheric temperature profile is caused predominantly by radiative

absorption by ozone (see Fig. 2.1).

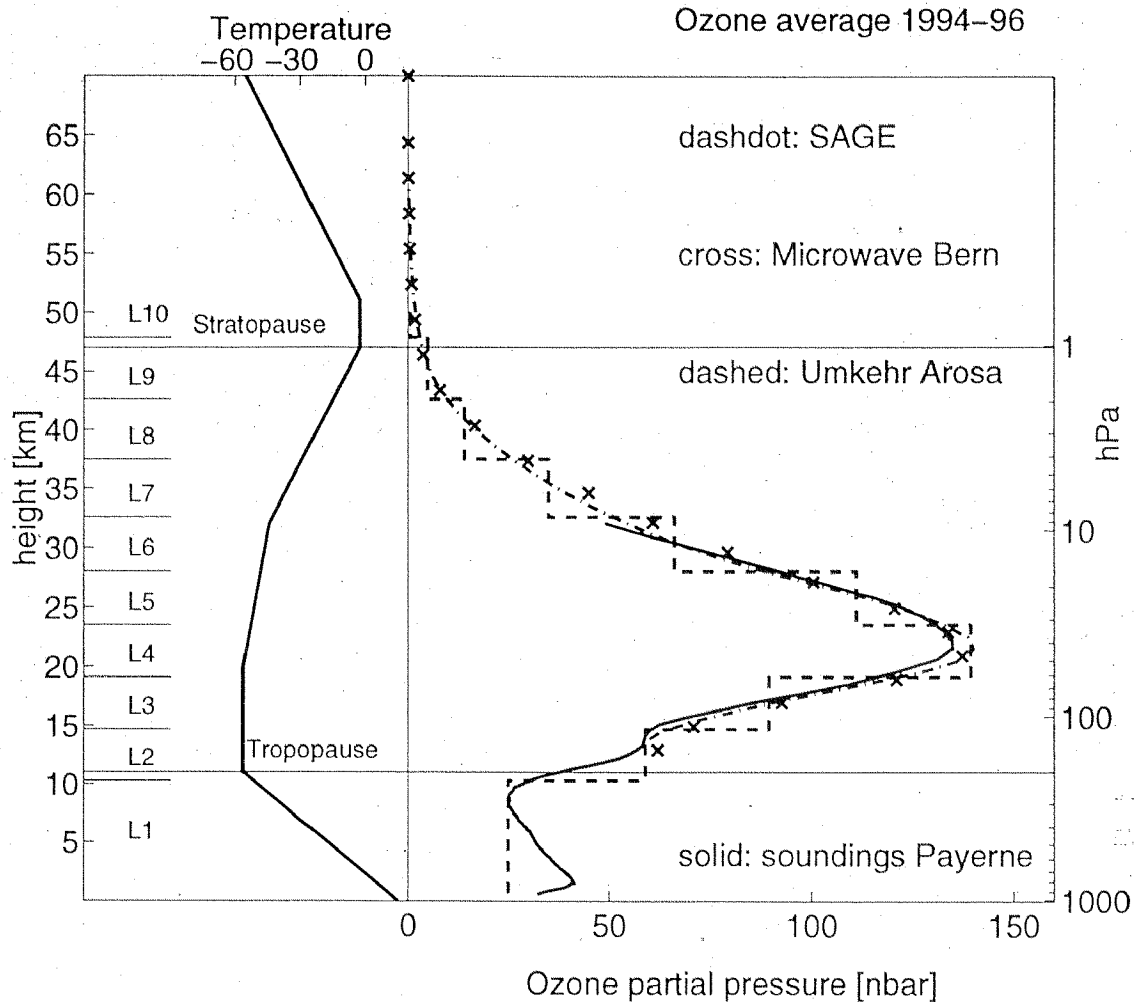


Figure 2.1: Different measurement systems, i.e., Swiss soundings, Umkehr, and Microwave supplemented by satellite (SAGE) are combined for a mean ozone profile. All available data of 1994-1996 were used. The Umkehr layers are L1:0-10.3 km, L2:10.3-14.7 km, L3:14.7-19.1 km, L4:19.1-23.5 km, L5:23.5-28 km, L6:28-32.6 km, L7:32.6-37.5 km, L8:37.5-42.6 km, L9:42.6-47.9 km, L10: above 47.9 km. On the left hand side, the US Standard Atmosphere (1976) temperature profile in °Celsius is depicted.

That ozone would form in the stratosphere was first recognized by Chapman (1930), who formulated a simple photochemical theory: short wave solar radiation splits oxygen molecules into free O atoms which quickly form O₃ with O₂. The O₃ molecules can also be split by solar radiation. The chemical equilibrium depends on the supply of solar radiation (for more details see Table 2.2). This theory explains the upper stratospheric ozone concentrations. Below, the solar short-wave radiation gets absorbed and cannot penetrate into the lower stratosphere because of the shielding of ozone above. In this part of the atmosphere, transport determines the ozone profile.

The altitude range between 25–35 km represents a transition region between photochemical and dynamical control in the stratosphere (WMO 1999). The bulk of stratospheric ozone is formed in the tropics. Ozone is supplied in the middle and higher latitudes through a net ozone transport from the tropics to the poles following the pole-ward slanted tropopause and the *isentropes*, which are levels of constant potential temperature. Thus, ozone is permanently transported from its photochemical production region over the tropics into the extra-tropical lower stratosphere. This circulation, historically referred to as *Brewer-Dobson circulation*, generates the pronounced ozone maximum at 20–25 km height over mid-latitudes (see Fig. 2.1) and explains in general the seasonal cycle of the total ozone.

In recent years, the understanding of this circulation changed. It is thought to be the meridional component of the global circulation which is driven by wave motions in the extra-tropical stratosphere (Holton et al. 1995). The global transport issue is further elaborated in Section 2.2.

For the ozone profile, the height of the tropopause is of importance. At the tropopause ozone-rich stratospheric air is in contact with ozone-poor tropospheric air. Therefore, the question how much of the atmospheric column is tropospheric and how much stratospheric, strongly influences the total ozone at a given longitude and latitude, and thus determines the global ozone distribution. In the tropics, the tropopause is at a height of about 16 km, over the poles at about 8 km. Hence, the ozone maximum is located at the poles (while highest ozone mixing ratios occur in the ozone source region over the tropics). This is the reason for another transport phenomenon: When lower stratospheric air is advected from the polar region, which happens mostly in winter and

spring, it is richer in ozone than mid-latitude air. In such episodes, a secondary maximum in ozone mixing ratios may appear in the lower stratosphere. In the averaged ozone profile (Fig. 2.1) over Switzerland, a bump is discernible which is due to such advection effects.

A large part of about 40% (Roelofs et al. 1997) of tropospheric ozone has its origin in the stratosphere. It is mixed in across the tropopause via tropopause folding and stratospheric intrusions. This mass transfer is part of the global meridional circulation (Appenzeller et al. 1996b).

There is also in situ formation of ozone in the troposphere, but this evolves via completely different chemical cycles — involving tropospheric photo-chemistry (Thielmann 2000) based on nitrogen oxides (NO_x) and volatile organic compounds (VOC). Half of the ozone produced this way is anthropogenic (Roelofs et al. 1997), i.e., caused by the primary pollutants (NO_x, VOC) from traffic and industry. The other half of photochemically produced tropospheric ozone is related to natural NO_x (flashes, soil emissions and forest fires) and biogenic VOC (emitted by plants).

2.1.2 Ozone variability

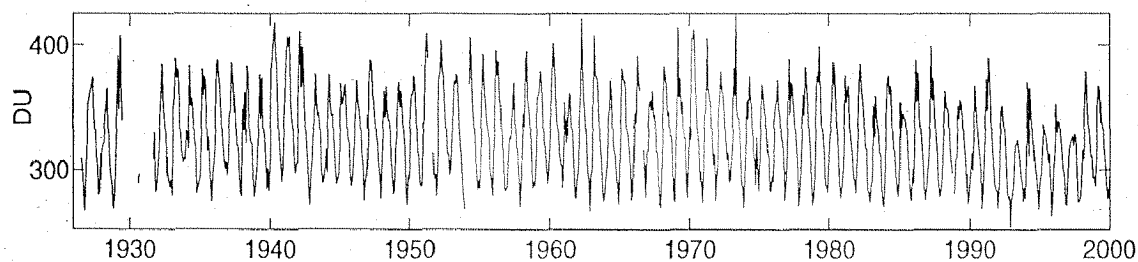


Figure 2.2: *Total ozone series of Arosa, monthly means.*

An impression of the total ozone variability in mid-latitudes is given by monthly means of the Arosa series (Fig. 2.2). The large day-to-day variability, which is connected with the weather, is not shown. The daily standard deviation is about 10% and has a seasonal dependency. The detailed numbers are given in Appendix A. In Fig. 2.2 the seasonal cycle is the most pronounced feature: Arosa total ozone is maximal in April and minimal in October–November. Also long-term variability can be discerned. There seems to be some sort of decadal variability. Remark-

ably much ozone has been observed in the years 1940–42 and 1969–70. In the mid-nineties, there was a period of particularly low ozone. Since the 1970s a decline in the maximum values, i.e. in springtime, is observable.

The variation of total ozone is the integral of variations along the ozone profile. The altitudes and ranges of variability are dependent on the season, as seen in Fig. 2.3. The variability is especially high from December to May, and reaches its maximum in the lower stratosphere, just above the tropopause in February. For some applications it is more useful to look at the pressure scale instead of the altitude scale, and to use ozone number density [particles per m^3] instead of partial pressure [nbar]. This is done in Appendix B (same figure as Fig. 2.3, but changed scales)

In order to determine anthropogenic ozone destruction, all natural influences must be specified the best possible way. In Table 2.1 known causes for ozone variability are listed.

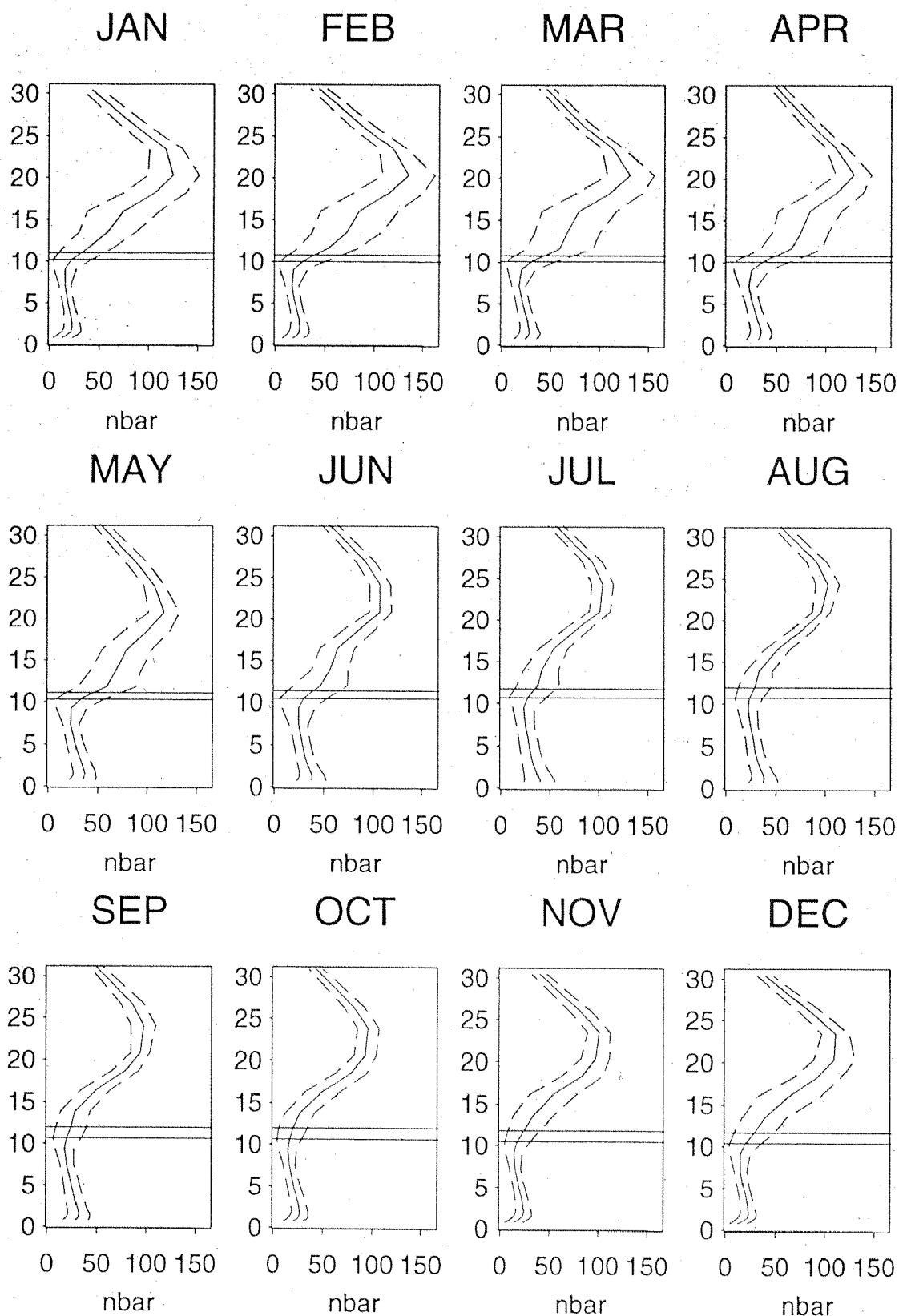


Figure 2.3: *Payerne soundings: mean (solid curves) \pm std (dashed curves) of ozone partial pressure. Horizontal lines are tropopause height + std and tropopause height - std. Variability is dependent on season and maximal in the lower stratosphere in February. Compare also with figure in Appendix B.*

	Feature	Time scale of variability
(1)	weather tropopause NAO / AO	days days-seasonal-interdecadal monthly-interdecadal
(2)	meridional circulation its variations	seasonal interdecadal
(3)	vortex dynamics polar chemistry	days to months since 1970s
(4)	QBO	biennial
(5)	ENSO	3–5 years
(6)	volcanic aerosols affect dynamics affect chemistry	by accident decadal injections months up to years
(7)	solar cycle	decadal
(8)	anthropogenic	since 1970s

Table 2.1: *A variety of factors influence ozone on the time scales from days to centuries. Weather and tropopause are connected to synoptic variability. The North Atlantic Oscillation (NAO) and Arctic Oscillation (AO) describe large scale structures in the atmospheric circulation. The meridional circulation, the polar vortex behavior, the Quasi-Biennial Oscillation (QBO) and the El Niño and Southern Oscillation (ENSO) all influence ozone via dynamics. The last two large volcanic eruptions had by chance a decadal interval and are therefore interfering with the 11 year solar cycle. Anthropogenic influence started in the seventies.*

Below, it is shortly described how these factors affect ozone. The dynamics and their interactions are explained in detail in Section 2.2 and only briefly mentioned here.

(1) Weather, tropopause, NAO and AO

Dobson et al. (1929) already found that the strong day-to-day variability of total ozone is connected with the weather. The mechanism is that low and high pressure systems deform the tropopause and cause flow in the lower stratosphere. To describe synoptic influences, meteorological parameters were used, e.g., the mountain Säntis temperature for Switzerland (Staehelein et al. 1998b). Further, several parameters describing tropo-

pause variability were found to be correlated with ozone (Schubert and Munteanu 1988, Vaughan and Price 1991, Steinbrecht et al. 1998, Ziemke et al. 1997).

There is evidence that dynamical changes could influence ozone in the long-term (Steinbrecht et al. 1998, Hood and Zaff 1995, Hood et al. 2000), see also Section 2.2 for a discussion. The North Atlantic Oscillation (NAO) and the Arctic Oscillation (AO) are climatic variables, both defined via sea surface pressure measurements. They describe the general weather situation over Europe and the Atlantic region, and are suitable to study inter-annual variation. Their influence on ozone is elaborated in Chapters 6 and 7.

(2) Meridional circulation

As the ozone is produced in the tropics and transported by the meridional circulation to the mid-latitudes, variations in the meridional circulation impact the global ozone distribution, especially in the middle and lower stratosphere where transport processes dominate over the in-situ chemistry. Inter-annual variations in up-welling planetary wave activity modulates the diabatic mean circulation and therefore ozone transport (Fusco and Salby 1999). The mean meridional circulation transports ozone away from its photochemical origin towards the poles. By this, fresh ozone-poor air is hauled continuously into the region where ozone is formed photochemically. Thus, mean meridional transport sustains the net production of ozone. The amount of ozone production in the tropics is influenced by the strength of the meridional circulation (Fusco and Salby 1999).

(3) Polar vortex dynamics and chemistry

The polar vortex dynamics affects the mid-latitudal ozone (Knudsen et al. 1998). Sudden stratospheric warmings in winter lead to the vortex breakup and release ozone from the otherwise rather isolated vortex. During these episodes, and at the annual vortex breakdown in spring, northern, ozone rich air is advected to mid-latitudes, causing the secondary maximum in the ozone profile of Fig. 2.1. Lower stratospheric air of polar origin is ozone rich compared to mid-latitudes because of the difference in ozone profiles. Because of the anthropogenic ozone destruction inside the Arctic vortex, less ozone is nowadays delivered this way to mid-latitudes.

This explains partly the observed downward trend of spring values in Fig. 2.2.

(4) **Quasi-Biennial Oscillation (QBO)**

The QBO is a prominent stratospheric phenomenon. Tropical winds circling the globe around the equator oscillate in their direction (east or west). The period is 26–29 months, i.e., somewhat longer than two years, therefore termed ‘quasi-biennial’.

The QBO causes ozone variations at mid-latitudes because of its dynamical influence on the extra-tropical stratosphere (Marquardt 1997). For ozone trend analysis, a proxy for the QBO is commonly included in the trend model to reduce variance, but the quasi-biennial period is short enough to cancel out in long-term analyses (Staehelin et al. 2000).

(5) **El Niño and Southern Oscillation (ENSO)**

An *El Niño* event is the switching from the normal mode to an unusual mode of winds and oceanic currents in the tropical Pacific. With this change, the up-welling of nutrition-rich deep water at the coast of South America stops, with disastrous impacts on fish stocks and the depending industry. This mostly happens around Christmas, giving the name for the phenomenon ‘El Niño’, the ‘Christ-child’. The *Southern Oscillation* is the signature of El Niño events in the sea level pressure.

The mean impact of El Niño on dynamics and therefore on ozone is found in the Southern Hemisphere (Langford et al. 1998). In connection to this global changes in the tropospheric circulation occurs, which are termed *teleconnection patterns*. As tropospheric dynamics in Europe is mostly determined by what is happening in the Atlantic region, only marginal influence is expected. For Switzerland, no influence of El Niño on ozone was found (Staehelin et al. 1998b) and therefore El Niño is not taken into account in this thesis.

(6) **Aerosol effects**

The stratospheric aerosols are small sulfuric droplets produced primarily through oxidation of sulfur dioxide injected into the stratosphere by volcanic eruptions. The major volcanic eruptions in the 20th century were Mount St. Helens on 18.5.1980, El Chichón on 3.4.1982 and the largest was Pinatubo on 15.6.1991. It takes some months until the volcanic aerosols are evenly distributed across the

hemisphere. The sulfate aerosols have a residence time (decrease to $1/e$) of about 12–18 months, and provide active surfaces for chemical reactions which accelerate ozone destruction (Solomon et al. 1996).

Furthermore, volcanic aerosols injected into the lower stratosphere absorb solar light and lead to strong local warming. The resulting dynamical changes in the stratosphere caused by major volcanic eruptions may be stronger than the ENSO-effects (Marquardt 1997).

(7) **Solar cycle**

The change of the solar constant between solar maxima and minima in the 11-year cycle is in the order of only 0.2%. Although the solar cycle is more pronounced at the UV wavelengths (in order of a few percent), it is hard to imagine a reasonable physical connection between ozone and solar activity. In principle, there are two possible ways that solar activity could influence ozone.

Firstly, the chemical equilibrium might be influenced by the amount on the UV radiation which is at disposal. Duetsch (1979) explained how the photo-dissociation rates of oxygen, ozone and NO are changed. This would give a noticeable contribution in the upper stratosphere, above about 40 km. Below this altitude, the so called *self-healing* effect prevents radiation changes to have an effect. Because the bulk ozone is situated below this region, this chemical in-situ solar effect should be too small to show up in total ozone. Secondly, and more likely, is the indirect influence via the dynamical changes, see Section 2.2.

(8) **Anthropogenic trends**

Ozone changes, which cannot be attributed to natural causes, are hypothesized to be caused by man-made chlorofluorocarbons and other ozone depleting substances. There is vast evidence for anthropogenic ozone destruction (WMO 1999, Solomon 1999) and the scientific questions are: in which way, how much and in which heights does this anthropogenic ozone destruction take place?

2.1.3 Anthropogenic ozone destruction

Gas phase chemistry

The basic chemical theory for stratospheric ozone was formulated by Chapman (1930). Ozone, molecular and atomic oxygen are in equilibrium according to the supply of solar radiation. The reactions are summarized in Table 2.2.

Chapman theory			
O ₃ production			
	$O_2 + h\nu(\lambda \leq 242\text{nm})$	\longrightarrow	$O + O$
	$2[O + O_2 + M$	\longrightarrow	$O_3 + M]$
net:	$3O_2 + h\nu$	\longrightarrow	$2O_3$
O ₃ destruction			
	$O_3 + h\nu(\lambda \leq 1140\text{nm})$	\longrightarrow	$O + O_2$
	$O + O_3$	\longrightarrow	$2O_2$
net:	$2O_3 + h\nu$	\longrightarrow	$3O_2$

Table 2.2: *Chapman theory for the formation and destruction of ozone under the influence of solar light with energy $h\nu$ (Planck's constant h , frequency ν , wavelength λ). M is a molecular collision partner which picks up momentum.*

Later work led to the recognition of substantial additional ozone destruction processes. These were presented first by Crutzen (1970) and Johnston (1971) who suggested that chemicals in low concentrations can act as catalysts for ozone destruction, as explained in Table 2.3. The radicals X and XO are such catalysts, and stand for either nitrogen compounds NO and NO₂ (Crutzen 1974), or chlorine Cl and ClO, (Molina and Rowland 1974). Further the bromine Br and BrO was found to play a role, and also HO and HO₂ (WMO 1999).

The nitrogen compounds in the stratosphere originate mostly from the photolysis of N₂O from micro-biological processes in (especially over-fertilized) soils (Graedel and Crutzen 1994). Less abundant, but more effective is chlorine as a catalyst. Molina and Rowland (1974) pointed out that it is the anthropogenic chlorofluorocarbons (CFCs) which release the anthropogenic chlorine upon photolysis in the stratosphere.

Catalytic gas phase O ₃ destruction			
	$X^\bullet + O_3$	\longrightarrow	$XO^\bullet + O_2$
	$O_3 + h\nu$	\longrightarrow	$O + O_2$
	$O + XO^\bullet$	\longrightarrow	$X^\bullet + O_2$
net:	$2O_3 + h\nu$	\longrightarrow	$3O_2$

Table 2.3: *The radicals X transform odd oxygen to even oxygen, and destroy ozone this way. They are highly reactive because of their unpaired electron •. As the X• are rebuilt at the end of the cycle, they are called catalysts. One X can destroy many O₃ molecules. X stands for NO, Cl, Br and HO.*

The CFCs are mainly CF₂Cl₂ (industrial name: CFC-12) and CFCl₃ (industrial name: CFC-11) but also include a large list of other industrial compounds (WMO 1995). The natural stratospheric background of chlorine compounds as originating from volcanos, sea spray and gas production by sea alga is much smaller, and anthropogenic chlorine is the main culprit for ozone depletion (Solomon (1999) and references therein).

The radicals also react with each other in a complex way (Staehelin and Duetsch 1989, Solomon 1999), and form reservoir gases which slow ozone destruction. The chemistry on and with surfaces of aerosols and polar stratospheric clouds (heterogeneous chemistry) reactivate reservoir gas, thus accelerate ozone destruction (Solomon et al. 1986, Solomon et al. 1996).

The ozone destruction observed in the higher stratosphere (near 40 km height) is shown to be due solely to the catalytic gas phase ozone destruction without heterogeneous chemistry (Crutzen 1974).

Heterogeneous chemistry

A special situation is encountered at the poles. In the polar night, a cold circumpolar vortex builds up and prevents air exchange with mid-latitudes. The temperature drops below -70°C , and polar stratospheric clouds (PSCs) form. Solomon et al. (1986) suggested the following mechanism: The clouds absorb the reservoir gases HCl and ClONO₂, which

react to HNO_3 and Cl_2 . As soon as the first sun light arrives in polar spring in Antarctica, a devastating ozone destruction occurs. The Cl_2 is photolysed and forms ClO , the catalytic ozone destruction (Table 2.3) begins. The chlorine destroys ozone, now unimpeded by the nitrogen compounds (i.e., no formation of the 'brake' ClONO_2). The nitrogen is still in the cloud or removed by falling particles which is termed *denitrification*.

Farman et al. (1985) discovered the ozone hole over Antarctica, which is caused by such heterogeneous chlorine activation and nitrogen deactivation. Since then, the ozone hole kept growing from year to year. The total ozone was depleted in the nineties to 1/3 of historical values and the depleted region had the size of the Antarctic continent. Molina and Molina (1987) discovered the catalytic ClO cycle involving Cl_2O_2 , which is now recognized to be responsible for 75% of the ozone removal in the ozone hole, another 20% are attributed to the bromine cycle (Solomon (1999) and references therein). The ozone depletion stops when the vortex breaks up and fresh air is mixed in.

Compared to the Antarctic, less severe ozone loss occurs in the Arctic. The heterogeneous chemistry is the same, but the dynamical conditions vary. Less PSCs form in the Arctic because it is warmer than the Antarctic. Still, denitrification was observed also in some years (Waibel et al. 1999). If the stratosphere cools due to the greenhouse effect, more denitrification and more ozone loss must be expected in future in the Arctic (Waibel et al. 1999).

Heterogeneous chemistry on volcanic aerosols was first demonstrated by Fahey et al. (1993) to play a role at mid-latitudes. On aerosol surfaces, nitrogen is transformed to inert compounds, and then no longer available for chlorine deactivation. In addition, there is chlorine activation occurring on aerosol surfaces. In particular, The ozone destruction connected with aerosols is considerably smaller than the one connected with PSCs, as the mass and effectivity of aerosols is much smaller than the one of the PSCs. However, after major volcanic eruptions, significant ozone decrease has been observed (Hofmann and Solomon 1989, WMO 1995).

2.2 Dynamical principles

For the circulation of the stratosphere, two processes are important: (1) the heating and cooling of the air through radiation and (2) the interaction of mean flow and waves. These processes give rise to the climatology of the stratosphere and its annual cycle. Because much of the ozone climatology and variability is determined by stratospheric dynamics, its basic principles are described below.

2.2.1 The meridional circulation

The observed temperatures in the stratosphere deviate from what would be expected from radiative equilibrium. The reason for this is a slow, global meridional circulation, a rising motion in the tropics and a descent over the poles of the winter hemisphere, historically referred to as the *Brewer-Dobson circulation* (Brewer 1949, Dobson 1956). These motions are accompanied by radiative heating and cooling, and therefore also called *diabatic circulation*. However, the actually observed meridional circulation is stronger than the different heating rates at the tropics and poles imply.

The additional drive of the meridional circulation is provided by dynamical processes that are interlinked with dissipating waves. The understanding of these phenomena has improved in the last years. Holton et al. (1995) explains the global circulation principle, which is referred to as *wave-driven extra-tropical pump*. Below, a simplified explanation is given.

These *waves* are perturbations in the mean flow, which propagate under favorable conditions from the troposphere into the stratosphere. When the waves are damped they weaken the zonal mean flow. The Coriolis effect converts the negative zonal acceleration into a meridional, poleward flow, thus establishing conservation of momentum. The damping of waves enforces the diabatic meridional circulation due to mass continuity. The air is pulled up from the tropics and pushed poleward and finally downward at high latitudes. This is why the tropical stratosphere is cooled below its radiative equilibrium, and in the high latitudes of the winter hemisphere, temperatures are higher than the radiative equilibrium would imply.

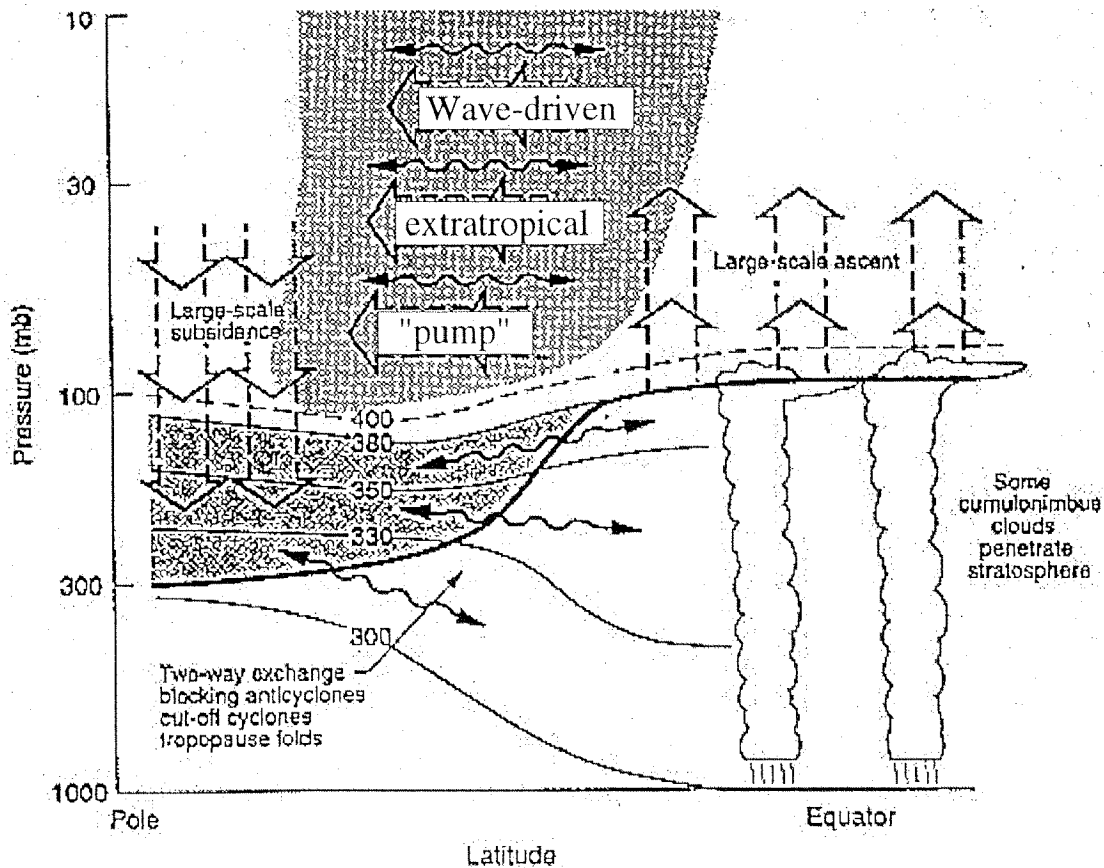


Figure 2.4: Figure from Holton et al. (1995). The 'extra-tropical pump' which gets its energy from wave dissipation, drives the global circulation. It causes uplift at the tropics and pushes air down at the poles. The broad arrows show the global circulation. Light shading denotes wave-induced forcing. The wave driven circulation is also responsible for the stratosphere-troposphere exchange. Thin lines are constant potential temperature surfaces (isentropes). The 380 K surface divides the 'over world', where isentropes are entirely in the stratosphere, from the 'lowermost stratosphere' which has exchange with the troposphere. The tropopause is the thick line. Wavy arrows denote eddy motions.

2.2.2 Wave origin and fate

One origin of the waves is the irregular land-sea distribution. The excited *Rossby-waves* have planetary scales and their restoring force is given from the Coriolis force varying with latitude. Smaller scale *gravity waves* are caused by great mountain chains, by stochastic perturbations from tropical convection cells, or are forced near strong wind jets. These waves are too small to feel the varying Coriolis effect. Their restoring force is given by the buoyancy of vertical displaced air parcels.

The criterion of Charney and Drazin (1961) determines whether a wave with a certain wave number propagates in a given zonal wind into the stratosphere or not.

The favorable conditions for wave propagation are (not too strong) west winds (Charney and Drazin 1961). This condition is given mostly in winter. In contrast, in summer, the stratosphere is determined by (weaker) easterly winds. Waves do not propagate in easterly winds. As a consequence the meridional circulation is strong in winter and weak in summer. During spring and autumn, the switch-over between the wind regimes happens, and weak west winds prevail in middle and high latitudes.

The breaking of the waves, a nonlinear effect, is favored with high wave amplitudes. These are reached in the upper heights, as wave propagation into the low pressure areas results in wave amplitude grow. Finally they get instable and *break*, i.e., dissipate. The irreversible angular momentum transfer due to dissipative eddy effects provoke an *eddy induced mean zonal force*. As described above, the effect of this force is not only felt locally, but also side-wards and below. This is the *downward control principle* which has been suggested by Haynes et al. (1991). The authors derived that the mean zonal force induced by eddy dissipation controls the vertical component of the mean circulation below. Although it is astonishing at the first glance with respect to pressure distribution, in fact dynamical disturbances can start in the upper stratosphere, and propagate downward.

In high latitudes, the breaking of planetary waves contributes significantly to the global circulation. In the tropics, gravity wave breaking and thermal dissipation (i.e. long-wave radiative transfer) of both planetary and gravity waves drive the QBO.

2.2.3 The polar vortex

The winter polar stratosphere is characterized by a large scale polar vortex. The *polar vortex* is characterized by strong zonal stratospheric west winds. The explanation is described in (Staehelin et al. 2000) as follows: The summer stratosphere is characterized by a polar temperature maximum because of the amount of sunlight. Due to the thermal wind balance this meridional temperature gradient is linked to easterly winds. The vortex starts to form in autumn, where less warming sunlight leads to colder temperatures at the pole relative to the lower latitudes. This implies westerly winds and an increase in the absolute value of potential vorticity (see Section 2.2.7) over the polar region. During winter, the vortex is strongest and the exchange of air across the edge of the polar vortex is strongly restricted. The strong potential vorticity gradient at the vortex edge acts as a mixing barrier. Thus, most of the polar air is trapped within the vortex, and is relatively isolated from mid-latitude air, which is well-stirred by Rossby waves and called the *surf zone* (McIntyre and Palmer 1983). The isolation of air is a prerequisite for the strong ozone depletion and the ozone holes which are observed.

Planetary waves with the wave numbers 1 to 3 generate a high variability of the vortex. For instance, a displacement of the polar vortex into middle latitudes is a planetary Rossby wave with zonal wave number 1. The elongation of the polar vortex is described with a zonal wave with number 2.

Sudden stratospheric warmings occur with wave breaking (vortex perturbations and vortex splitting). These events often begin in the upper stratosphere, even in the lower mesosphere, and propagate into the middle and occasionally further down into the lower stratosphere. Sometimes the vortex rebuilds, but after a final major warming, the vortex breaks down and does not regenerate, the circulation is switched to summer circulation. This can happen as early as in February, whereas the normal continuous changeover to the summer circulation happens between March and April.

2.2.4 QBO

In the tropics, a phenomenon called *Quasi-Biennial Oscillation (QBO)* occurs in the stratosphere. This are east-west tropical winds which oscillate with their reverse direction at a *quasi-biennial* scale. One period spans 26-29 months, i.e., somewhat more than two years. Observational and theoretical studies showed that vertically propagating equatorial gravity waves (internal, Rossby- and Kelvin waves) drive the QBO (Marquardt 1997). On the other hand, the QBO influences wave propagation, as waves can propagate upwards only in western winds (Charney and Drazin 1961). They break depending on direction and strength of the QBO.

The QBO is important for low frequency variations in the stratosphere, as Marquardt (1997) concluded from the response of the QBO and the global meridional circulation to the aerosol injection of Pinatubo: The meridional mean flow and the QBO interact with each other such that the QBO buffers anomalies of the meridional mean flow.

There are two mechanisms by which QBO affects ozone in mid-latitudes:

- (1) The QBO modulates the meridional transport of ozone from the tropics to mid-latitudes. (Marquardt 1997).
- (2) The break-up of the polar vortex is favored if there are winds in the opposite direction in the middle stratosphere. Therefore, ozone transport from the arctic vortex to mid-latitudes is enhanced when the QBO is in easterly phase (Holton and Tan 1980).

2.2.5 Solar influence

Labitzke and van Loon (1988) discovered a statistically significant connection between solar cycle and 30 hPa heights. The reason is suspected in either a modification of the tropospheric circulation via the tropical ocean surface or via the absorption of UV by the stratospheric ozone, creating temperature gradients responsible for more intense horizontal and vertical motions. Interestingly, the solar influence seemed to be only discernible when the data are grouped according to the QBO phase (Labitzke and van Loon 1988). The key seems to be the planetary wave activity. It responds to both solar and QBO forcings (Soukharev 2000). This idea is complemented by Haigh (1996) who found with a

general circulation model that in solar maximum, the easterly winds are strengthened in the summer stratosphere, which causes pole-ward shifts of the sub-tropical westerly jet.

Shindell et al. (1999) simulated in a numerical model the solar influence on climate via UV-uptake of stratospheric ozone. The changed UV-uptake alters the temperature distribution, and therefore geopotential heights. This influences the zonal winds, and these disturbances are expected to propagate downward as they change planetary wave propagation. To summarize this hypothesis: the dynamical changes originally caused by the chemical and radiation budget of the ozone, have a feedback on the ozone via redistribution of air masses.

2.2.6 NAO and AO

Already in the 1770's the missionary Hans Egede Saaby described a climatic oscillation: *In Greenland, all winters are severe, yet they are not alike. The Danes have noticed that when the winter in Denmark was severe, as we perceive it, the winter in Greenland in its manner was mild, and conversely* (van Loon and Rogers 1978). He observed a temperature effect that is linked to the North Atlantic Oscillation (NAO), which is the dominant mode of atmospheric multi-annual variability over the Atlantic sector, most pronounced in winter. NAO variability is found in many meteorological variables such as surface wind, temperature and precipitation which have impacts on agriculture and industry throughout Europe, Northern Africa, Asia Minor, and even eastern North America.

The NAO is characterized as a north-south pressure difference. Hurrell (1995) defined the NAO index as the pressure difference between Ponta Delgada (Azores) and Stykkisholmur (Iceland). Its signature appears in nearly all meteorological parameters in the North-Atlantic and Europe region and influences the troposphere-stratosphere system (Perlwitz and Graf 1995). Further, the pattern is present in the Atlantic sea surface temperature and salinity. The NAO attracted new attention in the late nineties (Marshall et al. 1997, Uppenbrink 1999) in connection with the anthropogenic climate trend issue.

The *Arctic Oscillation* (AO) is defined (Thompson and Wallace 1998) as the leading empirical orthogonal function of the wintertime sea-level

pressure field, i.e., via the whole hemisphere and not only by two locally characteristic measurement points as the NAO. The AO can be interpreted as the surface signature of modulation in the strength of the polar vortex aloft (Thompson and Wallace 1998).

On the multi-annual scale, the AO is resembling the NAO. The main difference is that AO 'feels' beside the pattern over the Atlantic also what is happening over the Pacific of the northern hemisphere.

At the present, the physical driving of NAO and AO is unknown. Numerical simulations of NAO show that a atmosphere-ocean interaction is indispensable for reproducing the climatic oscillation (Selten et al. 1999). Where the initial perturbations stem from remains unidentified. Some authors assume the initial perturbations come from the atmosphere (Marshall et al. 1997). The response of the oceanic circulation to wind-stress anomalies appears to be essential. Another troposphere-ocean interaction is suggested by Mysak and Venegas (1998): the feedback loop between polar ice coverage and surface winds.

As the AO was observed to propagate downward (Baldwin and Dunkerton 1999) and the signal was found to be strongest in the upper heights, it has been suggested that at least a part of the AO pattern comes from the stratosphere. Though, the planetary waves which transport the energy up to the upper stratosphere, are originating in the troposphere.

Clearly, the missing understanding of NAO/AO make forecasts difficult. But it is of vital importance for the climate research, whether the present trend in NAO is unique compared to historic behavior or not. This topic is discussed controversially (AGU 1999). There had been many attempts to reconstruct the climate and the NAO of the past, employing historical weather records, tree ring data and ice core data (Appenzeller et al. (1998) and references therein). Less work has been done with AO, as it requires the pressure field of the whole hemisphere which became available back to 1958 with the NCEP-reanalysis (Kalnay and et al. 1996).

Suggestions are that the NAO/AO behavior could be a random walk (Stephenson et al. 2000), or accumulated stochastic noise from weather and ocean or chaotic behavior which has intrinsic low frequency components and does not depend on external forcing (Christiansen 2000). This means that the observed NAO/AO long-term behavior is natural

variability. The other possibility implies an anthropogenic influence: a response to anthropogenic climate forcing (Paeth and Hense 1999) or (Shindell et al. 1999)

The climatic oscillations, among them NAO and AO, are connected with the planetary wave activity and the meridional circulation (Ohhashi and Yamazaki 1999). In Chapters 6 and 7 the influence of NAO/AO on the tropopause is shown to be a major mechanism for long-term ozone variations.

2.2.7 Tropopause

The tropopause separates the troposphere, with its decreasing temperatures with height, from the isothermal lower stratosphere. Often, the tropopause appears in the temperature profile as a marked temperature minimum. As sometimes there is also a temperature gradient in the lower stratosphere, the tropopause is defined thermically as the level where the temperature decrease with height falls below 0.3°C per 100 m (Liljequist and Cehak 1984).

The tropopause marks an important transport barrier, as the air below the troposphere is well mixed and above the stratification causes stability and less mixing. The potential vorticity PV (Ertel 1942) is a relatively conservative air mass tracer. It is a function of vorticity and static stability. Using the standard notation (Hoskins et al. 1985) and typically in the range -1 to 1 PV-units (see Hoskins (1991) for definition of PV-units) in the mid-latitudal troposphere and quickly rising in the stratosphere. Because of the static stability term, PV is much larger for the stratosphere than for the troposphere, which makes the PV a convenient marker of the tropopause. One common dynamical definition of the tropopause is $PV=1.6$ PV-units (WMO 1986). It was found more appropriate to use $PV=2$ PV-units (Appenzeller et al. 1996a), which is used in this thesis.

Some exchange of air occurs between the lowermost stratosphere and the troposphere by complicated mechanisms as tropopause folds and cut-offs.

2.3 Why ozone profile trend analysis

Besides its relevance to test the theory on ozone chemistry, monitoring ozone profiles is important for climate change research. Ozone absorbs ultraviolet, visible and infrared wavelengths and plays an important role in the radiative balance. Changes of ozone will affect the thermal and dynamical structure of the atmosphere. A large effect for the climate comes from the increasing tropospheric ozone due to industrial pollution and biomass burning. This contributes significantly ($0.3\text{--}0.5\text{ Wm}^{-2}$) to the greenhouse effect by warming the troposphere (Roelofs et al. (1997), and references therein). The decrease of stratospheric ozone cools the stratosphere. More visible and ultraviolet radiation can penetrate to the troposphere, but less thermal emissions will occur from less and colder stratospheric ozone. This radiative balance impacts the surface temperature. The sign of the climatic effect depends on details of the ozone profile (Ramanathan and Dickinson, 1979). The ozone depletion in the higher stratosphere has a small positive forcing (Forster and Shine 1997), which is contrasted by the estimate of Bintaja et al. (1997), who found no forcing. The majority of authors agree that lower stratospheric ozone depletion will cause a cooling of the troposphere-surface system (Shine and Forster (1999), and references therein). The magnitude of reported forcing from lower stratospheric ozone trends range between $+0.02\text{ Wm}^{-2}\text{ decade}^{-1}$ (Myhre et al. 1998) and $-0.19\text{ W m}^{-2}\text{ decade}^{-1}$ since the late 1970s (Hansen et al. 1997). The inconsistencies in the estimated climate forcing due to ozone changes are at least partly due to difficulties in defining the vertical and latitudinal profiles of ozone loss (Shine and Forster 1999). Coupling to the dynamics causes further complications. The forcing given by the ozone changes and the greenhouse gases is not able to reproduce the recent dynamical changes in the lower stratosphere (Graf et al. 1998, Shindell et al. 1999). These authors attributed the dynamical changes rather to natural variability, linked to the North Atlantic Oscillation (NAO). An analysis of the causes and magnitudes of the ozone profile trends is therefore highly desirable.

Large efforts to evaluate ozone profiles and to track their trends were undertaken in a collaborative effort of SPARC (Stratospheric Processes and their Role in Climate) of the World Climate research program, the International Ozone Commission (IOC) and the WMO's Global Atmospheric Watch program (GAW). Four measurement techniques produced records long enough to assess long-term trends: the satellites SAGE

(I+II) and SBUV, the remote sensing Umkehr method, and the ozone balloon soundings (SPARC 1998). The attempt to put together an overall trend versus altitude with instrumental and statistical uncertainties is depicted in Fig.2.5. In this figure, although constructed tentatively, essential points of observed ozone change are condensed. There are statistically significant negative trends throughout the whole stratosphere. The magnitude of trend depends on altitude. There are two main regions of ozone change, around 15 km and around 40 km. The maximum of ozone depletion in the higher stratosphere is consistent with the expected effects of industrial halocarbons outside the polar vortices (Crutzen 1974). The region of largest uncertainty, with respect to measurements as well as to interpretation, is between 10 and 20 km, i.e., the lower stratosphere. Actually only balloon soundings can provide estimates for ozone trends there, whereas SAGE may give some less reliable information (SPARC 1998), and Umkehr bulk estimates must be used with caution.

In Chapters 5 and 7, ozone profile trends are estimated for the Swiss profiling series, i.e., for the balloon soundings of Payerne and for the Umkehr measurements of Arosa. In the next chapter, the statistical means for proper trend analysis are provided.

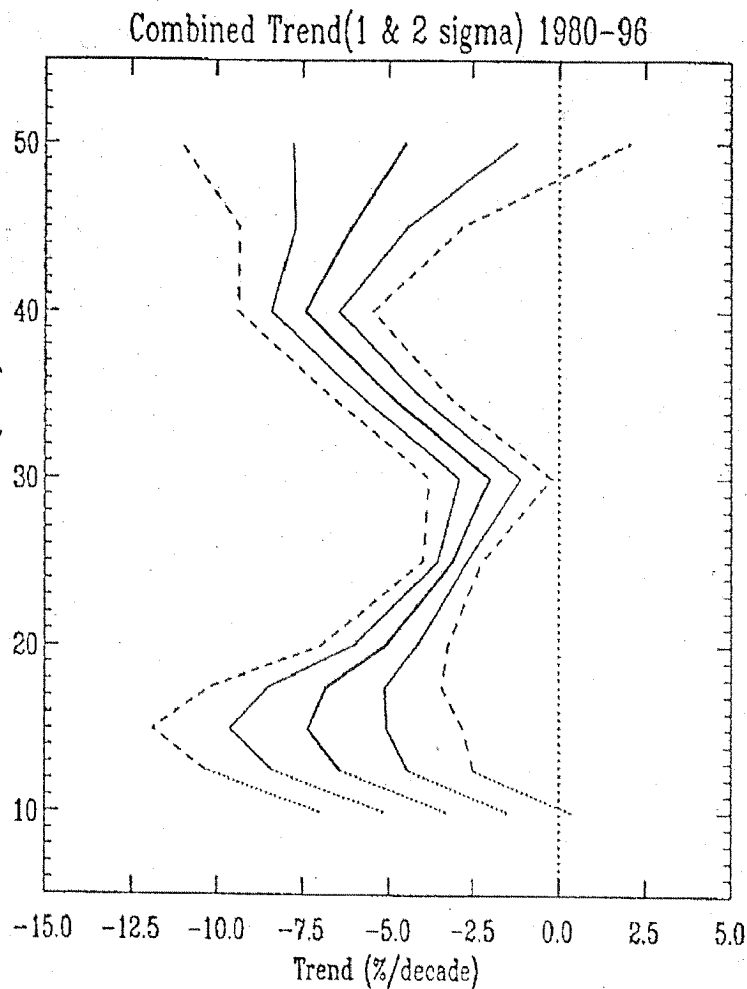


Figure 2.5: *SPARC-estimate of mean trend using all measurement systems at northern mid-latitudes (heavy solid line). Combined uncertainties are shown as 1σ (light solid line) and 2σ (dashed line). Combined trends are not estimated in the troposphere because the small sample of sounding stations have an unquantified uncertainty concerning their representativeness of mean trends. Figure from SPARC, 1998.*

Chapter 3

Statistical tools

The mathematical methods used in this thesis are shortly summarized to give the reader a quick reference. They are standard procedures described in many mathematical textbooks, for this thesis Bronstein and Semendjajew (1991) and Stahel (1995) were consulted.

3.1 Significance and p-value

Statistical quantities (e.g. the mean or correlation coefficient) are often given with their *significance* or with their '*p-values*'. This is for evaluating the quality of the estimate. Below, the meaning of this terms is explained. Most statistical tests begin with the *null hypothesis* that some statistical quantity θ of interest is zero. A measure for the uncertainty associated with the value of θ is its standard deviation of $\delta\theta$. With 68% probability the true value of θ lies in the interval $(\theta - \delta\theta, \theta + \delta\theta)$. With 95 % probability the true value of θ lies in the interval $(\theta - 2\delta\theta, \theta + 2\delta\theta)$. If these intervals do not contain the number 0, θ is *significantly different from zero* at the 68% or 95% confidence level, respectively.

The p-value is the level of significance for which the observed test statistic value lies on the boundary between acceptance and rejection of the null hypothesis. The confidence level is $100\%(1-(p\text{-value}))$. For exam-

ple, a p-value < 0.05 means that with at least 95% probability the statistical quantity θ is different from zero. This is a common choice for calling a quantity *statistically significant*.

3.2 Correlation

The question, whether two quantities are connected with each other, is often studied with the *correlation* or the *covariance* of the two quantities. The true covariance sequence $\text{cov}_{xy}(m)$ is a statistical quantity defined as

$$\text{cov}_{xy}(m) = E \{ x_n y_{n+m}^* \} \quad (1)$$

where x_n and y_n are stationary random processes, and n denotes number of the sample. Per definition n should cover all $-\infty < n < \infty$. $E\{\}$ is the expected value operator. The y^* denotes the conjugate complex which is in the application of real numbers the same as y . The lag m is the number of samples (e.g., time span) with which the series x_n and y_n are shifted against each other. The correlation γ_{xy} is the mean-removed and normalized covariance sequence:

$$\gamma_{xy}(m) = \frac{E \{ (x_n - \bar{x})(y_{n+m}^* - \bar{y}^*) \}}{\sqrt{E \{ x^2 \}} \sqrt{E \{ y^2 \}}} \quad (2)$$

For simplicity, series x_n and y_n are assumed to be normalized in the following, i.e., means are removed ($E\{x_n\}$ and $E\{y_n\}$ are zero) and the units are chosen so that $E\{x_n^2\}$ and $E\{y_n^2\}$ are set to one.

The *correlation coefficient* is $\gamma_{xy}(m = 0)$. If x_n and y_n are independent of each other, i.e., *uncorrelated*, then:

$$\gamma_{xy}(m = 0) = E \{ x_n y_n^* \} = E \{ x_n \} E \{ y_n \} = 0 \quad (3)$$

In reality, γ_{xy} must be estimated from a finite series. The formula is:

$$\hat{r}_{xy}(m) = \begin{cases} \sum_{n=0}^{N-|m|-1} x_n y_{n+m}^* & m \geq 0 \\ \hat{r}_{xy(-m)} & m \leq 0 \end{cases} \quad (4)$$

Equation (4) gives the correlation coefficient estimate $\hat{r}_{xy}(m)$ as a folding operation with x_n and y_n . This is equivalent to transforming x_n and

y_n in the spectral domain, multiplying the spectrum of x_n with the spectrum of y_n in the spectral domain, and transforming the result back into the time domain. Finite samples have in general an $\hat{r}_{xy} \neq 0$ whether the x and y are independent or not, just because they are finite samples and have therefore a non-zero spectrum.

For instance, if y is the series of annular ozone mean and x is the series of solar activity one should have a very, very long series, actually from $-\infty$ to ∞ to give the true correlation of both quantities. In fact, we have ozone $\{y\} = (y_0(1926), y_1(1927), \dots, y_{73}(1999))$ and, as we are interested in $m=0$ (i.e., no time lag) solar activity is $\{x\} = (x_0(1926), x_1(1927), \dots, x_{73}(1999))$. After normalization of the series, the estimate \hat{r}_{xy} is calculated from the finite sample (actually 74 years, i.e., $N=74$) as:

$$\hat{r}_{xy}(0) = \sum_{n=0}^{73} x_n y_n \quad (5)$$

Now \hat{r}_{xy} must be tested to understand whether it is different from zero just because of the finite sample length or whether there is a connection between ozone and solar cycle.

A standard procedure for this, the Pearson test, is implemented in the Splus-routine `cor.test`. This is used in the thesis for checking the correlation significance.

The *autocorrelation* $\hat{r}_{xx(m)}$, is the correlation of a series x_n with itself. For instance, if x_n is a series of monthly means, and there is seasonal cycle, then the autocorrelation $\hat{r}_{xx}(12)$ will be significantly different from zero.

Note that if both series are autocorrelated (e.g., if both have a seasonal cycle) the cross-correlation will be different from zero just because their similar spectra. An appropriate way to deal with this problem is to generate synthetic series with the same autocorrelation function and check whether this synthetic correlation is significantly different from the observed ones.

Finally, a time series where x_n is dependent on the previous values x_{n-1} , $x_{n-2} \dots x_{(n-l)}$, can be statistically modeled as an *autoregressive* (AR)

process of *order l*:

$$x_n = \sum_{i=1}^l a_i x_{n-i} + \epsilon \quad (6)$$

where the a_i are the parameters of the AR-process and ϵ is the normal distributed noise term. Such time series have autocorrelations $\hat{r}_{xx(m)}$ different from zero up to the lag m which is $m = l$. From this, the AR-coefficients a_i may be retrieved.

3.3 Linear regression

Multiple linear regression attributes the difference between the target variable y from its mean \bar{y} to the influence of several explanatory variables x_i :

$$y = \bar{y} + \sum_i c_i x_i + \epsilon \quad (7)$$

where the magnitudes of contributions c_i are found with a maximum likelihood method and ϵ is the error, also termed *residuals*. With residual analysis, the validity of the model can be verified.

If two explanatory variables are very similar, it cannot be distinguished which actually contributes to the variability of y , and the results are large error bounds and low statistical significance. This is the *collinearity problem* which can be avoided by using only one of this variables at a time in the model, and choosing the more significant of the two for the final model.

The model (7) can give only sensible significances and error bounds if the residuals ϵ are not autocorrelated, i.e., the residuals must be tested. In this case of autocorrelation, a regression method must be applied which accounts for this (Cochrane and Orcutt 1949).

3.4 The commonly used ozone trend model

For estimating the long-term total ozone trends, which are attributed to anthropogenic destruction, a model which is in principle the same as Eq.(7), is often assumed (e.g., Staehelin et al. (2000)):

$$y_t = \sum_{m=1}^{12} \bar{y}_m I_{m,t} + \sum_{m=1}^{12} \beta_m I_{m,t} R_t + \sum_{i=1}^k c_i \Theta_{i,t} + N_t \quad (8)$$

where t the index of the month, counted from the beginning of measurements, m the index of calendar month; y_t the mean of measured total ozone in the month t , \bar{y}_m the climatological mean of ozone in the appropriate calendar month, and $I_{m,t}$ an index which is 1 when the month t is matching the calendar month m and zero else. The aim of interest are the monthly trends β_m , the contributions of the explanatory variable R which is a linear ramp starting 1970 and rising 1 per decade. The model looks complicated because simple linear models as Eq.(7) are allowed for each month, with the requirement that the contribution c_i of the explanatory variable Θ_i is the same for each month. Further, the error term N_t is allowed to be autocorrelated, i.e., is defined to depend on the two months before (i.e., N_t is defined as x_n in Eq. (6) with $l = 2$).

The model Eq.(8) is the commonly used trend model for total ozone and ozone profile trend analysis (Bojkov et al. 1990) and was applied in the SPARC/IOC trends reports (SPARC 1998, WMO 1999). It is was employed for analysis of ozone sonde data (e.g., Logan (1994) and Logan et al. (1999)), satellite data (e.g., Stolarski et al. (1992) and Newchurch et al. (1998)) and Umkehr profiles (e.g., Reinsel et al. (1989) and Reinsel et al. (1999)).

The choice of the start of the *ramp* R was justified by the fact that concentrations of ozone depleting substances in the stratosphere almost linearly increased from the beginning of the 1970's to the middle of the 1990s. Therefore, long-term trends not explained by the natural factors $\Theta_{i,t}$ are commonly attributed to the anthropogenic release of ozone depleting substances. Many analyses start 1979 with the beginning of satellite records.

It would be desirable to have proxies $\Theta_{(i,t)}$ for all the factors affecting ozone summarized in Table 2.1. The most commonly used explanatory variables for $\Theta_{i,t}$ are the solar cycle, the QBO, ENSO and the aerosol

loading (see e.g., Harris et al. (1997), Bojkov et al. (1990), SPARC (1998)). Only a few authors have added a term for the synoptic variability (Staehelin et al. 1998b), or dynamical proxies (Hood and Zaff 1995, Steinbrecht et al. 1998).

The ozone balance Eq.(8) is additive, which is a sensible first guess from the knowledge that there is a certain variance observed and no jumps appear. For any contribution which would control ozone in a nonlinear, but polynomial manner, a linear first try is appropriate. The residual analysis is suitable to verify the assumptions. Further, it must be checked with which time lag the contributors affect ozone.

Non-linear suggestions for improving the ozone balance Eq.(8) are concerning the solar cycle, the QBO and the stratospheric aerosols loading. Labitzke and van Loon (1997) suggested linking the data according to the QBO phase, which is a non-linear dependence, but again a linear dependence within the subsample. Solomon et al. (1996) suggested linking the destruction of ozone by chlorine with the aerosol surfaces and Fusco and Salby (1999) used an *ozone depletion factor (ODF)* describing the nonlinear influence of both terms on the ozone balance in Eq.(8).

3.5 The new ozone trend model

An updated model is used in this thesis, starting from Eq.(8). There is no sensible reasoning why the explanatory variable Θ_i should have the same contributions on every month of year, therefore the ozone y_t is evaluated separately for each month or season in this thesis:

$$y_t = \bar{y} + \beta R_t + \sum_{i=1}^k c_i \Theta_{i,t} + N_t \quad (9)$$

This are 12 independent equations for the 12 months of the year. According to the results, months with similar trends and natural influences can be grouped into seasons, which reduces the scatter and allows more precise trend estimation. In Chapters 6 and 7, 3 seasons were found to be optimal, thus 3 independent equations of the form (9) are employed.

Actually, βR_t can be incorporated into the sum with $c_0 = \beta$ and $x_0 = R$ and x denotes now both the natural factors $\Theta_{i,t}$ and the trend term

βR_t describing anthropogenic destruction. The time index is dropped for convenience. This leads to the simple multiple regression formula as in Eq.(7):

$$y = \bar{y} + \sum_{i=0}^k c_i x_i + N \quad (10)$$

The errors N are identified by their autocorrelation to be an autoregressive process (Eq.(6)). Or, expressed in terms of the spectrum, there are unexplained frequencies which is an unexplained information content. This indicates an explanatory variable is missing and therefore an important physical mechanism for the ozone balance is ignored. There are two possibilities to deal with this. Ideally, a new variable is found which explains the information of the autoregressive noise and included in the model 8 and 3.5. The error term is not autocorrelated any longer and the standard linear regression procedure can be applied. If this is not possible, the appropriate procedure considering the autocorrelated errors must be employed to solve the linear model. Ignoring the autocorrelated errors and using the standard linear regression procedure for Eq. 10 means violating mathematical assumptions and produces wrong results. The values of c_i are not affected for a given model, but the error bounds and significances. These are not just accessory parts but determine the optimum choice of the model, and must therefore be calculated properly.

This may be done by fitting an autoregressive process Eq.(6) to the errors N of the least squares fit. Then, a Cochrane-Orcutt transformation (Cochrane and Orcutt 1949) is carried out to remove the autocorrelation of the errors. After this, the transformed model is fitted again using least squares. In this thesis the SPLUS-routine `autoreg` from Christian Keller (keller@stat.math.ethz.ch) is utilized. It estimates the c_i with its error bounds and also gives their significance. When the errors are not autocorrelated, the SPLUS-routine `lm` (MathSoft, 1993) is used instead of `autoreg`. This way some parameters less have to be estimated, as no AR-parameters a_i in Eq.(6) are to be determined.

For the optical profiling techniques, the ozone balance Eq.(8) and Eq.(10), respectively, include a measurement error due to aerosols in the aerosol term Θ_{aero} . This error is assumed to be in first approximation linear if heavily contaminated periods omitted. Therefore, c_{aero} is the sum of a real aerosol distribution to ozone change and of the measuring error due to aerosols.

Starting from the full model Eq.(10) with all explanatory variables, a *stepwise regression* is employed. With this procedure not significant terms are dropped one after each other, and the regression is repeated with the remaining terms. The SPLUS-routine `step` (MathSoft, 1993) was used. According to the C_p -statistics, a measure related to the Akaike's Information Criterion (AIC), not significant terms are dropped from Eq. (3.5). Stepwise regression is preferable to a fixed model, because unnecessary terms enlarge the error bounds of the estimates and falsify their significances.

Robust regression is useful when outliers are not easy to identify and should be suppressed in a large data set. It is not sensible to apply this to the ozone data used in this thesis because independent information (e.g., heavy aerosol distortion) allow a well-founded exclusion of specific data points and an inclusion when data quality is confirmed.

3.6 Cumulative differences for break detection

Break detection within long series is a common problem for climate research. It is not easy to resolve for intrinsic reasons, as explained below.

The basic problem is to test a measurement series, which is assumed to be stationary (i.e., mean, variance, kurtosis, skewness and all higher order statistical moments are constant). For this problem, reasonable mathematical tools exist to detect instrumental drifts and shifts. But if the series in question is not stationary, i.e., undergoes changes because of real, natural phenomena, the problem gets hard. With climatological series, the change is mostly gradually (e.g., a slowly rising mean). But also sudden changes (e.g., circulation changes) are conceivable. To detect instrument instabilities by purely statistical means, a domain must be found where non-stationarities can be attributed to the instrument with high probability. The judgment to find this domain is subjective in the sense it is decided by best knowledge, physical reasoning and experience and not from statistical considerations.

As the ozone (total and profile) is a highly variable quantity on scales

from days to centuries, it is not possible to do sensible break analysis with one of the present series alone. Large jumps can be found in specific situations, preferably accompanied by a documented technical change as happened successfully in Staehelin and Schmid (1991). But subtle changes can be detected only when natural ozone variability is suppressed.

This problem was tackled in Chapter 5 by working with the differences of two measurement systems. The difference is calculated for coincident days and for parts of the ozone profile where both measurement systems are supposed to be reliable. If jumps or drifts occur in the difference, this is attributed to an instrumental problem. To decide which of the two measurement systems is to be blamed, a third measurement system is applied as a referee. Still, the series of differences are very noisy, because of the limited resolution of the measurements. With a kind of integration process, i.e., cumulative summation of the series of differences, termed the *cumulative differences* in the following, some high frequency variation is suppressed:

$$cum(n) = \sum_{i=1}^n (oz_1(i) - oz_2(i)) \quad (11)$$

where oz_1 is the value from the first measurement system and oz_2 from the second.

Plotting $cum(n)$ against n gives a subjective tool for break detection as used in Chapter 5. An approximately zero difference ($oz_1 - oz_2$) would result in an approximately horizontal line. A constant difference shows up in a linear segment with constant slope. Changes in slope mark changes in the difference, the searched-for 'breaks'. In Figure 3.1 an example illustrates this idea.

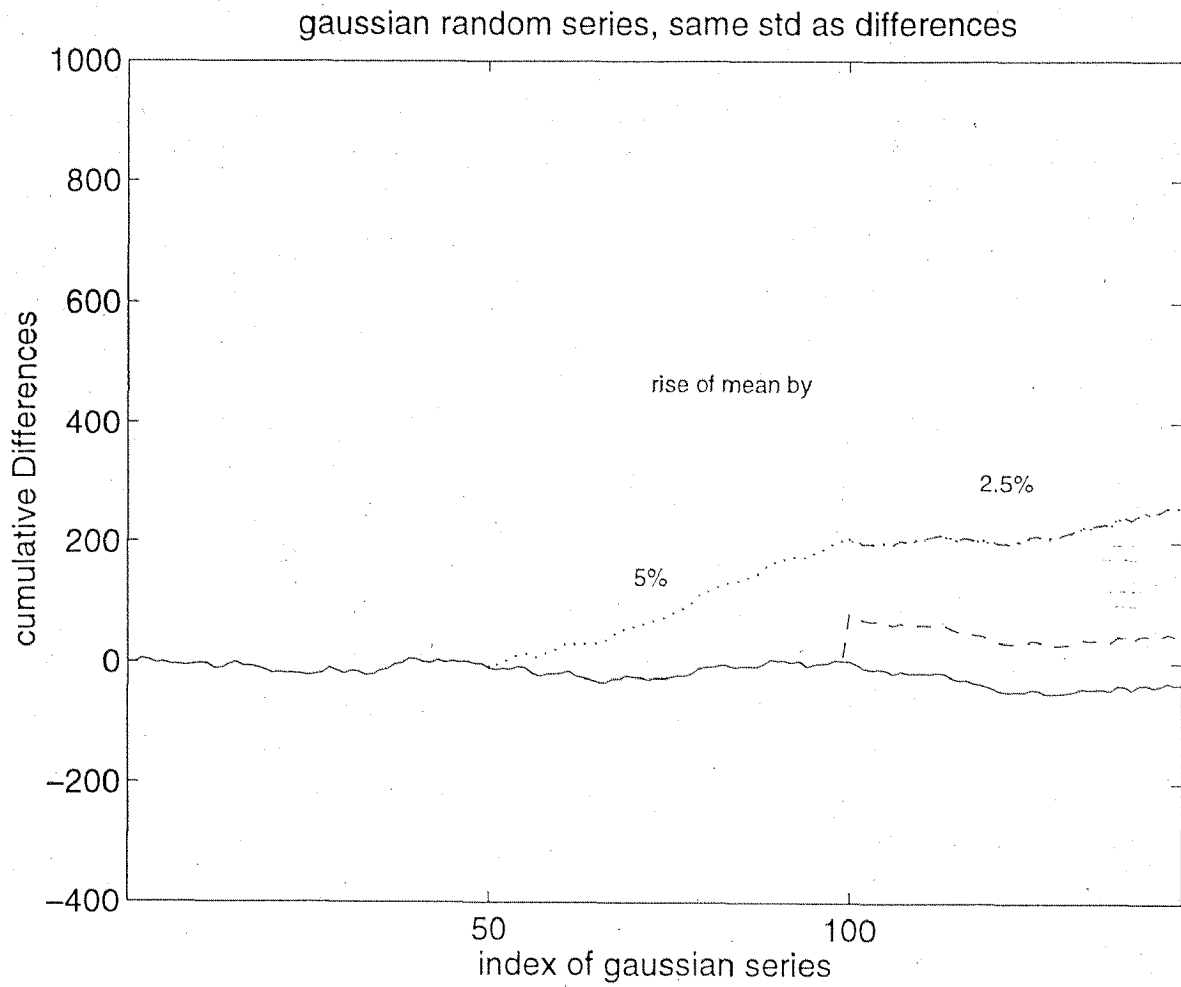


Figure 3.1: An example of synthetic cumulative differences $cum(n)$ plotted against n

Chapter 4

Data

The ozone data used in this thesis were obtained from several measurement systems: Ground-based total ozone and Umkehr measurements and balloon soundings carried out by the Swiss Meteorological Institute are used along with measurements from the American SBUV and SAGE satellite instruments. The ozone measurements and techniques are described with their individual advantages and drawbacks in Section 4.1. The proxies used for natural variability are referenced and depicted in 4.2. The data versions and sources of information for all measurements and proxies used are given. See Section D for Internet addresses.

4.1 Ozone measurement systems

Switzerland has the world's longest total ozone series, and two of the longest ozone profiling series, the balloon soundings of Payerne and the Umkehr measurements of Arosa. The series lengths are of high value for the statistical analysis, and invaluable because this way there is also information on the ozone before the anthropogenic influences occur. The series are especially valuable because of their careful maintenance and the reporting of the station history. Since the late 1970s a combined analysis with satellite data has become possible.

4.1.1 Total ozone

At Arosa the total ozone, i.e., the atmospheric column amount, has been determined with a remote sensing method based on sun photometry since 1926. Arosa is located at 46.78°N 9.68°E and 1820 m a.s.l. which is in the Swiss Alps. Today, the Observatory *Lichtklimatisches Observatorium* (LKO) measures total ozone with two Dobson instruments and three Brewer instruments (Hoegger et al. 1992, Weiss et al. 1999). Several Dobson instruments contributed to the total ozone series which was recently homogenized (Staehelin et al. 1998a), i.e., the instrumental effects were corrected and this high quality total ozone series (1926–1996) is now available from the World Ozone and Ultraviolet Radiation Data Centre (WOUDC) in Toronto, Canada. This homogenized total ozone series is used in this thesis up to 1996. The readings from instrument D101 have to be used to continue the series from 1997 to 1998. There are normally about 250–300 days per year with total ozone measurements (see (Staehelin et al. 1998a)).

The basic idea of the Dobson instrument (Dobson 1931) is to compare two wavelengths of solar light, one of which is strongly, the other one weakly absorbed by the atmospheric ozone. The two wavelengths are separated by a prism and slits, and an optical wedge is pushed in the way of the stronger beam until both beams give the same intensities at the photo-multiplier. The position of the wedge is used to derive intensity relation of the wavelength pair. A specially devised system averts temperature and internal stray light effects. To minimize the error caused by the turbidity of the atmosphere (scattering by aerosols), two wavelength pairs are used (pair A: 305.5 and 325.4 nm, pair D: 317.6 and 339.8 nm). The total ozone measurements with Dobson instruments require direct sunlight, at least for a few minutes.

The ozone amount is retrieved with the standard procedure recommended by the WMO (Komhyr 1980). The Dobson spectrophotometers are calibrated by the Langley-plot method (Staehelin et al. 1995) and also calibrated in side-by-side comparisons with the world standard instrument. Dobson comparisons took place at Arosa in 1986, 1990, 1995 and 1999. The accuracy of total ozone measurements is expected to be of the order of 3% (Staehelin et al. 1998a). The drift of the total ozone series of Arosa against the primary Dobson instrument was estimated to be less than 1% since 1978 (Staehelin et al. 1998a).

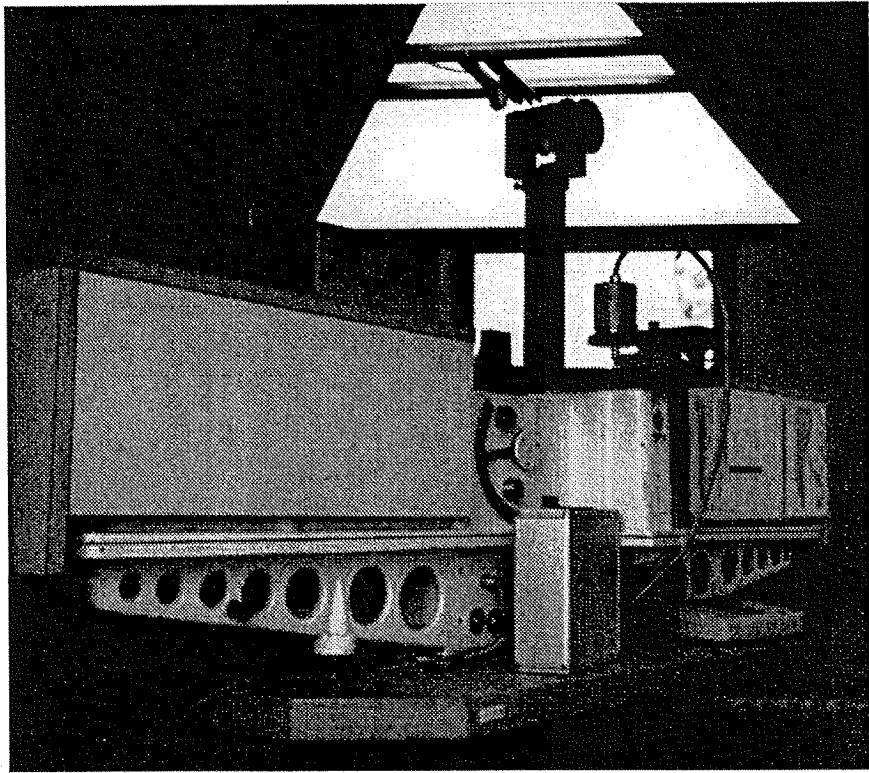


Figure 4.1: *The Dobson spectrophotometer D101 measures total ozone, whenever the meteorological conditions permit. Sun light enters the instrument through the black tube and is split into the spectrum. Intensity relations of two wavelengths pairs are measured, where at each case one wavelength is strongly, the other one weakly absorbed by ozone. From this, the total ozone amount can be calculated. The height of the depicted instrument is about 50 cm.*

The total ozone is subject of research on its own, as well as an important input parameter for the ground based ozone profiling techniques: balloon soundings and Umkehr measurements.

4.1.2 Umkehr

Measurements

Umkehr is an optical remote sensing method. The first Umkehr measurements at Arosa were performed by Götz et al. (1934). Operational measurements started in 1956. The same type of instruments as for total ozone (Fig. 4.1) are used for Umkehr measurements. But, in the case of Umkehr, zenith sky light is measured. There is only one wavelength pair used (pair C: 311.5 and 332.4 nm). The logarithmic intensity relation of these two wavelengths is measured during sunrise and sunset, for several hours. These are the raw Umkehr measurements, called *R-values*. They are converted with R/N tables to *N-values* which take into account the instrumental constants and include a scaling by factor 100 for historical reasons.

$$N(\mathbf{x}, \theta) = 100 \log_{10} \left(\frac{I_{\lambda_2}(\mathbf{x}, \theta)}{I_{\lambda_1}(\mathbf{x}, \theta)} \right) + C_0 \quad (1)$$

where I_{λ_1} and I_{λ_2} are the intensities of zenith sky light at the wavelengths 311.5 and 332.4 nm, which depend on the ozone profile \mathbf{x} and the solar zenith angle θ . C_0 contains the extraterrestrial difference of both intensities and also their instrumental sensitivity differences. The standard operational measurements from Arosa, i.e., with instrument D15 until 12/1987 and with instrument D51 thereafter, are sent as *N-values* to the World Ozone and Ultraviolet Radiation Data Centre (WOUDC), Toronto, Canada. Schill (1994) wrote a detailed description of Arosa Umkehr records.

In this thesis, the Umkehr trends has been calculated from the standard Umkehr *N-values*. The supplementary readings from the instruments D51 and D101 and D15 are used for stability checks.

The total ozone amount required for the Umkehr inversion is usually deduced by switching to direct sun observations (wavelengths pair C) of the same instrument. In the following, the total ozone is taken from

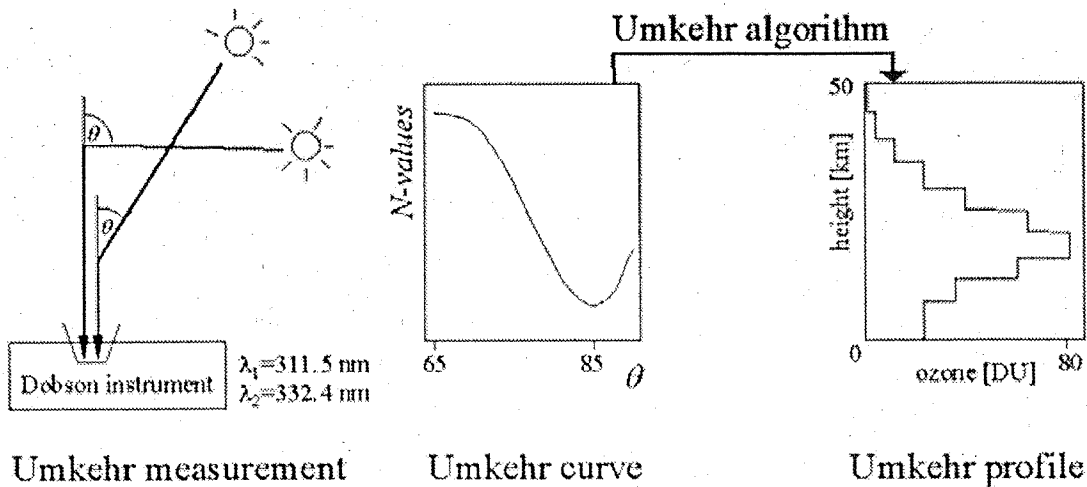


Figure 4.2: The Umkehr is a remote sensing technique. Zenith sky light is measured at two wavelengths and their intensity ratio is plotted against solar zenith angle, giving the Umkehr curves. From this an inversion algorithm calculates the Umkehr profiles.

the homogenized series of Arosa (Staehelin et al. 1998b). As total ozone has a strong influence on the result, this best estimate must be used.

Information on the ozone profile is deduced from the solar light passing through the atmosphere at different angles (Fig. 4.2). The change in solar zenith angle produces a scanning effect. With increasing solar zenith angle, the altitude at which most of the solar radiation is scattered downwards into the instrument moves up through the atmosphere. Absorption and scattering increase with the length of the light path in the atmosphere, but not in the same way for both wavelengths, which differ with respect to absorption by ozone. Therefore the intensity relation of both wavelengths is a function of solar zenith angle and the ozone profile. The *N-values*, plotted against the solar zenith angle, give U-shaped curves, named *Umkehr curves* after the German word for turnaround. They are used to deduce information about the ozone profile with a rather sophisticated Umkehr algorithm.

Retrieval algorithm

In this thesis the Umkehr FORTRAN code developed by Dr. Carl Mateer was used (mk2v4.NEWCUMK, revised version of Nov 20, 1994). The program is obtainable from the WOUDC. It is based on Rodgers optimal estimation (1976), and described in detail by Mateer and DeLuisi (1992). Below, a short summary is given. The input are the N -values at the solar zenith angles θ of 60° , 65° , 70° , 74° , 77° , 80° , 83° , 85° , 87.5° , 88° , 89° and 90° and total ozone which is provided by a separate measurement.

The procedure first removes the unwanted effects C_0 from Eq.1 by subtracting N_{60° :

$$\mathbf{y} = N_\theta - N_{60^\circ} \quad (2)$$

where \mathbf{y} is the vector $(y_{65^\circ}, y_{70^\circ}, \dots, y_{90^\circ})$. Then the ozone profile is searched which yields such measurement \mathbf{y} . For technical reasons, Mateer and DeLuisi 1992, retrieved the logarithm of ozone contents of the layers instead of the contents itself. Thus \mathbf{x} with $(x_{L1}, x_{L2}, \dots, x_{L3})$ is searched for, where x_{Li} denotes the logarithmic amount of ozone (in DU) within the layer i .

First, starting from an *a priori* profile which is determined by latitude, season and observed total ozone, the respective N -values are computed. For this, the radiance in the zenith direction is calculated. This procedure is called *forward modeling* and is carried out for a clear, dry, spherically homogeneous atmosphere, with molecular (Rayleigh) scattering and temperature-dependent ozone absorption (Mateer and DeLuisi 1992). The result is the \mathbf{y} which represents the primary scattered N -values belonging to this *a priori* profile. Further, in this forward modeling, multiple scattering and refraction corrections are applied. The forward model also provides the derivatives $\frac{\partial(N\text{-values})}{\partial \ln(\text{Layer ozone})}$, i.e., the weighting functions. They describe the change in observation for a change in the ozone profile.

Second, with these weighting functions, the difference of modeled and measured \mathbf{y} and the *a priori* knowledge of the ozone profile, a new estimate \mathbf{x} for the ozone profile is computed. The statistical solution for this was provided by Rodgers (1976) and worked out for the Umkehr inversion by Mateer and DeLuisi (1992).

Next, the first step, i.e., the forward modeling, is repeated with the new estimate \mathbf{x} , yielding a new modeled \mathbf{y} and its derivatives. With these results the second step can be repeated to obtain an even further improved estimate \mathbf{x} for the ozone profile. By repeating these two steps, the non-linear inversion problem is tackled iteratively. The iteration is terminated when a convergence criterion is met. After successful iteration, each layer i is attributed its ozone content as $\exp(x_{Li})$.

With the so-called *averaging kernels* one can evaluate how well the algorithm performs. The *averaging kernel matrix* is a transfer function which maps the difference between the true and *a priori* profile into the difference between the retrieved and *a priori* profile (Mateer and DeLuisi 1992). For instance, if the true profile departs from the *a priori* in Layer 4 and nowhere else, then the retrieved profile will be changed according to the averaging kernel marked with diamonds in Fig. 4.3. For an ideal measurement, the kernel should be one in the belonging layer and zero outside.

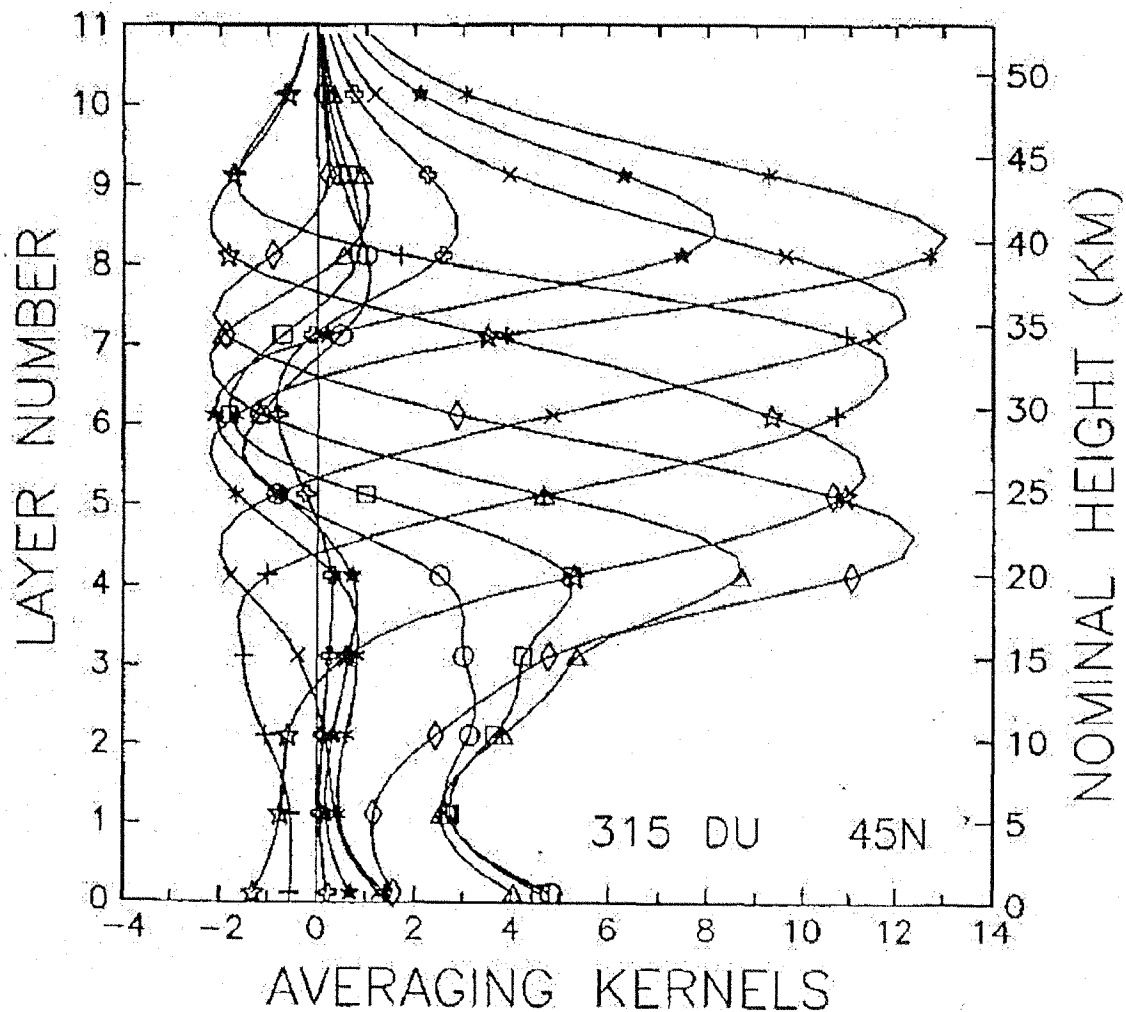


Figure 4.3: Umkehr kernels from Mateer et al. (1996): Averaging kernels for 1992 Umkehr algorithm for total ozone 315 DU at 45 N for layers 1 (circles), 2 (squares), 3 (triangles), 4 (diamonds), 5 (open stars), 6 (plus signs), 7 (crosses), 8 (asterisks), 9 (solid stars), and 10 (swiss crosses). Averaging kernel units are 100 $[\log(\text{retrieval}/\text{a priori})/\log(\text{true}/\text{a priori})]$.

Resulting profiles

The result is an ozone profile in 10 Umkehr layers from ground to 50 km height. Except for the lower-most layers, they are approximately 5 km thick and centered at a height which is about layer number times 5 km. The Umkehr ozone contents in the ten layers are not independent from each other and the information content varies considerably. This is because the *N-values* at the 12 solar zenith angles are strongly dependent on each other. As Mateer (1965) showed, there are only four pieces of independent information on the vertical distribution of ozone in the Umkehr, i.e., the Umkehr profile is heavily smoothed. One should consider only the sum of the lower-most layers (1 to 3) and uppermost layers (8 to 10) for interpretations, whereas the middle layers are reasonably defined by the Umkehr kernels (Mateer et al. 1996). The Umkehr profile is forced to match the total ozone. Especially sensitive to the total ozone are layers 1 to 3, as their *a priori* is a quadratic function of the total ozone (Mateer and DeLuisi 1992).

Problems

Umkehr measurements suffer from the following methodical problems: (1) they are disturbed by clouds, (2) have a clear weather bias and (3) are susceptible to aerosol disturbances. Further, there are the intrinsic problems of the inversion algorithm, as (4) restricted kernel resolution and (5) *a priori* dependence. In the following, these are discussed.

- (1) Zenith sky measurements require a clear (blue) zenith. Small, passing clouds can be detected and their effect is removed by the observer. Larger clouds are flagged and these data are not used for trend analysis or instrument comparisons in this thesis. Luxmeters are employed to evaluate the cloud situation and perform cloud corrections on the flagged data. This is done with tables which were obtained from observations with a quickly changing clouds and assuming clouds have low altitude.
- (2) Meteorological situations entailing clouds are under-sampled. Deep pressure systems and advection of polar air is normally connected with clouds and more ozone. To exclude this clear weather bias, for instrument comparisons only coincident days of

measurements are used.

- (3) Aerosols disturb the measurements noticeable, especially when the sun is low. Therefore the error shows up most distinctly in the upper layers. To account for the effect on the radiative transfer, one needs the optical depth, i.e., their *effect* on the radiation, and the vertical profile of the aerosols. A theoretical study of the effect of multiple scattering from haze on the Umkehr curve is provided by DeLuisi (1979). He concluded that this effect (which happens mainly in the troposphere) would decrease the ozone concentration at the level of ozone maximum, and increase concentrations below 15 km in order of a few percent.

Much larger is the effect of stratospheric aerosols, most of which are injected into the atmosphere by large volcanic eruptions. They fake a sharp drops in ozone values in the upper layers after volcanic eruption events. With theoretical work employing several aerosol profiles, the effect on the Umkehr measurements is found to be strongly dependent on the vertical aerosol distribution (DeLuisi 1979) but could be accounted for satisfactorily when the vertical distribution and optical depths are known. Absorption and scattering phase function are of secondary importance (DeLuisi 1979). The effect of stratospheric aerosols with 0.02 stratospheric optical depth is of order of -15% fictitious ozone change at 45 km and about -5% in the vicinity of the ozone maximum (DeLuisi 1979). Umkehr measurements were seriously disturbed in the Pinatubo period, where the maximum effect reached in 02/1992 with 0.17 AOD and reached 0.02 in 05/1994 and pre-Pinatubo values were reached not until 01/1996. Correction for Umkehr were worked out in DeLuisi et al. (1989) with 5 Umkehr stations, including Arosa, and aerosol measurements by 5 lidar instruments including Garmisch-Partenkirchen, Germany, which is in a distance of 135 km from Arosa. These corrections were applied for experimental purpose, and found to be not adequate for use in this thesis. Maaier and DeLuisi (1992) found a significant impact of aerosols in Layer 7+ (aerosols account for about half of the trend) whereas in the layers below the aerosol effect is small. Other authors exclude periods with heavy stratospheric aerosol loading (Miller et al. 1995, Reinsel et al. 1989) or employ empirical corrections (Reinsel et al. 1989, Newchurch et al. 1998). Newchurch et al. (1998)

suggested a correction of Arosa Umkehr data which is only half of the effect calculated by Mateer and DeLuisi (1992). Nevertheless, the correction appears to be still too large when applied to the Arosa data for strongly contaminated periods.

The ozone trend is influenced by the way the aerosol effect is accounted for. For Umkehr trend analysis in this thesis, the aerosol effect is assumed to be a linear regressor in each layer, described by stratospheric optical depth (AOD). A one year period after Pinatubo is removed for the layers 7+.

- (4) The Umkehr kernels (Fig. 4.3) show that the information is smeared across the whole profile. The kernels peak only adequately in layers 4 to 8, therefore, only these layers can be used for trend analysis (WMO 1988). The other ones must be regarded as a mixture of atmospheric information which does not necessarily stem from the heights assigned to the layers.
- (5) The inversion algorithm requires *a priori* information. The result is somewhat dependent on the *a priori*: In Layers 9 and 10, there is less information other than *a priori* information. The layers below have been tested (Mateer et al. 1996) according to their response to the ozone profile trends as observed by the Payerne soundings. They showed that trends in *a priori* influence the Umkehr trends in Layers 1 and 3 significantly. No change is found in Layers 2, 5, 6 and 7+. Layer 4 is not significantly influenced according to 2σ confidence, but would be with 1σ confidence. The conclusion is, that the trends in Layers 1, 2 and 3 can be tuned by *a priori* trends, and the trends in Layers 5 and above cannot. Mateer et al. (1996) also concluded that the observed differences of sounding and Umkehr in Layers 4 and above cannot be explained by *a priori* trends.

Further, Newchurch (*personal communication*) found that the change of gravity g with height must be accounted for. This results in an upward shift of ozone from layers 5 and below (less than 1%) into layers 6 and above. The maximum effect appears in layers 7 and 8 (about 2%). But the effect is small and does not affect trends.

The Umkehr measurements constitute the only available archive for ozone trends in the upper stratosphere before continuous satellite measurements (SBUV) started in the late 1970s. This justifies the effort

in spite of all the problems. From the 9910 Umkehr measurements in the years 1956–1996, 9560 matched the convergence criteria. There had been clear sky or small, passing clouds on 4510 days.

4.1.3 Brewer-Mast soundings

Since 1969 electro-chemical ozone soundings are launched three times a week at the Station Aérolologique Payerne (SMI), Switzerland (46.80 N 6.95 E, 490 a.s.l.), together with meteorological radio soundings. Until 1996, 3497 soundings were performed which reached 23 km height and 1873 soundings were launched on a day where an Umkehr profile was measured under fair weather conditions.

The balloons reach 20–30 km height and give a high resolution ozone profile. The sensor is a Brewer-Mast sonde (Brewer and Milford 1960). This is an electro-chemical cell with potassium iodide (KI) solution, in which the surrounding air is pumped. Ozone reacts with the KI and H₂O to KOH and I₂ and O₂. The I₂ absorbs electrons at the platinum cathode, to get as I⁻ into the solution. The result is a current which is proportional the ozone amount pumped in, and this signal is radioed to the ground station.

These raw values are converted to ozone profiles by division by the *flow rate*, i.e., how much air is pumped into the electrochemical cell. This is a complicated task, as the pump loses efficiency with decreasing ambient pressure. At Payerne, a *pump correction* is applied according to the Standard Operation Procedure of WMO (Claude et al. 1987), which is based on laboratory studies. The procedure for optimal pump correction is still under discussion (Steinbrecht et al. 1997). Further, the pump efficiency is suspected to be not stable with time because of manufacturer changes (De Backer et al. 1998).

The relative changes along the ozone profile are generally assumed to be more reliable than the absolute value of the measurements (SPARC 1998). Therefore, the integrated soundings are scaled to the total ozone. The ozone residing above balloon burst is assumed to have a constant mixing ratio when 17 hPa is reached. If the balloon reached 30 hPa, but not 17 hPa, the SBUV climatology is taken to estimate the residual ozone. Then the profile is scaled to match the total ozone measured at Arosa. If this is unavailable, satellite measurements are taken. If no total

ozone measurements are available, an estimate is derived from the days before and after, taking into account the meteorological situation. In this work, for scaling, the homogenized total ozone of Arosa (Staehelin et al. 1998a) is used.

The outstanding advantage of ozone soundings is, that they measure *in situ* and provide the best resolved ozone profiles. However, they do not reach the upper stratosphere. Further, they are single-use instruments and cannot be controlled for long-term stability. Several technical problems with the soundings have been reported which give rise to doubt the long-term stability (see Staehelin and Schmid (1991) and references therein). For instance, the launch time has changed, which influences ozone measurement results in the planetary boundary layer (above no effect is expected). A report of the station history of Payerne (Giroud 1996) documents changes of the radio soundings and the launch times and other technical changes. A statistical approach to homogenize the sounding series is applied in Neuhaus (1997), the influence of technical changes between 1984 and 1992 is investigated in Kegel (1995). Known problems are accounted for with the homogenized series of Payerne soundings (Stuebi et al. 1998b, Stuebi et al. 1998a) which is used in this thesis.

The scaling factor for scaling a sounding to match the total ozone is called the *correction factor* (CF). It is the ratio of integrated amount of ozone measured by the sonde plus residual ozone to total ozone from the Dobson spectrophotometer. Ideally, the CF should be unity. Large deviations $CF > 1.2$ indicate data quality problems with the sounding, although a $CF \approx 1$ is no guarantee for the reliability of the sounding (Logan 1994). The CF 's before 1984 have high values, which were annual means $CF = 1.2$ or larger. Since the mid-1980s, the CF 's are much smaller, which can be regarded as an improvement of the sounding data quality (Staehelin and Schmid 1991).

In summary, soundings are the best instruments for single profiles up to the middle stratosphere, but long-term stability of the series is hard to evaluate. The Station Aérologique Payerne provided quality checked soundings and a homogenized series 1969–1996 corrected for known problems.

4.1.4 SBUV

The Solar Backscatter Ultraviolet (SBUV) instrument (Frederick et al. 1986) on board the Nimbus 7 spacecraft provides ozone profile data (Hilsenrath et al. 1995) from 1978 to 1990. SBUV measures the ultraviolet sunlight scattered back by the earth's atmosphere between 255 and 340 nm. The shorter wavelengths do not penetrate deep into the atmosphere. Thus, a wavelength scan bears information on the ozone profile. The inversion algorithm for ozone profile retrieval is based on the same mathematical method as the Umkehr (Rodgers 1976). The resulting ozone profile is given in Umkehr layers, although the vertical resolution of the SBUV is approximately 8 km in the upper stratosphere and drops significantly in the lower stratosphere. The ozone profiles of SBUV suffer principally from the same type of problems as the Umkehr: The vertical resolution is even worse and the profiles are disturbed by large volcanic eruptions. The kernel function show that information is smeared in a similar way, but with the difference that kernel resolution is best in the uppermost layers (9–12) because SBUV is viewing from space. For details of SBUV inversion see Bhartia et al. (1996). In this thesis, the data version SBUV-035.N7S (obtained from Dr. R. McPeters, NASA) with distance weighted SBUV ozone over Arosa is used. SBUV/2 and successors are not studied. The 1915 overpasses over Arosa matched on 633 days Umkehr and balloon soundings of Payerne within 24 hours time span.

4.1.5 SAGE

The Stratospheric Aerosol and Gas Experiment (SAGE) II sensor was launched aboard the Earth Radiation Budget Satellite (ERBS) in October 1984. During each sunrise or sunset encountered by the orbiting spacecraft, attenuated solar radiation is measured through the Earth's limb. The exo-atmospheric solar irradiance is also measured in each of the seven channels (Poole 1999). Thus this solar occultation technique is self-calibrating. The transmittance measurements are inverted (Chu et al. 1989) using the 'onion-peeling' approach to yield 1-km vertical resolution profiles of ozone. The focus of the measurements is on the lower and middle stratosphere, but may extend well into the troposphere under non-volcanic and cloud-free conditions (Cunnold et al. 1989). The

method is also susceptible for aerosol interferences, but aerosol profiles are provided by SAGE. SAGE and Umkehr ozone profiles were compared in Newchurch et al. (1998) and similar trends were found.

SAGE version 5.96 (from Jim Craft, NASA) was used in this thesis, SAGE I was excluded from analysis because of homogeneity problems (personal communication, 1998, with Dr. Zawodny, NASA). The quality of SAGE was required to be less than 12% error (as suggested in SPARC (1998)). Coincidence with ground based measurements is defined to be within one day difference to a day with a ground-based measurement, and 0–20 degree longitude and 42–52 degree latitude overpass. These were found to be safe choices for the time and longitude window, but the latitude has an influence on the ozone profile which must be considered. There were only 160 days for which SAGE, Umkehr and balloon soundings are available within the coincidence criterion. Therefore, SAGE was compared with soundings (527 matches) and with Umkehr (350 matches) separately.

4.2 Used proxies for natural ozone variability: AOD, QBO, solar activity, NAO/AO and tropopause pressure

As explained in Section 2.1 there are many factors influencing ozone. These should be included in the ozone trend model of Section 3.4. However, the natural variability of ozone is not perfectly understood by now. Furthermore, only few proxies for natural variability were recorded at a time span long enough for ozone trend analysis. The aerosol loading, the solar activity and the Quasi-Biennial Oscillation are commonly used for ozone trend analysis and described below. In addition, in this thesis the North Atlantic Oscillation (NAO), Arctic Oscillation (AO) and tropopause pressure are investigated with respect to their contribution to the ozone balance (Eq.(10) in Section 3.5). The Internet data sources are listed in Appendix D.

Aerosols - AOD

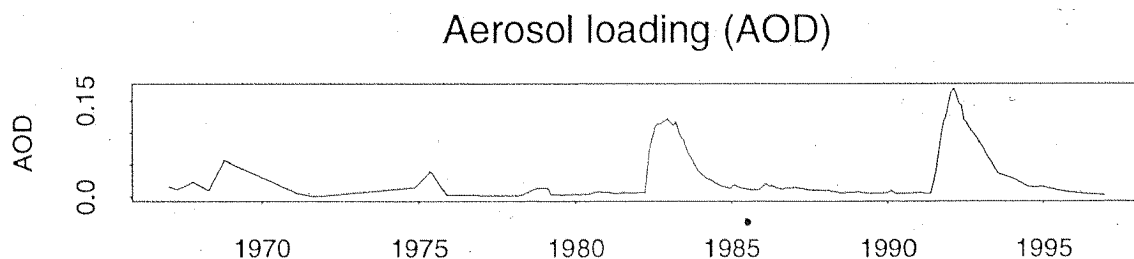


Figure 4.4: *Aerosol optical depth (AOD) is used as a measure for aerosol loading to describe ozone variability and measurement errors caused by aerosols*

The aerosols are important for several reasons: (1) They scatter and absorb radiation which causes errors for the optical profiling measurements. (2) Aerosols also influence dynamics by affecting the atmospheric energy balance. (3) On aerosol surfaces, heterogeneous reactions take place which lead to ozone destruction. Unfortunately, these effects cannot be distinguished by the means used in this thesis. As the disturbance of optical profiling measurements is the largest effect, the stratospheric aerosol optical depth is used as linear proxy for the radiative aerosol effect (1) and is assumed to include in first approximation also effects (2)

and (3).

Solar activity (F107)

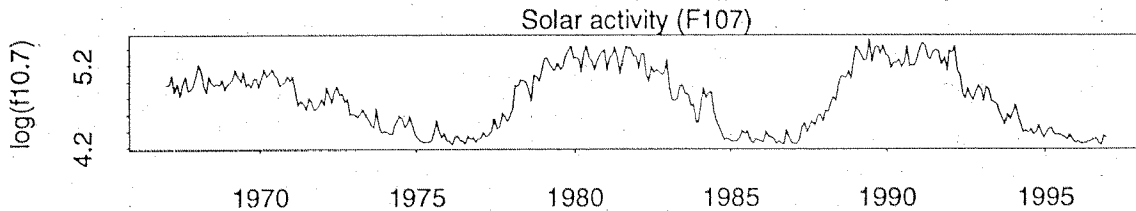


Figure 4.5: *Solar radio flux at 10.7 cm is used to determine possible solar activity influence on ozone.*

The solar UV-radiation is partly absorbed by the atmosphere. Thus, the solar flux at the wavelength of 10.7 cm is commonly used to describe solar activity. The logarithm of this was chosen following (Staehelin et al. 1998b) to describe as first approximation the possible influence of solar activity (see Section 2.2 for the physical background). Before 1948 no F107 solar flux measurements are available. A correlation between F107 and sun spot number was used to extend the series backward (Staehelin et al. 1998a). The data were obtained from NOAA.

Quasi-Biennial Oscillation QBO

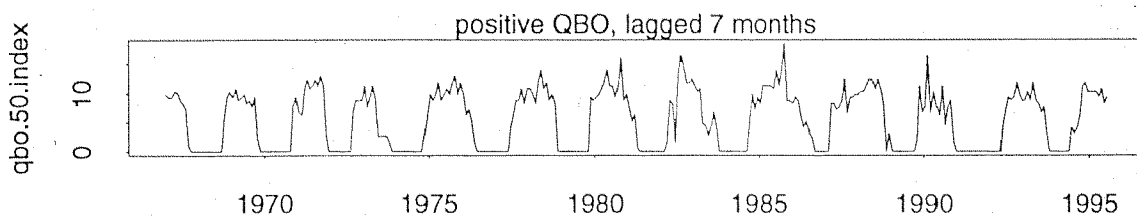


Figure 4.6: *The Quasi-Biennial Oscillation (QBO) influences the total ozone in mid-latitudes. Only the positive QBO phase is considered. A lag of 7 month is applied which was found statistically as the most significant.*

The QBO-index is based on the winds measured at 50 hPa over Singapore and was provided by the NOAA. For the ozone balance (Eq.(10 in Section 3.5) only the positive QBO phase is considered with a lag of 7 month. It is interesting to note that the full qbo index shows to

be not significant, as well as a biennial proxy. Using only the negative phase of the QBO results in a significant, weak signal in February only, whereas the positive phase QBO is significant during several months at certain heights. The lag of 7 month is found statistically as the most significant. The lag does not necessarily mean a physical time lag. One possible interpretation is that the downward propagating QBO signal should be matched in an other height than 50 hPa. Choosing the positive QBO only is most appropriate from the statistical point of view but also favorable for describing a possible solar influence Labitzke and van Loon (1988) as explained in section 2.2.

NAO/AO and tropopause pressure

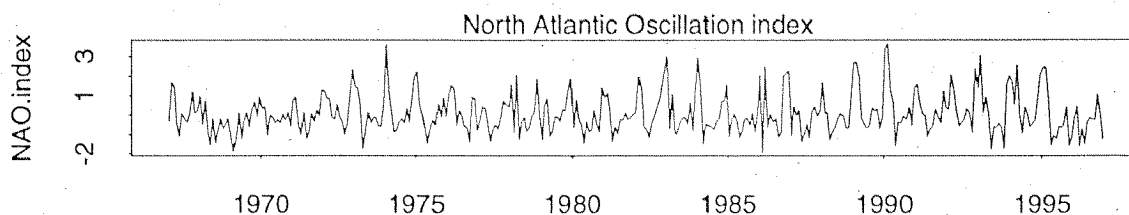


Figure 4.7: *The North Atlantic Oscillation is shown in Chapter 6 to influence mid-latitudal ozone strongly in winter–spring. The NAO index is measured according to (Hurrell 1995) as a pressure difference between the Azores and Iceland.*

The North Atlantic Oscillation (NAO) index, the Arctic Oscillation (AO) index and tropopause pressure shown below are based on the NCEP/NCAR reanalysis. The NAO index and tropopause pressure were supplied by Christof Appenzeller (apc@sma.ch) and the AO index by Dave Thompson (davet@atmos.washington.edu). Units for AO and NAO are arbitrary and for each application the used period is normalized.

The NAO index is measured as the sea level pressure difference between Ponta Delgada (Azores) and Stykkisholmur (Iceland) (Hurrell 1995). The NAO-index is shown for the whole year. Note that the usual interpretation of the index as the NAO phenomenon is valid only in winter–spring.

The AO index is the leading empirical orthogonal function (EOF) of the wintertime sea level pressure (SLP) pole-ward of 20N (Thompson and Wallace 1998).

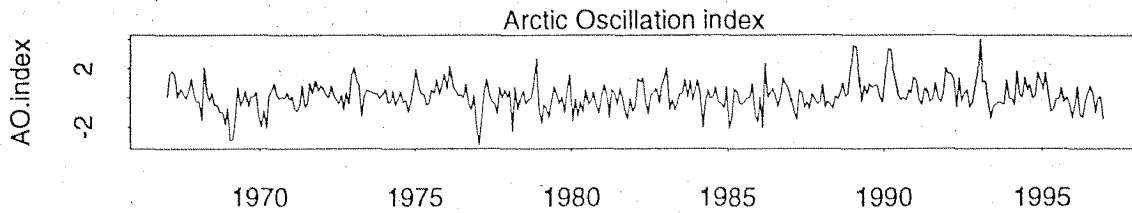


Figure 4.8: *The Arctic Oscillation (AO) index is defined via the sea level pressure anomaly field pole-ward of 20N.*

The tropopause is defined as the level of $PV=2$ (see Section 2.2). The pressure data of this level are taken from NCEP-reanalysis data as tropopause pressure over Switzerland and over Iceland.

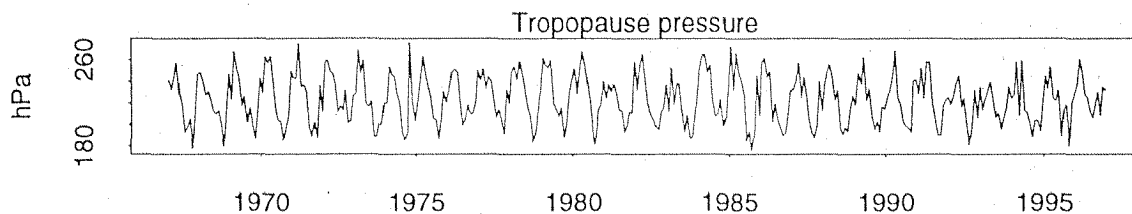


Figure 4.9: *The tropopause pressure series over Arosa (Switzerland) is calculated from NCEP-reanalysis.*

Seite Leer /
Blank leaf

Chapter 5

Results of Homogeneity checks

The data quality of the measurements used for trend analysis is assessed. The ozone balloon soundings of Payerne and the Umkehr measurements of Arosa both include profile information extending to an altitude of approximately 30 km. Both measurements are compared in Section 5.1 covering the entire period since 1969. The aim of this chapter is to point out that Payerne soundings and Arosa Umkehr measurements yield significantly different trends throughout the ozone profile. The supplementary instruments of Arosa are used for homogeneity tests in Section 5.2 and show that Umkehr measurements from different instruments agree in their contradiction to the soundings. In Section 5.3 the Swiss ozone profile measurements are compared with two instruments from satellite available from 1979.

5.1 Difference of Payerne soundings and Arosa Umkehr results

Although the physical principles of the in-situ measuring ozone sondes and the remote sensing Umkehr method are different, similar estimates

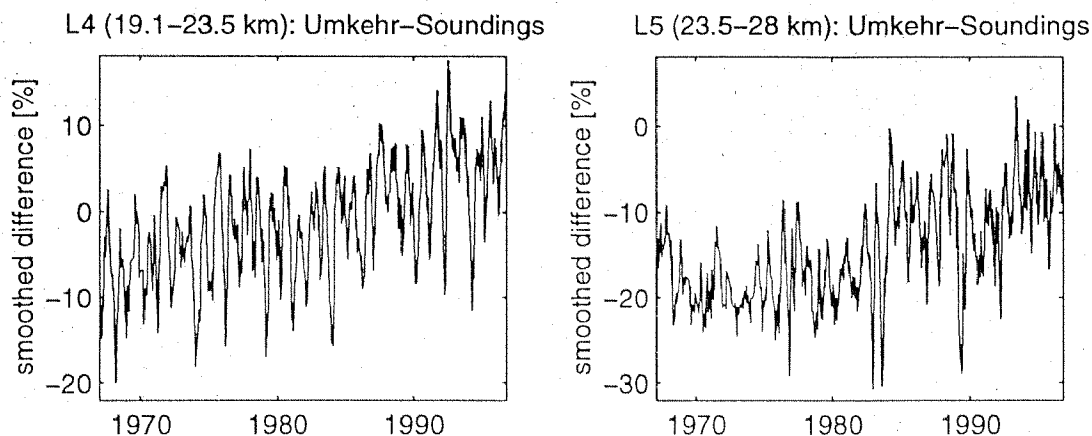


Figure 5.1: *The difference between the ozone of Arosa Umkehr and integrated Payerne soundings are shown for a) Layer 4 (19.1–23.5 km) and b) Layer 5 (23.5–28.0 km). Only coincident days of measurement were considered, and a moderate smoothing is applied. The seasonal cycle can be attributed to a seasonal error of the Umkehr, suffering from the rougher resolution. Large long term changes are easily seen and question the long term stability of the sounding series.*

of long-term trends are expected, at least in the altitude 20–30 km. Umkehr measurements yield a rough estimate of the ozone profile up to 50 km height (see Fig. 2.1 for an average profile and precise heights of the layers). The vertical resolution in the first three Umkehr layers, i.e., below 19 km, is bad, but the sum of these three layers is believed to be reliable. The Payerne soundings were integrated respectively to the Umkehr layers and converted to Dobson Units (DU). Because the soundings have information on height as well as pressure and temperature, the conversion is sensible in this direction. The formula is given in Appendix B.

5.1.1 Clear contradiction in measurements

Both methods claim to yield correct results in the sum of ozone in the column below 19.1 km, in the height of ozone maximum L4 (19.1–23.5 km) and in layer L5 (23.5–28 km). Note that both profiling methods are scaled to the total ozone measurements of Arosa. Umkehr and Balloon soundings can be compared in L4 (19.1–23.5 km) and L5 (23.5–28 km). In fact, there are substantial discrepancies in the ozone measurements (see Fig. 5.1). Umkehr and soundings differ by an amount of up to

20%. Even worse, there is a systematic change over decades. In L4, the difference rose from -10% to +10%, in L5 it was constant with a magnitude of -20% to the eighties, and rising thereafter to -5%.

5.1.2 Different trends of soundings and Umkehr

The change of the difference between soundings and Umkehr with time is reflected in the trends. Trends were calculated with multiple linear regression with autoregressive errors as explained in Section 3.5. Results are depicted in Fig. 5.2. The Umkehr instruments exhibit the largest ozone trends in the upper stratosphere (30–40 km), and less trends below. At the altitudes of the ozone maximum no trend is present in the Umkehr results. There is even a slight, but not significant positive trend in L5 which was found to be significant using a more sophisticated statistical model (Newchurch et al. 1999). The soundings, on the other hand, show a clear decrease of ozone in L4 (-4.3 ± 0.8) and L5 (-3.1 ± 0.5). Above L5, the sounding coverage is limited.

The Umkehr trend estimate in the lower part of the profile is the trend of the bulk ozone in the column below 19.1 km, Umkehr cannot provide better resolution. The soundings reveal a strong increase in troposphere, and a strong decrease in lower stratosphere. Nevertheless, the bulk estimates should be comparable. There is a striking difference between the Umkehr trend (-2.7 ± 1) DU per decade and sounding trend ($+2.9 \pm 1.5$) DU per decade for the sum of the Umkehr layers 1 to 3.

As both methods claim reliability, especially in the region of 20–30 km, this is a serious contradiction. To exclude a possible fair-weather bias of the Umkehr, only coincident days of measurement were used for the above estimated trends.

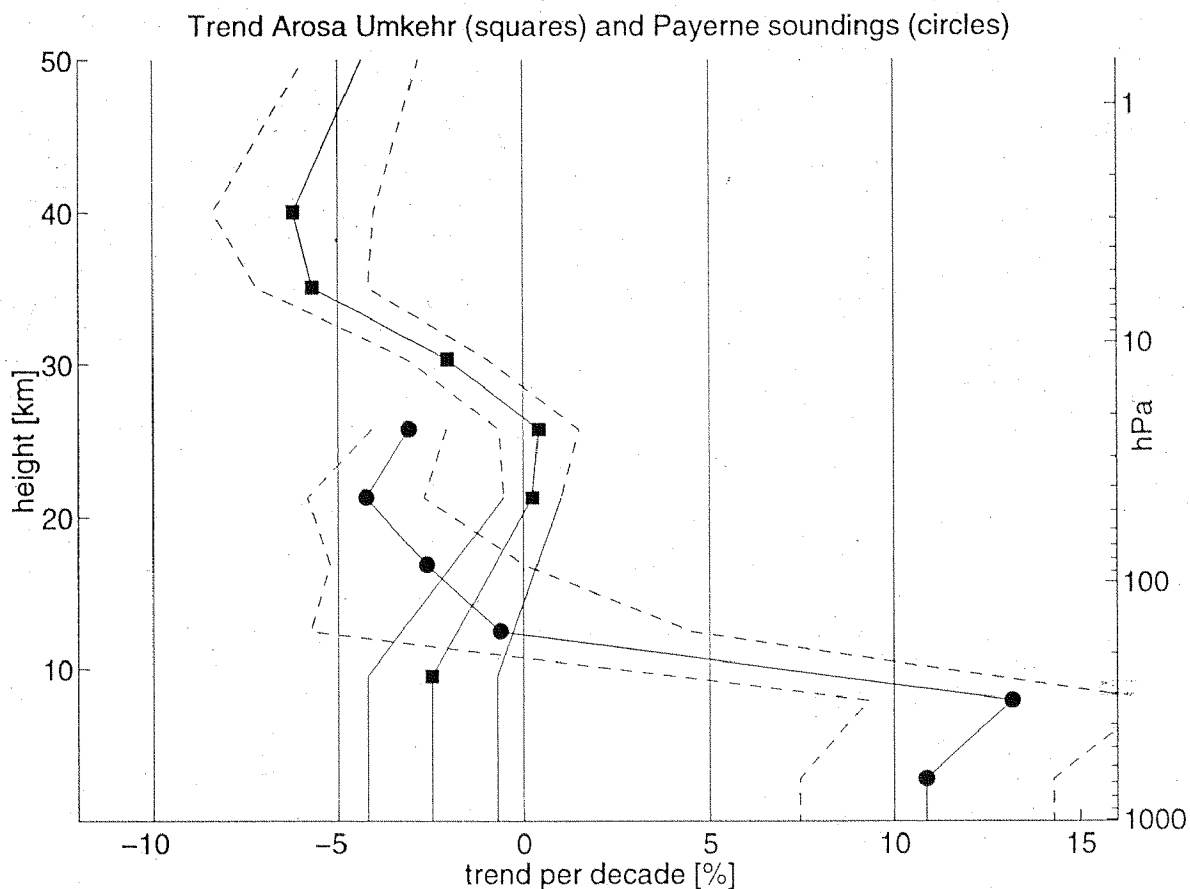


Figure 5.2: Trend analysis including autoregressive errors show a clear statistically significant contradiction of Umkehr trends (squares) and sounding trends (circles) in the middle stratosphere, at 20–25 km (i.e., Umkehr Layers 4 and 5). Below Layer 4, the Umkehr can give only information for the bulk of ozone (0–19.1 km). The trends are depicted in the middle of their layer. The dashed lines give the 2- σ confidence interval for the trends. Heavily aerosol contaminated periods are omitted, slight aerosol loading ($AOD < 0.02$) was modeled as a linear error contribution for the Umkehr trend analysis.

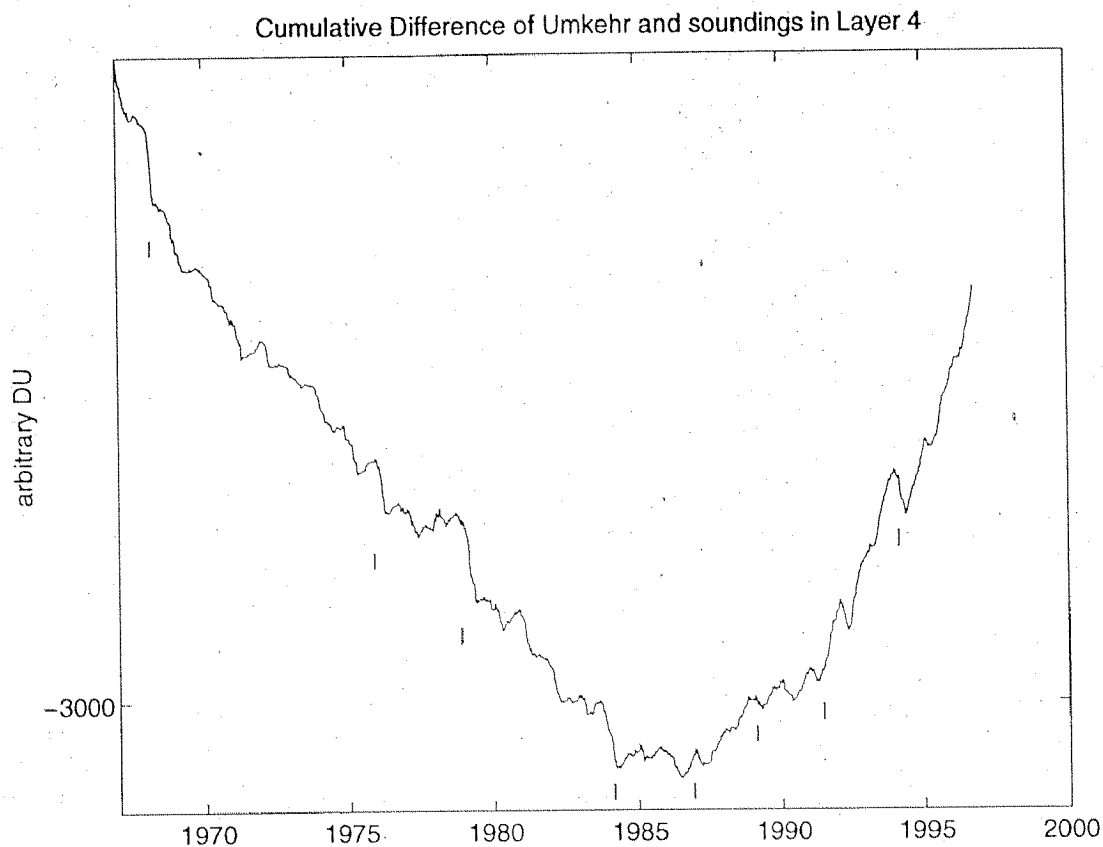


Figure 5.3: Break detection with cumulative differences. Dashes indicate breaks, which are subjectively chosen as explained in Section 3.6. Breaks in the difference Umkehr-Payerne soundings in Layer 4 seem to be: 1969, 1975, 1978, 1984, 1986–87, 1988, 1991, 1993. For Umkehr the standard series of Arosa (D15 and D51) is used.

5.1.3 Searching for the culprit

A semi-objective break detection employing cumulative differences (as explained in Section 3.6) was used to identify the times where the relative behavior of Umkehr versus soundings changes. Breaks are the points which separate linear parts in Fig. 5.3. The most prominent feature, the change of sign in the slopes in the middle of the eighties means that the difference (*Umkehr* – *soundings*) changed its sign. The exact time of break is quite subjective, however, one can see intervals which are linear and that many of them must be separated. One sensible suggestion of breaks is: 1969, 1975, 1978, 1984, 1986–87, 1988, 1991, 1993. Of course, they must be checked in detail and verified with other studies.

In the next Section (5.2) the Umkehr instrument stability is tested. It is not possible to do the same with the Payerne soundings because there is no redundancy as with the Umkehr. It was not attempted to compare the ozone sonde records of the nearby station Hohenpeissenberg with the Payerne record to ensure independence of both sounding records. Section 5.3 will employ satellite measurements to shed more light on the problem.

5.2 Homogeneity checks with the Umkehr series of Arosa

In this section the stability of the Umkehr series is investigated. This is of general interest for all who use this series in their analysis, and therefore this section will also be published in the Internet, in April 2000 with co-authors who gave advice (Weiss et al. 2000).

5.2.1 Umkehr records and stability tests at Arosa

Different Dobson spectrophotometers were involved in the Umkehr series at Arosa. The series can be divided in two main periods, the period when all readings were taken manually (1956–1987) and the automated period since 1/1988. In the ‘manual’ period, the standard instrument was D15. Another instrument, D101 was also run operationally since 1968 for control purposes. In the automated period, the completely automated Dobson instrument D51 is the standard instrument, and for control purposes about 1 to 3 times per month manual readings were taken with the instrument D101. As third instrument, D15 served for occasional manual readings from 1/1988–8/1992. After 8/1992, the D15 was out of action and D62 served as third instrument for occasional manual readings. In Fig. 5.4 the different periods and instruments are sketched.

Only instruments D101 and D62 were regularly tested at side by side comparisons with world Dobson standard instruments which took place at Arosa in 1986, 1990, 1995 and 1999. This comparison of direct sun measurements are used to check and correct the instrumental constants.

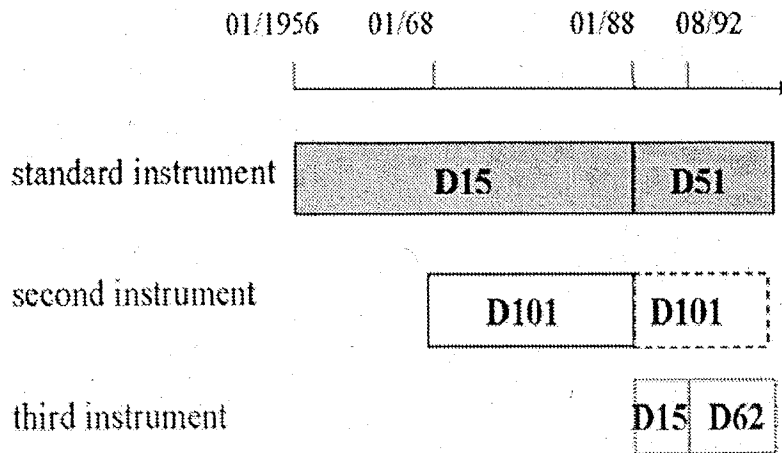


Figure 5.4: *Periods of Umkehr observations at Arosa with instruments D15, D101, solid frames denote operational measurements, dashed frames occasional readings. The standard operational measurements (shaded) are sent to WOUDC.*

The wedge calibrations of the instruments D15, D101 and D62 are listed in Table 3 of Staehelin et al. (1998b). However, instrument D51 was not included in such inter-comparisons because of technical difficulties. The last wedge calibration of D51 was performed 1986.

Mercury lamp tests and standard lamp tests were regularly performed at Arosa. Since 1989, about 15 times per year lamp tests with three lamps are performed with all instruments, allowing a well-founded correction for drifts of the instruments. The standard lamp tests are designed for the quality control of total ozone measurements, and give an additive constant to the instrument readings. These tests indicate drifts in the instrumental constants of all instruments, with D101 showing the largest drift. For instrument D101, the lamp correction dN changed from -6 (1989) to -42 (1999). D51 has a drift which is opposite in sign, i.e., growing lamp correction dN from 0 (1989) to 17 (1999). D15 had inaccuracies of $dN = -6$ between 12/89 and 8/92, D62 has a maximum lamp correction of $dN = -4.2$ level from 8/92 to 6/99.

Apart from allowing a qualitative (and subjective) judgment on the instrument stabilities, lamp tests are not applicable to the Umkehr measurements. From the definition of the test, adding dN to each measurement is the most reasonable correction. Adding a constant to an Umkehr

curve does not change the retrieved profile. Therefore, one cannot make use of the lamp tests to correct for possible Umkehr measurement drifts. A wedge calibration could shed more light on this potential problem.

5.2.2 Confirming the results of the standard series

From 1968–1988, the standard instrument D15 can be compared to instrument D101. These two Umkehr instruments differ much less from each other than from the sounding series, as shown in Table 5.1. The correlations of the differences are given, after the mean yearly difference is removed, which otherwise would falsify implications. It is proven by Table 5.1, that the difference from the two Umkehr instruments to the Payerne soundings are highly correlated. The implication is that either the whole Umkehr method is subject to drifting or the sounding series of Payerne is not stable.

The similar behavior of D15 and D101 is mirrored in nearly identical figures resulting when Figure 5.1 and 5.3 are repeated with substituting D15 by D101 from 1968–1988.

Share on the contradiction attributed to the instruments			
	D15	D101	soundings
	$\text{cor}(a, b)$	$\text{cor}(a, c)$	$\text{cor}(b, c)$
L1	0.01	-0.23	0.97
L2	-0.03	-0.29	0.97
L3	0.01	-0.25	0.97
L4	0.18	-0.09	0.96
L5	0.16	-0.34	0.87

Table 5.1: Correlation between the series of differences which are $a=D15-D101$, $b=D15\text{-soundings}$, $c=D101\text{-soundings}$. Data used were from 1969 to end of 1987, because D15 was replaced by D51 after.

5.2.3 N-values of the instruments

It was recently discussed in the context of the REVUE project that the N-values of the zenith sky observations show a significant trend since

the middle of the 1980s (see Figure 5.5). These N-values are obtained from the original R readings after conversion with the R/N table which includes the instrumental constants. It was discussed whether the decreasing N-values must be attributed to instrument D51 which was used as standard instrument 1988.

In Fig. 5.5 the series of N-values for the standard instruments (D15 to 1987, D51 from 1988) are reported while in Fig. 5.6, the equivalent data for the instrument D101 is given for comparison. The series of the much sparser data of D101 after 1988 looks rather different than the standard series. This impression changes, when only coincident data are plotted (Fig. 5.7).

As the fine structures are well reproduced on both systems, it is obvious that the behavior of the N-values is not an artifact of D51. However, the relative difference (Fig. 5.8) reveals also instrumental problems: D51 seems to have had readings 5% smaller than D101 in 1988, and up to 25% smaller than D101 in 1996.

It is difficult to emphasize whether it is a continuous drift (like the readings at solar zenith angle of 60 degree suggest) or if the changes are step-like with plateaux over sub-periods (e.g., readings at Z-angles of 85 degrees suggest 1988.5, 1992.5, 1994, 1995). The important question is, how the ozone profiles retrieved from those N-values are affected. This is addressed in the next section.

5.2.4 Implications from the instrumental differences on the retrieved ozone trends

The propagation of the instrumental differences into the calculated profiles is not trivial since the Umkehr algorithm is nonlinear. Using a heuristic approach, the ozone content per layer is calculated separately for each instrument and the results are compared: The simultaneous measurements of D101 and D51 (since 1988) are used. The results of this comparison provide evidence (see Fig. 5.9), that the retrieved profiles of D51 are similar to those of the other instrument. Fig. 5.10 shows how the instrumental differences as seen in Fig. 5.8 influence the derived ozone trends. Generally, the scatter is too large to quantify small instrumental drifts. It is interesting to note that the relative differences

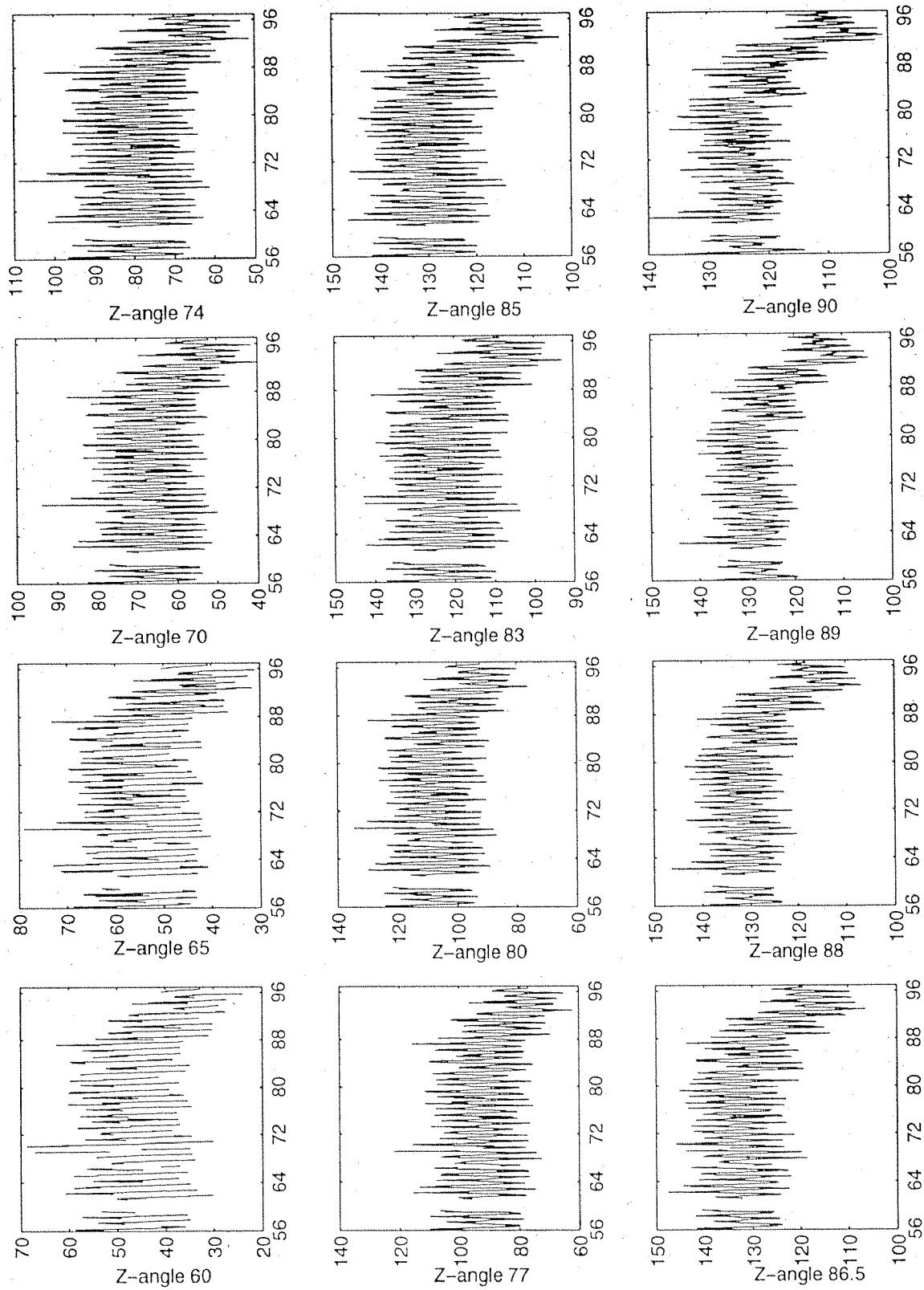


Figure 5.5: Monthly mean N -values from operational Umkehr instruments. These zenith sky measurements are used to derive the standard Umkehr profiles for Arosa. The series is combined from instrument D15 before 1988 and instrument D51 thereafter.

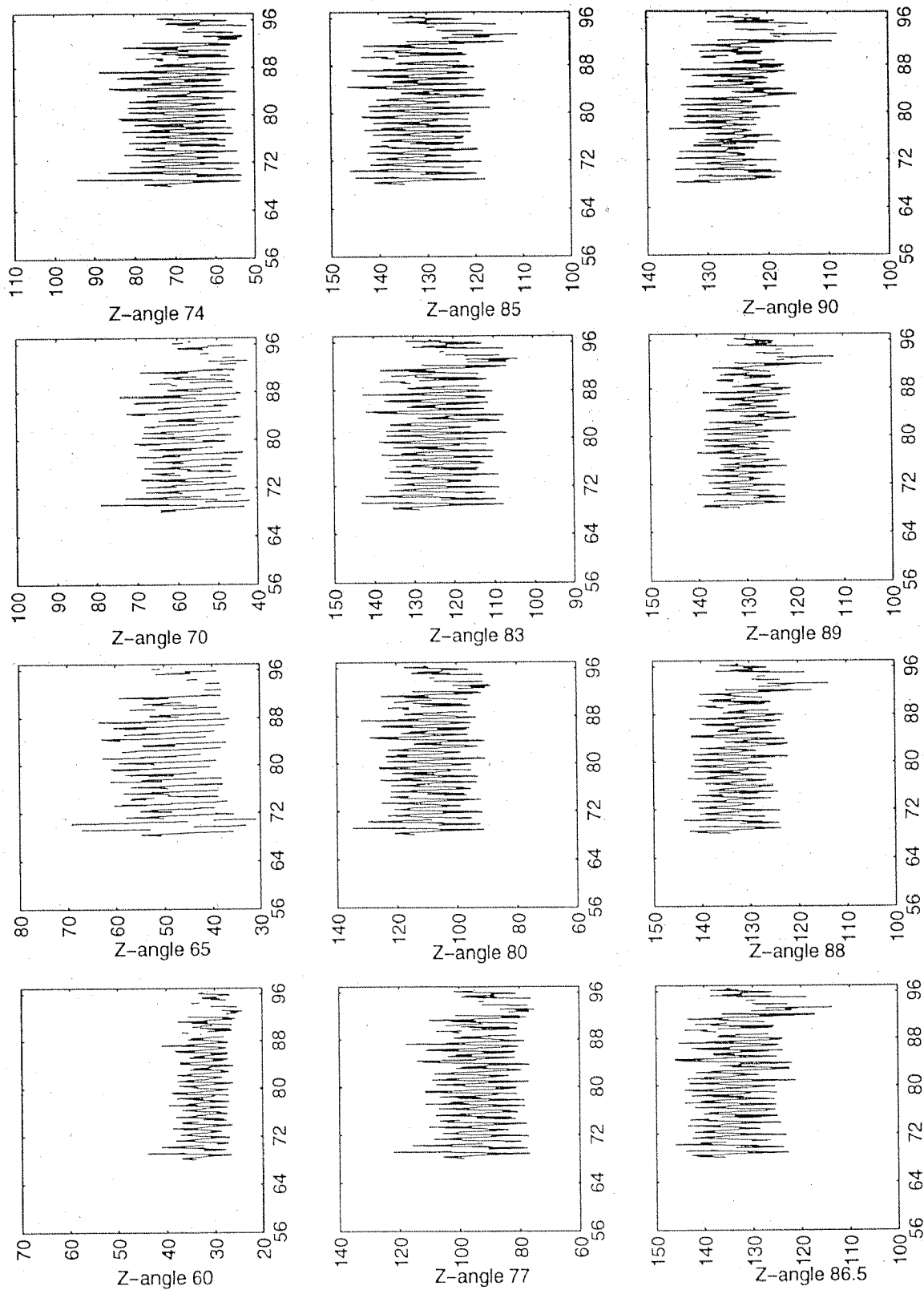


Figure 5.6: Time series of instrument D101 N-values (monthly means). These zenith sky measurements are used to derive supplementary Umkehr profiles. After 1986, only occasional measurements were performed.

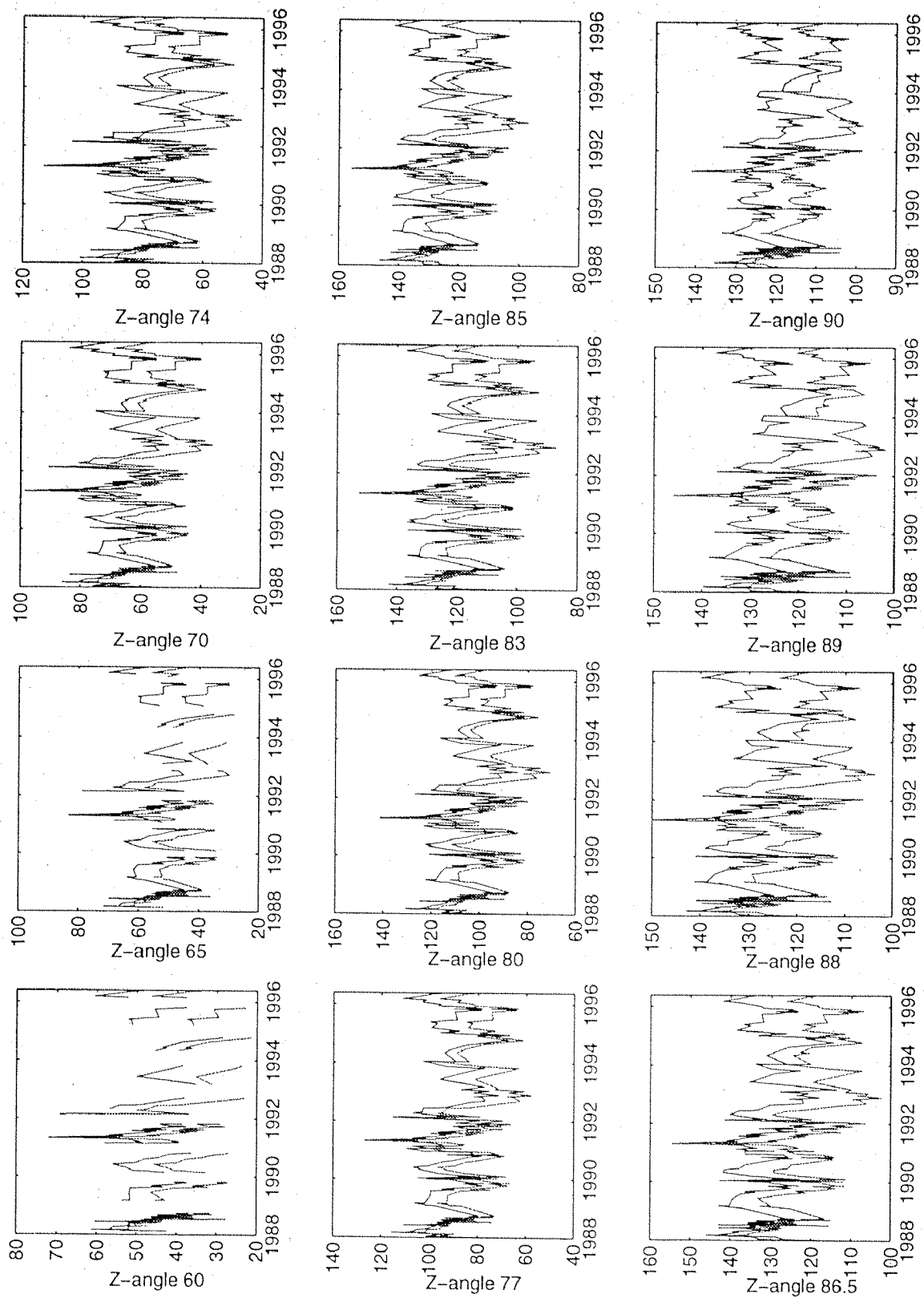


Figure 5.7: Monthly means of D51 (red) and D101 (blue) N-values at coincident days of measurement.

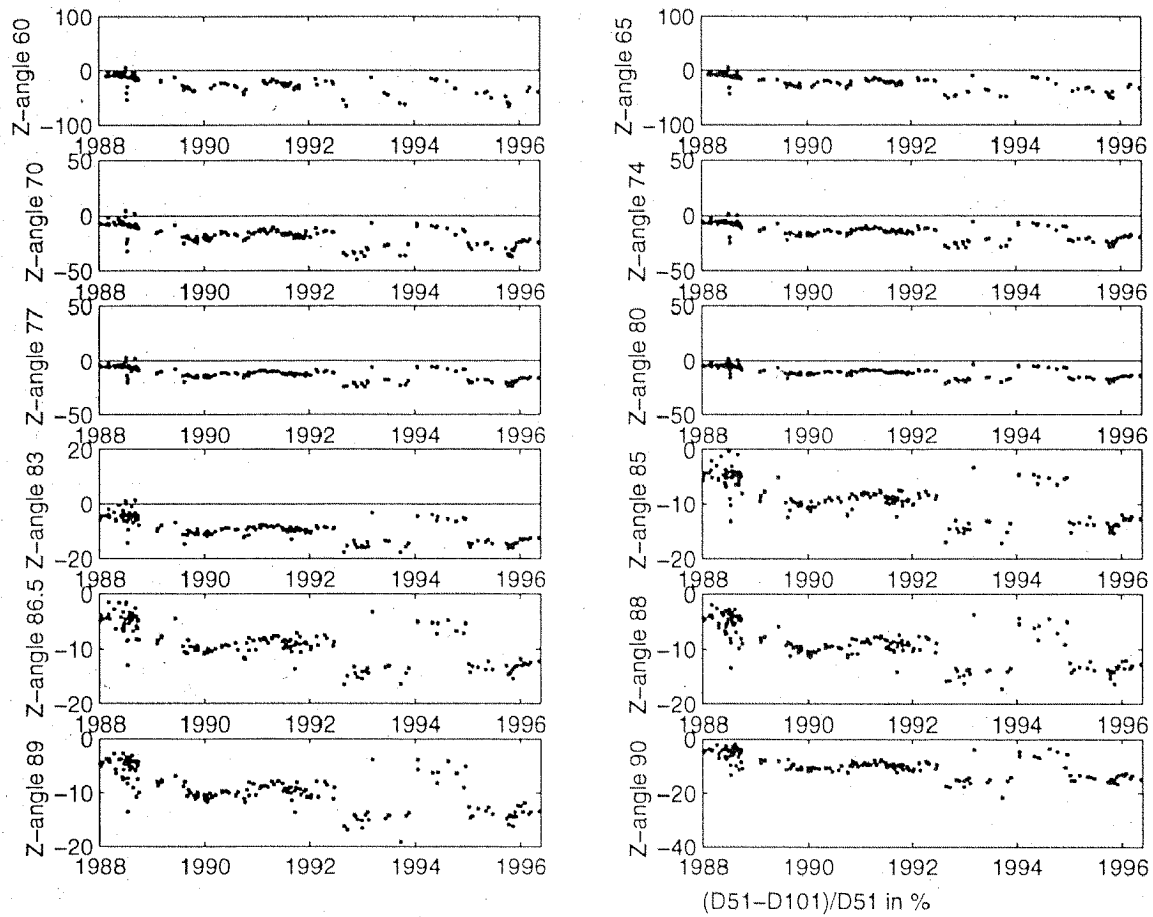


Figure 5.8: *Relative difference of N-values as depicted in Fig. 5.7) $(D51-D101)/D51$ in percent.*

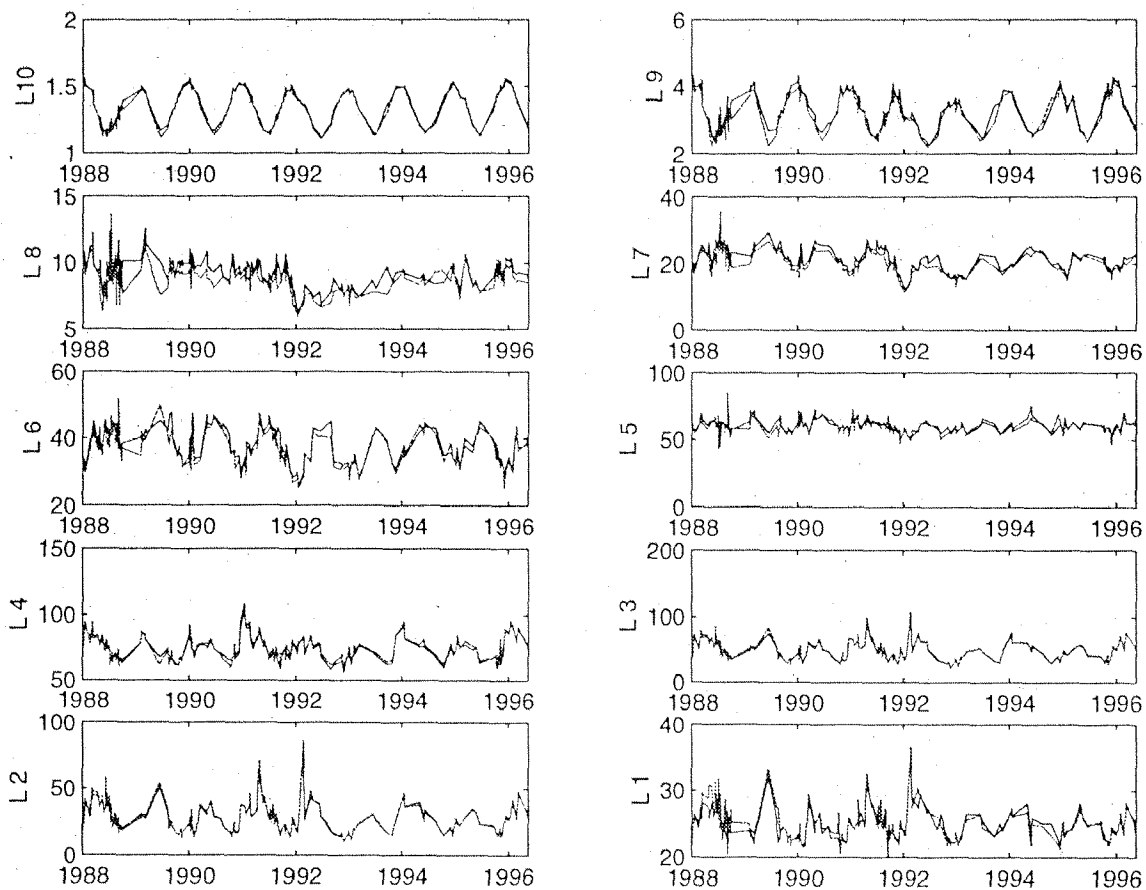


Figure 5.9: Ozone content of the two instrumental series D51 (red) and D101 (blue) of Arosa after 1988. The Umkehr layers are defined as L1:0-10.3 km, L2:10.3-14.7 km, L3:14.7-19.1 km, L4:19.1-23.5 km, L5:23.5-28 km, L6:28-32 km, L7:32-37.5 km, L8:37.5-42.6 km, L9:42.6-47.9km, L10:above 47.9 km.

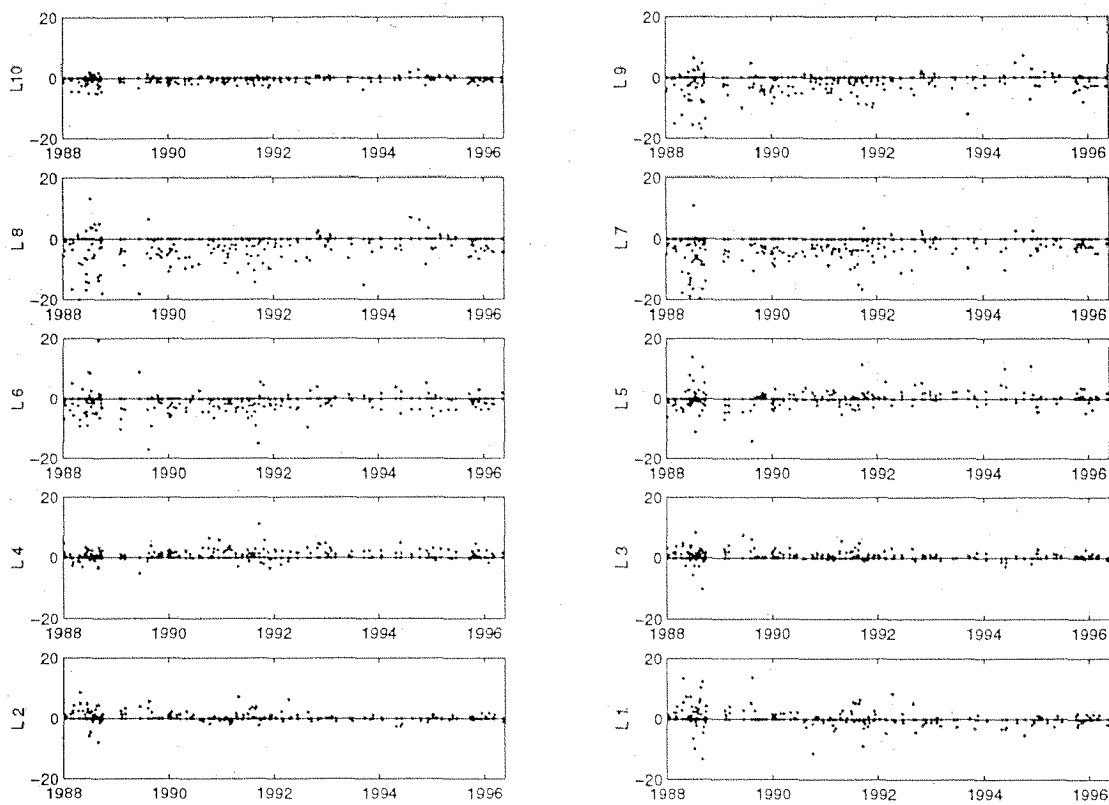


Figure 5.10: *Relative differences of the layer ozone content of the two instrumental series $(D51-D101)/D51$ in %.*

in ozone content are much smaller than the differences in the raw data. There is also some difference between the individual layers. The smoothness of Layer 10 is caused by the strong *a priori* dependence there. Layer 8 has the largest scatter, this is a region where the ozone retrieval is falsified by lower stratospheric aerosols. Rather surprising is the considerable scatter (note the scale) in Layer 5 which should give good Umkehr results.

The period 1988–1989 stands out because of particularly large scatter. In this period instrument D101 was partially automated. As instrumental changes and problems are reported for D101, it is assumed to be responsible for the differences in this period. Therefore, the standard instrument is assumed to be more reliable in 1988–1989. This unstable period is excluded for statistical tests on whether the instruments drift.

For the other years there cannot be conclude which instrument is more stable. With the statistical linear regression model the significance of a drift is tested. The so-called *p-value* gives the probability that the drift would occur by chance. A *p-value* p is considered clearly significant if $p < 0.01$, in which case a drift is statistically confirmed.

There is a suggestion of a linear drift of the instrument's relative difference (Fig. 5.10) for the layers 7 and above ($0.05 > p > 0.01$), it is less significant for layer 2 ($p = 0.09$) and not significant ($p > 0.1$) in all other layers. Still, this includes a possibility of drifts in the order of some percent per decade. As one can deduce from Fig. 5.10, D101 seemed to see more ozone in layers 7 and above in the late eighties and early nineties, and developed to nearly no difference at present times. Therefore, the ozone series derived from D101 declines quicker than the one derived from the standard instrument D51. That means, the D101 ozone trends in the upper stratosphere are larger than the ones derived from Arosa standard Umkehr.

5.2.5 Conclusions for the Umkehr series

Simultaneous Umkehr data of the operational instrument and occasional observations of another instrument were compared. The same main features, i.e. the dropping of N-values, provide hints that at least part of the observed changes are caused by atmospheric changes. The differences of the series also shows possible instrumental drifts. The measurements of

instrument D101 drifted in the period since 1988 requiring lamp readings to correct the total ozone measurements. However, standard lamp corrections are not a suitable tool to correct the Umkehr measurements.

There is no justification for applying corrections to the N-values by a statistical procedure. Such artificial adjustments would mask real physical changes in this long, and therefore especially valuable time series of Arosa Umkehr measurements. Only further careful study including all information available at the Lichtklimatisches Observatorium Arosa might possibly allow to correct for known problems.

On the other hand, the comparison between D15 and D101 Umkehr observations in the period of 1968 to 1988, show some minor inconsistencies which are less relevant for long term trend analysis than the eye-catching patterns in N-values as discussed above. However, the probably less stable instrument D101 yields larger upper stratospheric trends by some percent per decade, compared to the standard Umkehr series of Arosa, which is reported at the WOUDC.

5.3 Using satellites as referees

In this section the Swiss ozone series are compared with satellite data available since 1979. The results presented here take into account the satellites SAGE II and SBUV which serve as a referee between the contradicting sounding and Umkehr trend results. No general conclusions can be drawn.

5.3.1 Comparisons with SBUV

Coincident days between each combination of two out of the systems: (SBUV, soundings, Umkehr) were selected. These three difference series were binned into monthly means and cumulated. For detecting breaks as described in 3.6 one must identify linear parts. A change in slope indicates a break in the difference. Occurs the break in two differences at the same time, the common instrument is the culprit. From the cumulative differences (Fig. 5.11 and 5.12) it can be seen, that there are less changes in the difference between Umkehr and SBUV than between

soundings and SBUV. Therefore, SBUV supports Umkehr stability. In Layer 5 (Fig. 5.12) two breaks in the sounding series can be identified: 1984 and 1988. There seem to be something wrong with the satellite data in 1989 (also Fig. 5.12). In Layer 4 (Fig. 5.11), the situation is blurred. The break 1984 in the sounding series is confirmed, but not so the one 1988. One would rather assign a break to 1987 to the soundings. The difference between Umkehr and SBUV seems rather smooth, except 1980 or 1981 which seems to be a irregularity in all three differences.

This analysis suggests that the long term stability of the Arosa Umkehr is superior to the record of the ozone balloon soundings of Payerne. SBUV supports stability of the Umkehr 1981–90, confirming a break in the sounding series at 83/84, and 87 or 88.

It must be noted that SBUV uses a similar inversion algorithm as Umkehr and is therefore not completely independent of Umkehr with respect to drifts originating from the principles of the method.

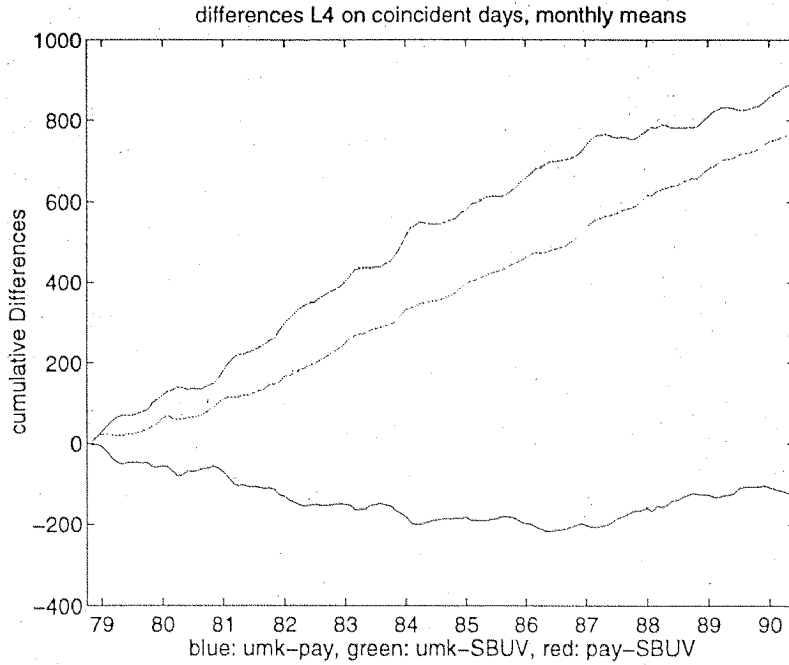


Figure 5.11: *Cumulative differences in Layer 4 of soundings-SBUV (red), Umkehr-SBUV (green) and Umkehr-soundings (blue).*

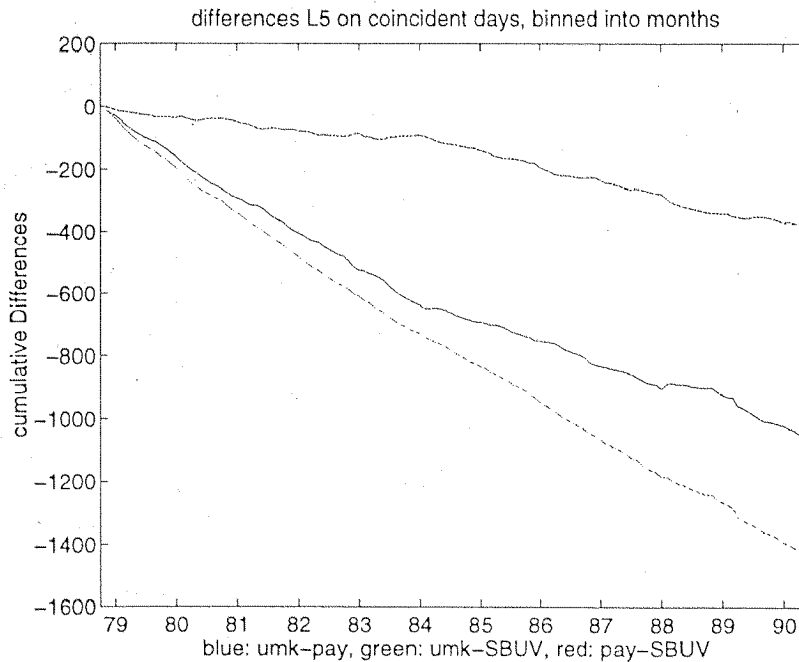


Figure 5.12: *Cumulative differences in Layer 5 of soundings-SBUV (red), Umkehr-SBUV (green) and Umkehr-soundings (blue)*

5.3.2 Comparisons with SAGE II

Since 1984 also measurements of the instrument SAGE II are available for comparison. More confidence is placed in the trends from SAGE than in that of SBUV (Randel et al. 1999). SAGE and Umkehr results has been found to match reasonably well (Newchurch et al. 1998).

Unfortunately there are again very few days which were covered by soundings and Umkehr and SAGE II. Therefore, soundings and SAGE II were compared (Fig. 5.13) and Umkehr and SAGE II were compared (Fig. 5.14) separately. For smoothing, the differences are binned into monthly means. Missing data indicate months where no coincident high-quality satellite overpass was available.

Too many missing values of the resulting series of differences do not allow to calculate the cumulation of differences, because the results depend too much on how the missing values are inserted.

SAGE II agrees with the sounding that the Umkehr gives too little ozone at Layer 5 (23.5–28 km) and agrees with Umkehr with respect to a negative offset of the soundings Layer 4 (19.1–23.5 km). Plotting all difference series over each other (not shown) reveals that safe conclusions cannot be drawn because of high scatter. SAGE II more likely attributes the breaks 1986–87 to the Umkehr, and also 1991, whereas 92/93 is more likely attributed to the soundings. But this indications must be verified with other methods. No definite conclusions are possible from this data comparison because of two little resolution and therefore too much scatter of the data.

Comparing SAGE II to Umkehr yields different characteristics for different layers. The main feature of the upper stratospheric data are the aerosol contaminated periods in Layer 7, 8 and 9. The last two years of Layer 6 exhibit a suspicious downward drift, and in Layer 5 there are several inhomogeneities within the series. Because of the large scatter, one cannot interpret them as breaks or shifts. The rising difference of Fig. 5.14 in Layer 4 and the lack of trend in Fig. 5.13 in Layer 4 implies that SAGE II agree qualitatively with soundings that there is a negative trend at the height of the ozone maximum. On the other hand, there are long-term variations in Layer 5 (Fig. 5.14) which imply SAGE II and soundings do not agree.

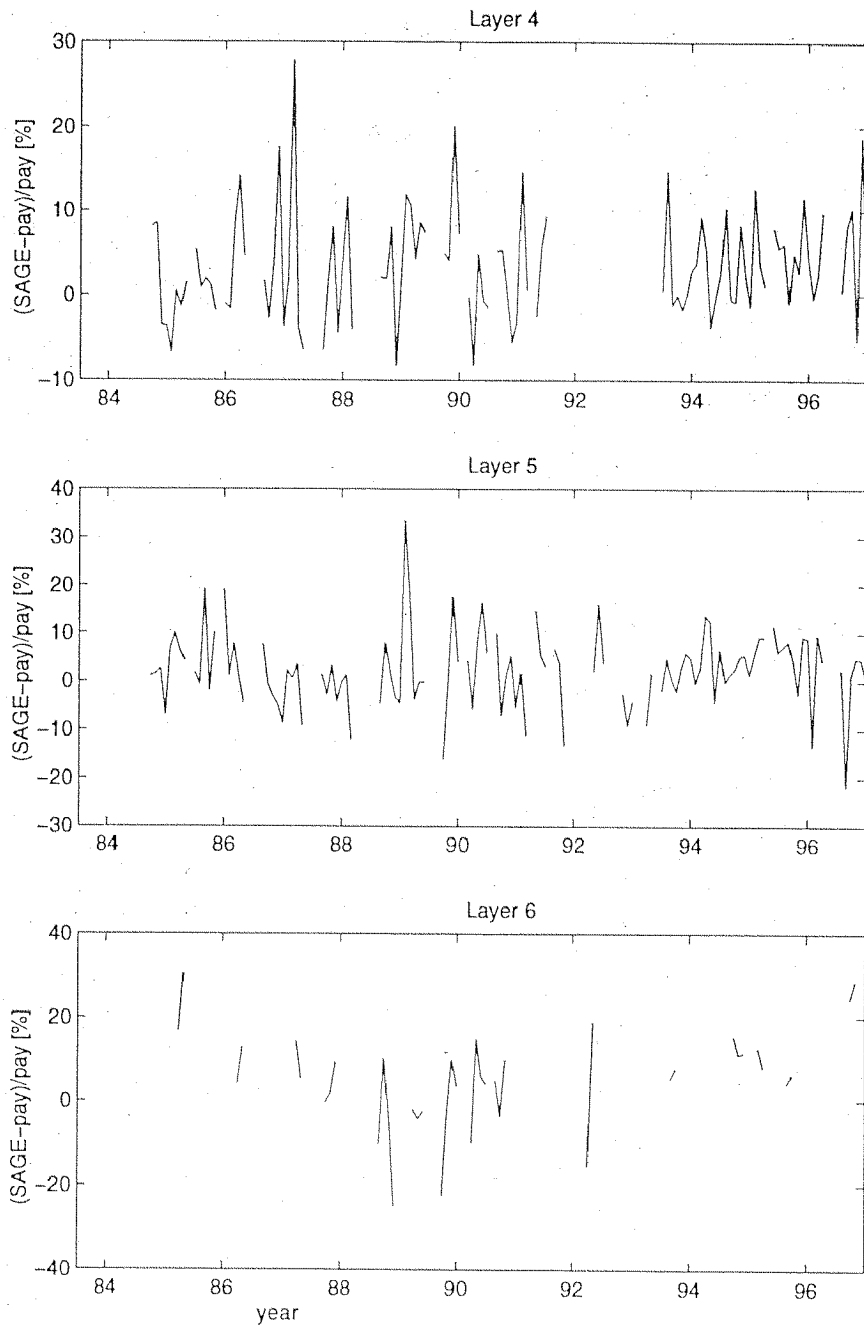


Figure 5.13: *Relative difference in monthly means of coincident SAGE II and Payerne soundings.*

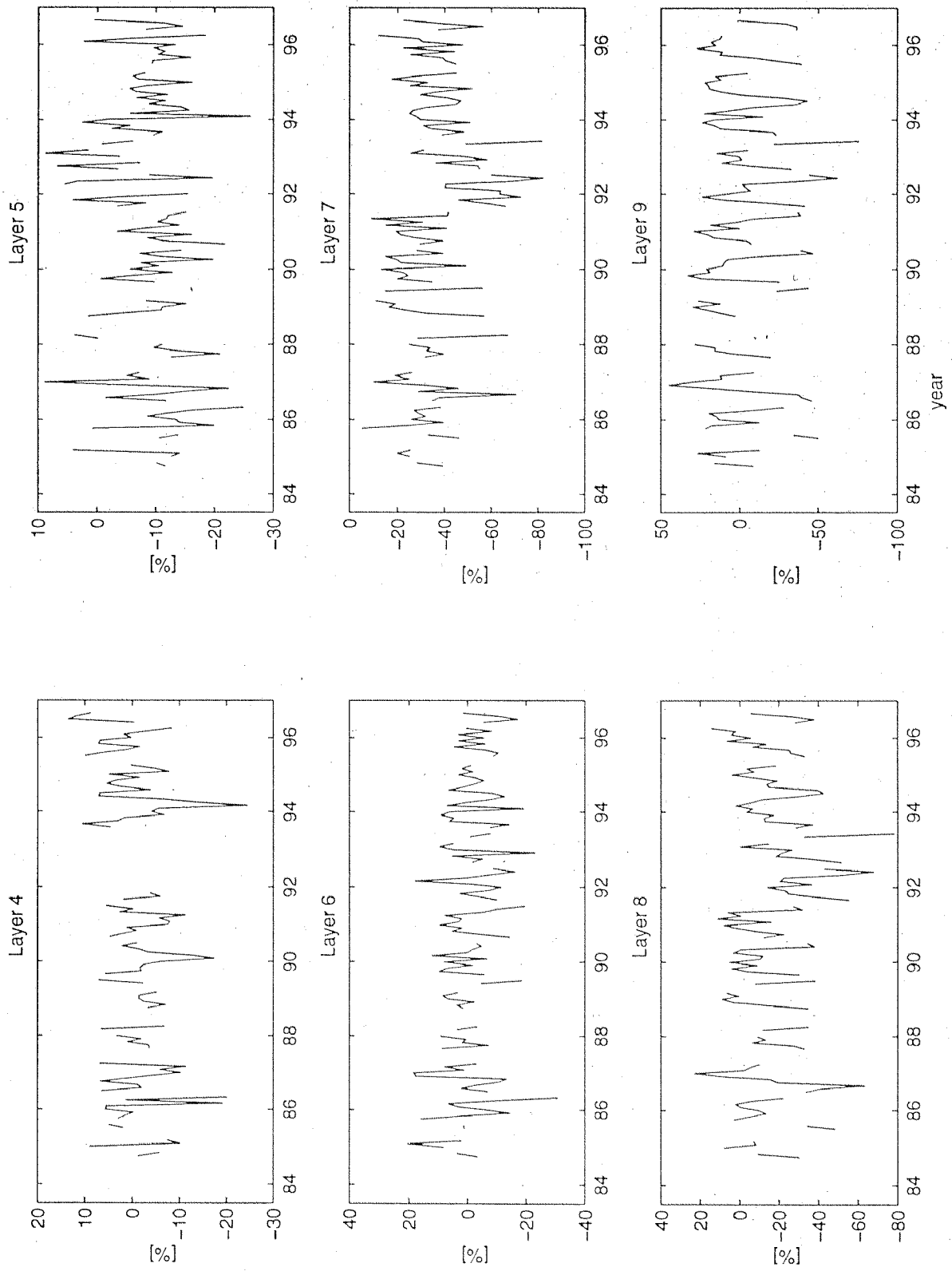


Figure 5.14: *(Umkehr-SAGE II)/Umkehr on coincident days, binned into months.*

The fact that the three systems SAGE II, Umkehr and soundings seem to have different long-term behavior in different months, rises the question whether there is a physical change in the atmosphere, which somehow has different behavior at different seasons and is reflected in varying ways by the three measurement systems. The solution is complicated by the fact that the mean latitude of SAGE II overpass changes with time, and exhibits different changes in different months. There are too few data with too much scatter to describe single month's drifts.

SAGE II does not give a decision whether soundings or Umkehr are more stable between 1984 and 1996. But it could be possibly used to verify single breaks. Reason of concern is that the information of different Layers is contradicting.

5.4 Conclusions from homogeneity checks

Ozone trends derived from Payerne soundings and Arosa Umkehr are contradictory, especially at the height of ozone maximum. The Umkehr instruments differ less from each other than from the Payerne soundings.

The stability of the standard Umkehr instrument of Arosa is studied in view of the reliability of the derived ozone trends. The time evolution of the N-values from the Dobson instrument D51, which is used for the regular Umkehr measurements, shows significant changes after the middle of the 1980s. The simultaneous measurements of another Dobson spectrometer (D101) from Arosa show in principle the same behavior regarding to the soundings, but also a small drift between Umkehr resulting from D51 and D101. The implication is that the upper stratospheric ozone trends would get somewhat larger if D101 were used instead of the standard instrument.

As the fault does not lie with a single instrument, either the Payerne soundings or the whole Umkehr method must cause the difference. SAGE and SBUV data are employed to explain the difference, and the drifts and shifts in the difference between Arosa Umkehr and Payerne soundings at each height. SBUV seems to give more support to the Umkehr, but comparison has the drawback that SBUV and Umkehr use the same type of retrieval algorithm. SAGE does not give a clear judgment between soundings and Umkehr.

It is not expected that with refined homogenization tools the satellites can give better judgments. There are too little coincident data for this.

The conclusion is, that there is no simple approach to validate drifts and shifts in the sounding or Umkehr series. Statistical 'corrections' should not be applied as in (Hogrefe 1996) and (Staehelin and Weiss 1998) and (Kosmitis 1999) before physics behind are understood.

The observed contradictions could originate in following problems:

1. instrumental instabilities

The standard Arosa Umkehr instruments have been shown to be too stable to be responsible for the contradiction to the soundings. Change in Umkehr standard instrument is definitely not the cause. Manufacturer changes of the soundings could be thought of being responsible, but are not that large, as Chapter 7 will reveal. Further, well understood problems (Neuhaus 1997) have already been accounted for in the homogenized series of Payerne soundings (Stuebi et al. 1998b).

2. methodological reasons

The Umkehr inversion is susceptible to a priori drifts. However, Mateer et al. (1996) expounded that the effect on trends for Layer 4 and 5 should be smaller than the observed difference to the soundings. The soundings have a systematic error due to scaling to total ozone. This effect is too small. The trend of the ozone above balloon burst is according to the Umkehr Layers in DU per decade: L10+L9: 0.1, L8: 0.7, L7: 1.4, L6: 0.8 which is together 3 DU per decade, approximately 1% of total ozone which is much too small to explain the observed differences between Umkehr and sounding trends.

3. unknown changes in the atmosphere

It is possible that Umkehr drifts are caused by a trend in turbidity of the air, i.e., a growing tropospheric aerosol loading, feigning a increase (or less decrease) in ozone values. This should have the largest impact in summer when the mountain resort Arosa is within the inversion layer. But the difference shows up also in spring. Therefore, tropospheric aerosol loading is dismissed as a reason for the conflicting trends. Further, increasing sub-visible

cloud coverage because of boosting air traffic could cause complicated error effects. For exploring cloud effects, cloudy Umkehr which are known to be slightly incorrect, and morning and evening Umkehr which probably differ in sub-visible cloud coverage, were compared. There was no large systematic effect found which could support this (sub-visible) cloud arguments.

The striking difference of Payerne sounding trends and Umkehr trends are endorsed with the general disagreement of Umkehr and sounding trends at Northern mid-latitudes. At the altitude of ozone maximum these two methods yield conflicting results (SPARC (1998), especially Fig. 3.53 therein). Also, the agreement of SBUV with Umkehr and the draw from SAGE is found again.

There could exist a parameter relevant for ozone variation, which is 'seen' differently by soundings and Umkehr. Further, the parameter must have long-term changes with a monthly dependency.

In Chapter 7 the ozone balloon series is used for trend analysis. Although this choice seems somewhat arbitrary from data quality consideration, the physical explanation for favoring the balloon sounding data becomes evident from the results presented in Chapter 7.

Seite Leer /
Blank leaf

Chapter 6

Total Ozone Trend Analysis

Total ozone trend analysis is improved in this chapter by considering a new parameter for dynamical variability. The foundations for using a dynamical proxy were explained in Section 2.2. To calculate the new trend estimates taking into account dynamical variability, the revised model which was derived in Section 3.5 has been applied. Below, the effect of the North Atlantic Oscillation (NAO) and of the tropopause pressure which is governed by this is verified statistically. The long-term dynamical changes are shown to lead to long-term total ozone changes which have the same sign as the anthropogenic ozone trends over Arosa. In contrast, in Reykjavik (Iceland), the long-term dynamical changes and anthropogenic changes have opposite sign and tend to cancel out each other in 1990–1996. These findings are in concordance with the physical explanation presented below.

The content of this chapter has been published in Appenzeller et al. (2000).

6.1 Total ozone and tropopause pressure

Over mid-latitudes strong variability in total ozone occurs with the passage of low and high pressure systems (Dobson et al. 1929). Due to the dynamical constraints on the large-scale flow, a surface low/high pressure system is associated with a distinct structure in the upper-troposphere lower-stratosphere. As shown in Figure 6.1, a low pressure system is connected with an enhanced potential vorticity anomaly, a warm potential temperature anomaly and a tropopause pressure higher than normal as Hoskins et al. (1985) explains. Similar to the surface pressure the tropopause pressure is an integral measure of the flow changes. Within a positive potential vorticity anomaly vertical vortex tubes are stretched and hence due to mass conservation the total mass (and similar total ozone mass) above a unit square is increased as reflected in an enhanced tropopause pressure (compare the tubes in Fig. 6.1). The converse holds true for the surface high pressure system which results in a reduced tropopause pressure and a shrunk tube in Fig. 6.1 and therefore less column ozone.

Hence from dynamical constraints one expects a simple linear relation between variability in tropopause pressure and total mass of ozone in the lower stratosphere (which contributes substantially to the total ozone value). A correlation between total ozone and tropopause variability has been documented for example by (Schubert and Munteanu 1988, Steinbrecht et al. 1998, Vaughan and Price 1991), the one between total ozone and other lower-stratospheric upper-tropospheric atmospheric parameters for example by (Ziemke et al. 1997).

Here we show that this relation also holds for multi-annual or decadal variability in total ozone. Figure 6.2 A shows winter mean total ozone measured over Arosa (46.78N, 9.68E), Switzerland (Staehelin et al. 1998a) together with the corresponding tropopause pressure data calculated from the NCEP reanalysis data set (Kalnay and et al. 1996). About half of the total variance (53%) can be explained with a simple linear relation (Table 6.1). Figure 6.2 B shows the same analysis for tropopause pressure and total ozone measured over Reykjavik (64.13N, 21.9W), Iceland. Since at Reykjavik sun photometric measurements are sparse during the December–January period the winter mean was restricted to a February–March (FM) mean. In addition only 25 of 41 possible winters had more than 15 measurements per month and were

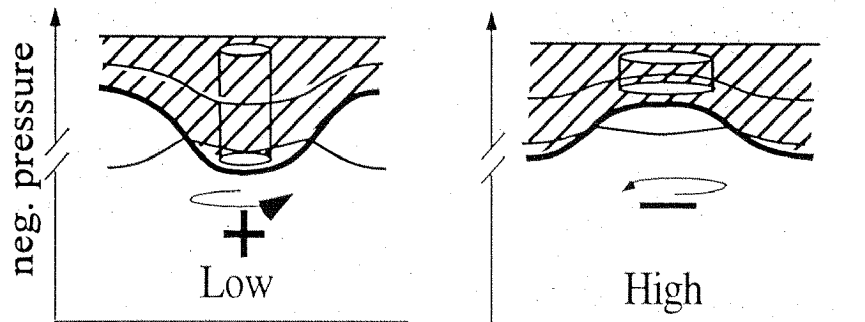


Figure 6.1: Schematic diagram showing the stretching/shrinking of a tube of air in the lower stratosphere due to the difference in the dynamical structure associated with a low and high pressure system (Hoskins et al. 1985). The tropopause is given as a thick line, potential temperature surfaces as thin lines and \pm indicate sense of vorticity.

used to calculate the FM mean values. At Reykjavik even a higher amount (67%) of the total variability can be explained with a linear relationship between total ozone and tropopause pressure.

6.2 Total ozone and NAO

On multi-annual time scales European winter climate is strongly linked with the North-Atlantic Oscillation which is typically measured with an index representing the strength of the meridional surface pressure difference across the North-Atlantic e. g. between Ponta Delgada (Azores) and Stykkisholmur (Iceland) (Hurrell 1995). NAO-like variability occurs in a large number of atmospheric and oceanic key climate variables (Wallace and Gutzler 1981, Hurrell 1995) and encompasses the entire troposphere-stratosphere system (Perlwitz and Graf 1995, Thompson and Wallace 1998). Figure 6.3 shows results of a correlation analysis between winter mean NAO index and winter mean tropopause pressure over the North Atlantic European region. Both the tropopause data and the NAO index for the period 1958 to 1998 were calculated from NCEP reanalysis data (Kalnay and et al. 1996). The correlation pattern shows a clear tri-pole pattern. During positive NAO phases tropopause pressure is higher at high latitudes and lower at mid-latitudes, as would be expected from an enhanced Icelandic low and Azores high

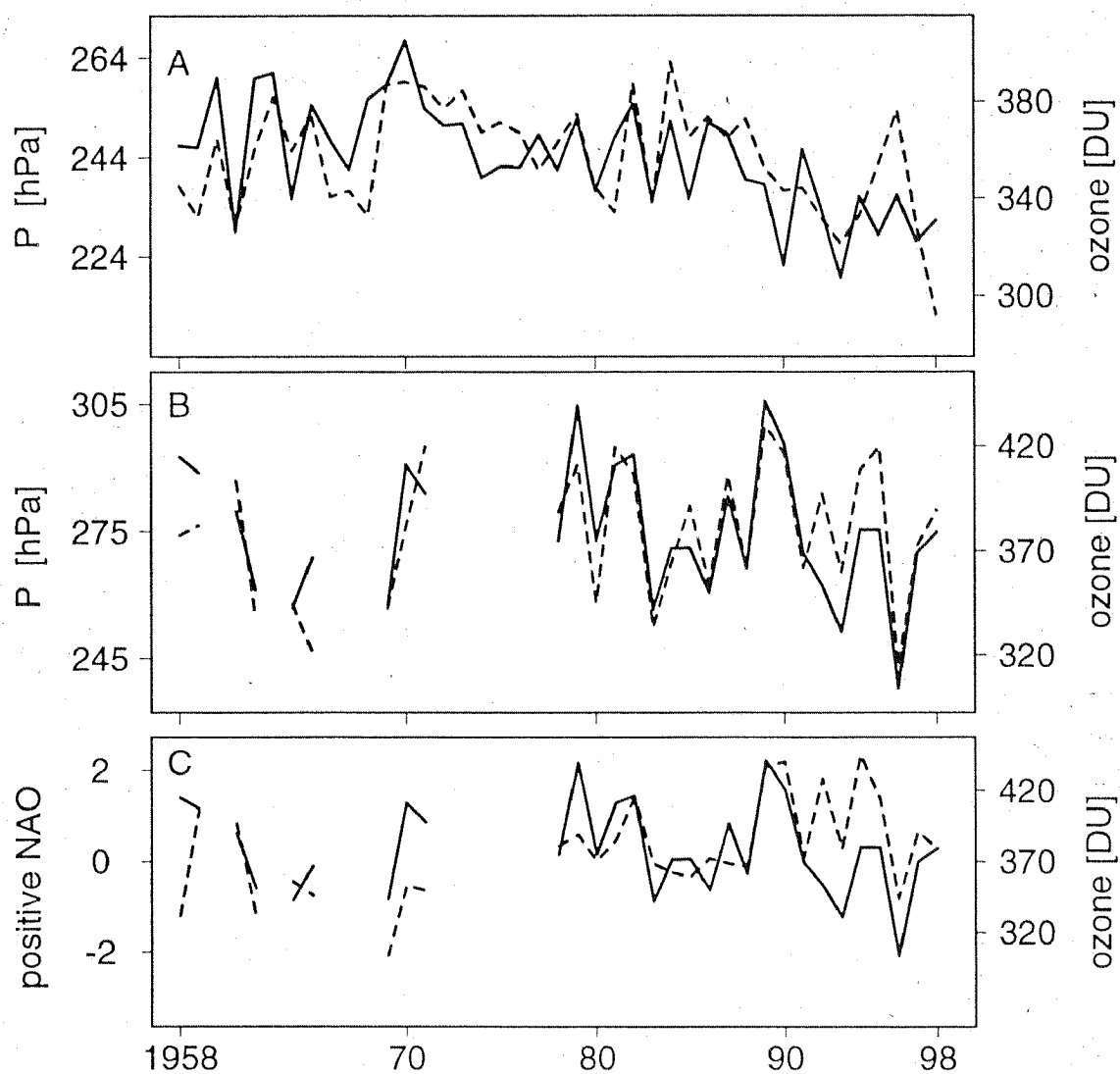


Figure 6.2: Panel A: February-March (FM) mean total ozone (solid line, in Dobson units) and tropopause pressure derived from NCEP reanalysis data (dashed line, in hPa) for the period 1958 to 1998, over Arosa, Switzerland. Panel B: As Panel A, but for Reykjavik, Iceland. Panel C: As Panel B but December to March means, and instead tropopause pressure with NAO index (dashed line) based on NCEP reanalysis data.

pressure system. The sub-tropical band with positive correlation is not directly associated with a surface feature. It is shifted towards the end of the Atlantic storm-track region and coincides with the location where stratospheric streamers and cut-off lows are frequently observed, e. g. (Appenzeller et al. 1996a).

Since tropopause pressure variations are proportional to total ozone variations one expects a similar space dependent correlation between NAO and total ozone. Figure 6.4 shows that during positive NAO phases winter mean total ozone is reduced at Arosa whereas over Iceland (Figure 6.2 C) total ozone values are enhanced as expected from Figure 6.3. At both stations a linear relation explains roughly one third of the total variance (Table 6.1). This result is also stable when the Arosa winter mean time series (1932 to 1998) is split into two equal parts, with the first part not disturbed by any trend or possible anthropogenic influence.

From the 60's to the early 90's the NAO index showed a continuing increase towards positive values with the exception of the winter 1996. This positive bias over the last 30 years had a direct impact on a large number of climate variables e. g. (Hurrell 1996, Thompson et al. 1999). Since total ozone is varying in concert with the NAO index one might speculate that a similar bias occurred in the observed total ozone trends. This hypothesis can be supported using a linear statistical trend model with the NAO index as additional explanatory variable.

6.3 Extended total ozone trend model

An earlier trend analysis for the winter mean total ozone measurements at Arosa (Staehelin et al. 1998b) showed that the solar radio flux (SF) at 10.7 cm (lagged with 32 months) and a measure for stratospheric aerosol loading (AOD) due to volcanic eruptions (Sato et al. 1993) were statistically significant. The anthropogenically induced chemical ozone destruction was quantified using an artificial ramp (R) starting in January 1970. However, an unexplained autocorrelated error suggested that major (autocorrelated) influences on total ozone were not accounted for.

In order to be consistent with the earlier analysis (compare Section 3.3)

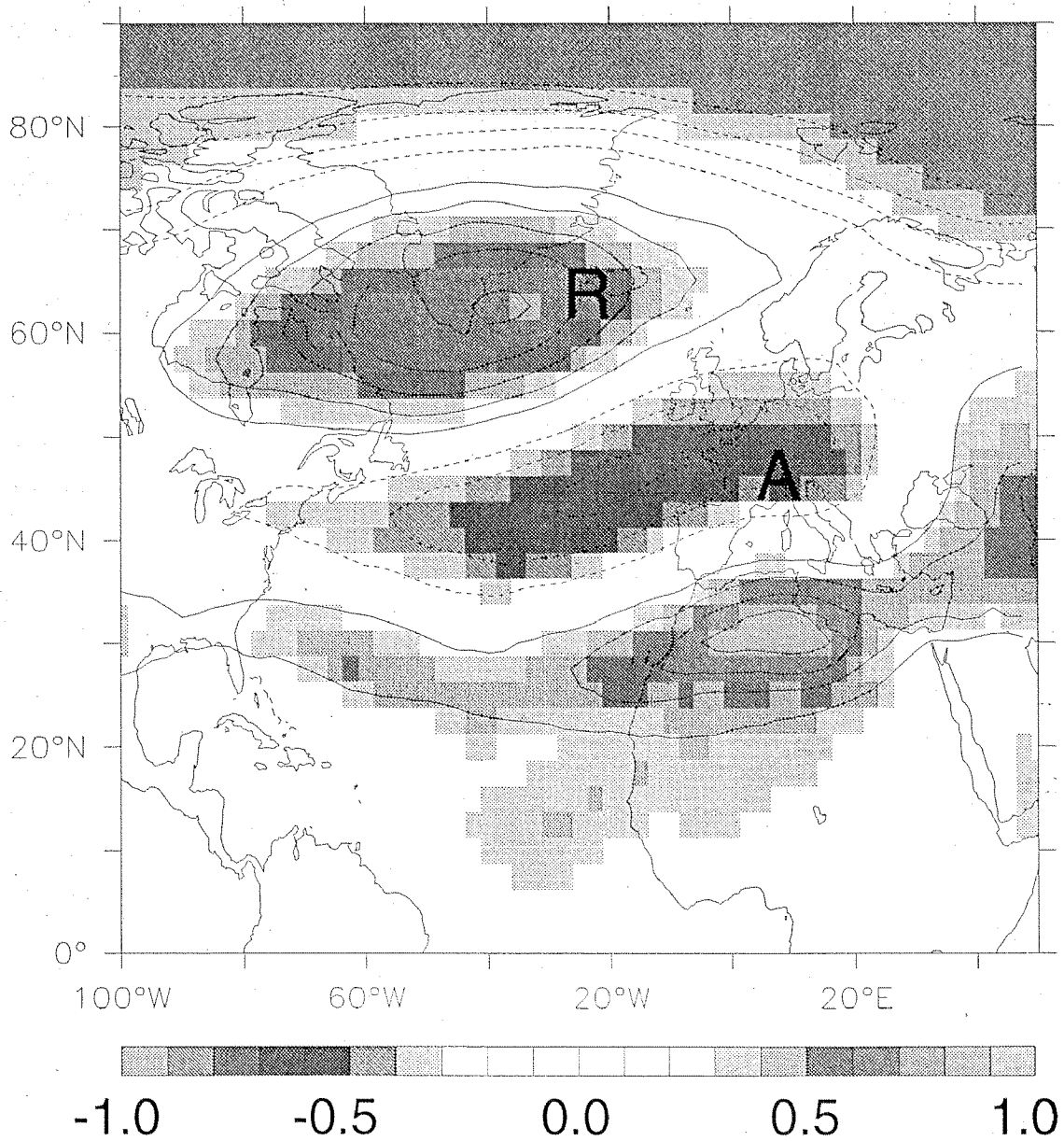


Figure 6.3: Cross correlation map (in colors) between winter mean (December to March) tropopause pressure and NAO index both derived from NCEP reanalysis data for the period 1958 to 1998. Only correlation coefficients above/below ± 0.3 are shown. Contours indicate tropopause pressure variation (in hPa) associated with +1 SD in NAO index, (A) location Arosa and (R) location Reykjavik.

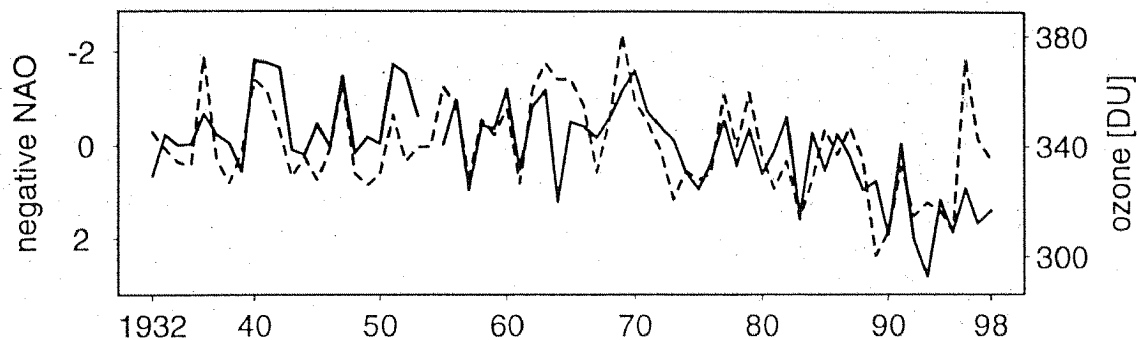


Figure 6.4: Total ozone (solid line, in Dobson units) over Arosa and normalized NAO index (dashed line), scaled with -1.0 , based on pressure data from Iceland and Azores for the period 1932 to 1996. Compare to Figure 2 Panel C.

a revised linear model for total ozone (N) is assumed

$$N = \bar{N} + c_1 NAO + c_2 R + c_3 SF + c_4 AOD + \varepsilon \quad (1)$$

with the additional explanatory variable NAO , the normalized NAO index (or the tropopause pressure P -tropo for the alternative model). The term \bar{N} denotes the ozone mean value and ε an error term.

The dynamically corrected anthropogenic winter mean total ozone trend estimated from (1) is $(-2.4 \pm 0.5)\%$ per decade. This corresponds to a reduction in trend amplitude of a quarter compared to analysis without considering the NAO $(-3.2 \pm 0.6)\%$ or another meteorological parameter representing the NAO behavior. The results of the best models found with stepwise linear regression are summarized in Table 6.1. In addition note the following two points. The inclusion of the NAO index removed the autocorrelation in the error term (ε) and resulted in better error bounds and p-values. Second the statistical significance of the lagged SF disappears for the period when the Quasi Biennial Oscillation (QBO) data were included (available from 1954 onward) as was tested in a separate model run. The QBO is excluded in the final model because it does not affect trends but introduces collinearity problems with NAO or tropopause pressure.

The same statistical modeling procedure was used for the Reykjavik total ozone measurements. Due to the sparse December - January ozone data coverage the analysis was again restricted to a February/March (FM) average. The NAO index proved to be a significant variable explaining $\approx 30\%$ of the ozone variability. The dynamically corrected FM

trend estimate is a negative trend of $(-3.8 \pm 1.4)\%$ change per decade (compared to no trend without NAO contribution). The trend seems to be higher than the revised FM trend over Arosa $(-2.8 \pm 0.8)\%$ as expected from 2D chemistry models (see also Table 6.1).

Using directly tropopause pressure instead of the NAO index as an explanatory variable leads to revised trend estimates that are comparable to the one described above (see Table 6.1). The tropopause pressure model setup performs even better than the one using the NAO index. This is consistent with the assumption that the changes in the dynamical structure of the atmosphere, as reflected in the tropopause pressure, are the immediate driving force for total ozone fluctuations, whereas the NAO is the climate oscillation associated with the observed multi-annual fluctuations.

6.4 Conclusions from total ozone trend analysis

The North Atlantic Oscillation (NAO) is modulating the Earth's ozone shield such that the calculated anthropogenic total ozone decrease is enhanced for the last 30 years over Europe (Arosa, Switzerland) whereas over the North Atlantic region (Reykjavik, Iceland) it is reduced. Including the NAO in a statistical model suggests a more uniform chemical winter trend by -2.4 to -3.2% per decade since 1970, compared to the strong longitudinal variation reported earlier with -3 to -5% over Arosa and 0% over Iceland. The revised trend is slightly below the predictions by 2D chemical models. Decadal ozone variability is linked to variations in the dynamical structure of the atmosphere, as reflected in the tropopause pressure. The latter varies in concert with the NAO index with a distinct geographical pattern.

Finally, note the following two points. First the apparent inconsistencies in total ozone trends in Western Europe and the North Atlantic are explained when allowance is made for the dynamical variability associated with the NAO. This effect is particularly strong for the TOMS period (1978 to 1994), where the revised trends are now consistent with, though slightly less than, those calculated using a 2D chemistry model (Jackman et al. 1996, Stolarski et al. 1992). The revised trend for e.g.,

Total ozone winter trends				
Ozone model	% Trend	[DU]/ [NAO]	[DU]/ hPa	R^2
Arosa DJFM				
with NAO	-2.4 ± 0.5	-7.8 ± 1.2		70
without	-3.2 ± 0.6			47
Arosa FM				
with NAO	-2.8 ± 0.8	-7.6 ± 2.9		50
without	-3.6 ± 0.8			39
Reykjavik FM				
with NAO	-3.8 ± 1.4	18 ± 5		39
without	not sign.			8
Arosa FM				
with P-tropo	-3.2 ± 0.8		0.9 ± 0.3	53
without	-3.6 ± 0.8			39
Reykjavik FM				
with P-tropo	-2.7 ± 1.0		1.1 ± 0.2	67
without	not sign.			8

Table 6.1: Trend estimates in % per decade, based on a linear regression model as equation (1). DJFM denotes winter averages December-March, FM February-March only. Full model is used for Arosa DJFM with data from 1932-1996 for comparison with literature (Staehelin et al. 1998b). All other models with FM means are calculated from 1958-1998, without SF and AOD as not significant variables for this series. Highly aerosol disturbed data ($AOD \geq 0.02$) were excluded. R^2 is total explained variance in %.

March ozone at Arosa is -2.2% instead -5% , for Reykjavik -5% instead 0% compared to -3 to -5% for 2D chemical models. Second, it has been suggested that the NAO can be considered as a sub-pattern of a hemispheric Arctic climate oscillation (AO) (Perlwitz and Graf 1995, Thompson and Wallace 1998). The AO index is comparable to the NAO index and hence a similar statistical relation between total ozone and AO index is expected (Thompson et al. 1999) which is confirmed in the next chapter. The advantages in using NAO are that a longer data set is available and that NAO is a more regional proxy for Europe.

Seite Leer /
Blank leaf

Chapter 7

Ozone Profile Trend Analysis

Ozone profile trends are revised with a new ozone trend model that includes the dynamical influences which showed up already in the total ozone (Chapter 6). Tropopause pressure variations are identified as the most important driving mechanism for dynamically induced ozone changes in the lower stratosphere, extending the results of Chapter 6. The influence of the North Atlantic Oscillation (NAO) and the Arctic Oscillation (AO) are compared. The ozone variability, and their attribution to dynamical influence and aerosols as well as anthropogenic trends are investigated in the different seasons and heights.

This chapter will be submitted slightly changed to JGR.

7.1 Searching for the cause of the vertical structure of O₃ trends

The interpretation of the observed ozone profile trends in mid-latitudes is still a subject of discussion. Compared with observations, the chemical models seem to disagree partly. The NASA Goddard Space Flight

Center (GSFC) two-dimensional model of stratospheric transport and chemistry (Jackman et al. 1996) provides the following picture: There is a strong maximum of ozone depletion which peaks at 40–45 km, consistent with measurements and theory. The model overestimates this ozone depletion somewhat, but this can be attributed to some difficulties of the model with a certain chemical reactions. In the middle stratosphere, about 25–35 km, the model is in perfect agreement with the measurements. Below 20 km, only half of the observed trends can be reproduced by the model.

There were efforts to explain the observed trends with chemical theories and with dynamical changes. One reason for the observed ozone trends in mid-latitudes is that ozone depleted air which originates from the vortex is mixed in (Hadjinicolaou et al. 1997).

Knudsen et al. (1998) estimated the impact of polar ozone destruction on polar stratospheric clouds (PSC) to the latitudinal band of 20°–90° to be in the range of 2–4% of total ozone in the mid-nineties. This is about 1/3 to 1/2 of the observed trends in mid-latitudes. The maximum contribution of this dilution loss (4%) was found 1997, a winter with little PSCs outside the vortex. Therefore, the dilution loss corresponds to the PSC-induced depletion inside the vortex.

An alternative to PSCs as the cause of ozone trends at mid-latitudes are sulfuric acid aerosols of volcanic origin. They can act as catalysts for heterogeneous chemistry as explained in Section 2.1.3.

Overall, the chemical models seem not to be capable to reproduce the full observed trends in mid-latitudes (WMO 98, figure 7-24). The modeled ozone changes had to be scaled by 1.5 to approximately match the magnitude of observations (Solomon et al. 1996). The results get closer when a temperature offset of -2K is assumed and suggest that mid-latitude ozone loss may be dominated by extra-vortex chemistry (Solomon et al. 1998).

With the three-dimensional chemical transport model SLIMCAT (Chipperfield 1999) there has been found evidence that the polar processes influence the mid-latitude ozone in spring and summer, but not further into the year than November. Interestingly, the strong ozone decrease in winter 1992/93 was reproduced by the model without taking into account the impact of possible ozone chemistry of volcanic aerosols, which

should show up particularly strong there because of Pinatubo eruption.

Hence, there is strong evidence for also non-chemical contributions to the observed mid-latitudal ozone changes. An early paper found a correlation between sea surface temperature (SST) and stratospheric ozone (Komhyr et al. 1991). Steinbrecht et al. (1998) used tropopause height to explain a substantial part of the long-term ozone change. Hood and Zaff, 1995 and McCormack and Hood, 1997 explained the dynamical influence on ozone trends as observed by satellite. They found that half of the observed trends are caused by adiabatic transport and therefore reversible redistribution. Fusco and Salby (1999) use a meridional mean in order to eliminate the reversible component. They showed that variations in the meridional mean of total ozone can be attributed to planetary wave (also called Rossby wave) activity. Hood et al. (2000) confirmed that in February and March as much as 40% and 25 %, respectively, of the zonal mean total ozone decline may be attributed to long-term trends in Rossby wave breaking behavior. Up to now, only total ozone was investigated.

In the next section, tropopause pressure changes are identified as the cause for ozone changes in certain parts of the ozone profile. The tropopause pressure itself is governed by the North Atlantic Oscillation (NAO) which exhibits long term changes (Chapter 6). The Arctic Oscillation (AO) includes the NAO signal, and on long time scales, the NAO and the Arctic Oscillation (AO) are similar (see Section 2.2 for explanations).

The influence of tropopause pressure, NAO and AO on ozone is statistically tested in Section 7.3. In the following the physical background is explained.

7.2 Tropopause pressure and ozone

The tropopause pressure difference induces a flow in the lower stratosphere. Because the ozone profile has a strong gradient from the troposphere to the lower stratosphere, the amount of stratospheric air in the column determines the amount of ozone. In Figure 6.1 this mechanism is sketched, below, a mathematical deviation is given that the total ozone change is proportional to tropopause pressure change. The

deviation was done in collaboration with Christoph Appenzeller.

Assuming an idealized ozone profile, a linear relation between tropopause pressure and total ozone can be derived. The total ozone (N) is the vertical integral of all ozone molecules in an atmospheric column. Using the hydrostatic equation, N may be written as

$$N = - \int_{P_s}^0 \frac{m(p)A}{Mg} dp \quad (1)$$

where $m(p)$ is the ozone mass mixing ratio, A the Avogadro number, M the molecular weight of ozone and P_s the surface pressure, p the pressure over which is integrated. Ozone mass mixing ratios peak in the mid-stratosphere. In the troposphere and above the stratosphere m is a magnitude smaller and will in the following be taken zero. Although large-scale planetary disturbances can propagate upward into the stratosphere, synoptic or sub-synoptic scale disturbances decay with height and leave most of the stratosphere unchanged. These disturbances displace the tropopause and change the tropopause pressure but not the tropopause ozone mass mixing ratio if an adiabatic motion is assumed. Hence the deviations (N') from a long-term mean total ozone value (N) can be written as

$$N' \approx - \frac{A}{Mg} \left[\int_{P_T}^{P_L} m(p) dp - \int_{P_{T0}}^{P_L} m_0(p) dp \right] \quad (2)$$

with the pressures P_T of the actual, P_{T0} of the mean tropopause and P_L the pressure at the level the flow disturbance is decayed. The ozone mixing ratios, m the actual and m_0 the mean, are both taken to be zero at the tropopause and equal m_L at the penetration depth P_L . In the lower stratosphere the mixing ratios m_0 and m are increasing functions with decreasing pressure and as a zero order approximation both will be assumed to have a linear shape between P_L and P_{T0} with $m_0 = \frac{-m_L}{(P_{T0}-P_L)}(p - P_T)$. In addition we assume that the disturbed O_3 profile can again be approximated by a linear profile between P_L and P_T with $m = \frac{-m_L}{(P_T-P_L)}(p - P_T)$. Integrating equation (2) using these approximations leads to $-\frac{A}{Mg} [\frac{m_L}{2}(P_L - P_T) - \frac{m_L}{2}(P_L - P_{T0})]$ and therefore

$$N' \approx \frac{A}{2} \frac{m_L}{Mg} P'_T \quad (3)$$

with $P'_T = P_T - P_{T0}$ the tropopause pressure anomaly. Equation (3) suggests that the dynamically induced total ozone disturbance N' is

proportional to the associated tropopause pressure anomaly P'_T but is also dependent on how deep the flow disturbance is penetrating into the stratosphere (represented by m_L).

Here it was shown that tropopause pressure is justified to be used as a linear contribution for the ozone balance.

7.3 Natural influences and anthropogenic trends

We perform ozone trend analysis with a stepwise linear regression model, starting with Eq. (10) of Section 3.3. The ozone profiles used here are Payerne balloon soundings (Stuebi et al. 1998b) which were integrated into six layers according to the Umkehr layer definitions (L1:0–10.3 km, L2:10.3–14.7 km, L3:14.7–19.1 km, L4:19.1–23.5 km, L5:23.5–28 km) and for L6 the special restriction 28–30 km was used, because only few balloons exceed this level.

For each layer, a separate ozone balance was set up. The trend model explains the deviation of the measured ozone from the seasonal mean as contributions of explanatory variables and a residual error term ϵ :

$$oz_i = \overline{oz}_i + c_1 * pTropo + c_2 * AOD + c_3 * SF + c_4 * QBO + c_5 * R + \epsilon \quad (4)$$

where the target variable is oz_i , the ozone content of a certain layer i and \overline{oz}_i is its climatological mean. The explanatory variables are: the tropopause pressure $pTropo$, which is controlled by NAO/AO, the aerosol loading AOD , the solar activity SF , the seven months lagged Quasi-Biennial Oscillation QBO of which only positive phase is used, and R a ramp starting 1970 and rising one unit per decade. The contribution c_5 of the ramp R is the trend which is attributed to anthropogenic ozone destruction.

A stepwise regression (see Section 3.5), is performed for each season and layer. This yields the contributions c_i of the different explanatory variables to the ozone balance (4). The results are discussed in the next sections.

7.3.1 Significance of tropopause pressure with respect to season and height

Variability in tropopause pressure is the primary source of total ozone variability. It explains up to 40% variability between 10 and 20 km height. The response of ozone is prominent in the season with large dynamical variability in tropopause region, which is spring season for Europe. But also in the other seasons, tropopause pressure is linked with ozone, see Fig 7.1 for an example of data and Fig. 7.2 for statistical significance.

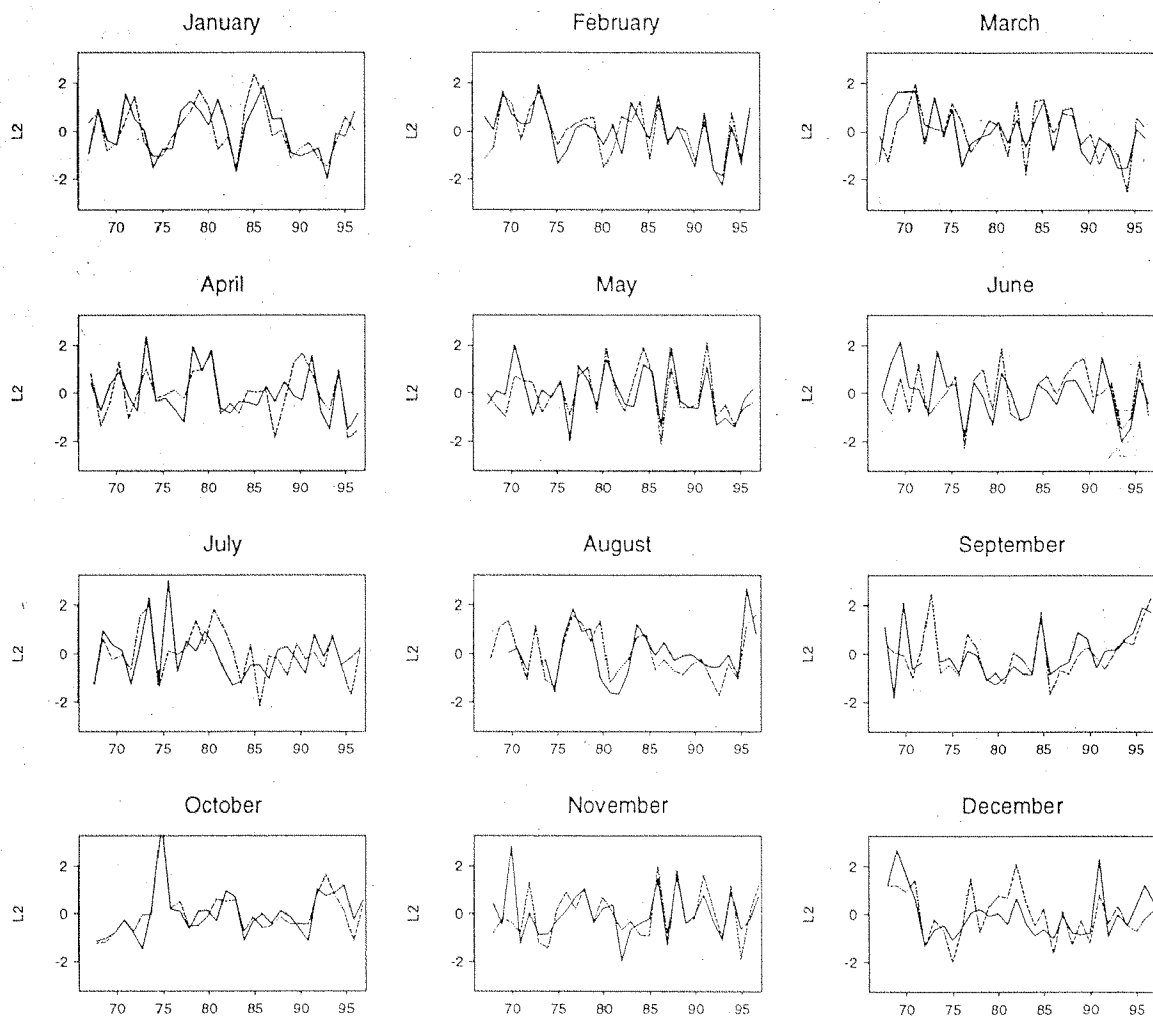


Figure 7.1: Example of normalized layer ozone (L2:10.3–14.7 km, integrated Payerne soundings) compared to normalized tropopause pressure (red).

From the example in Fig. 7.1 one can discern that the correlation of tro-

popause pressure and ozone content is important on longer time scales. As derived in the section above, ozone changes are linearly connected with tropopause pressure changes. Therefore, long-term changes in tropopause pressure contribute to long-term ozone trends.

The correlation of tropopause pressure and ozone is valid for all months, but the long-term tropopause pressure behavior is not the same for all months. For example (Fig. 7.1), in March tropopause pressure has fallen from the 1970s to mid of 1990s, whereas in September it has risen. June and December do not show a clear long term change. The strongest correlation of tropopause pressure and layer ozone is found in the lower stratosphere, as expected (see Fig. 7.2).

With the Pearson test (Section 3.2) it is checked whether there is a discernible trend in tropopause pressure. Single months cannot provide sufficient significance. Seasonal averages of spring and winter months show a significant upward trend in tropopause pressure. Summer has some indications to a upward trend (not significant) and autumn suggest a downward trend (not significant). It is necessary to reduce scatter by combining the months with similar tropopause behavior in order to perform meaningful ozone trend analysis. This considers besides the influence of tropopause pressure also other variability of ozone, and aims on the detection of anthropogenic destruction.

For trend analysis, the optimal choice is to consider 3 seasons: January–April (JFMA), May–August (MJJA) and September–December (SOND). Averaging over these or even somewhat changed ensembles give smooth results. The reduced scatter allows to check for more subtle influences (Fig.7.3).

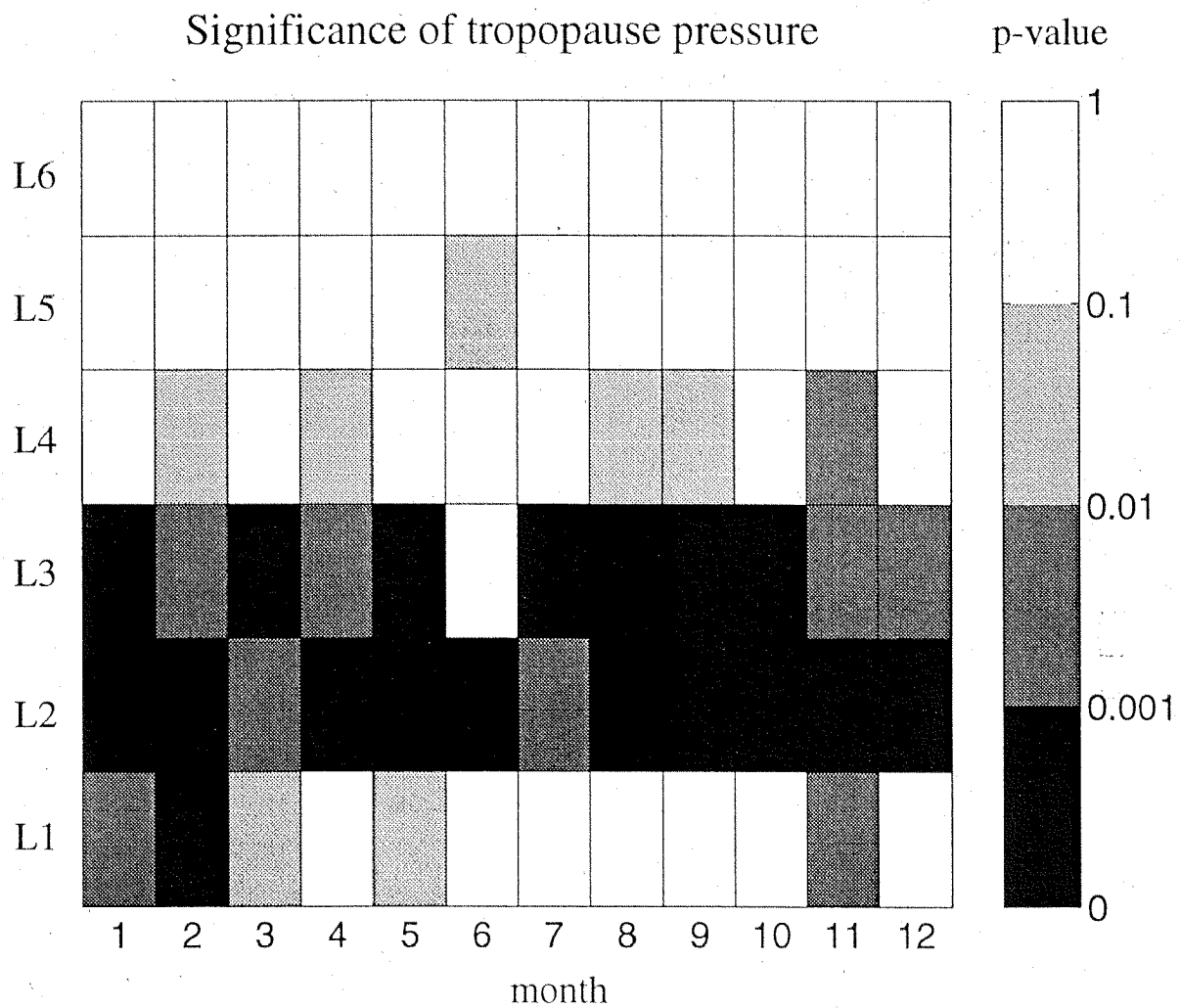


Figure 7.2: Significance of tropopause pressure (where highly significant: $p < 0.001$ is black, not significant: $p > 0.1$ is white) with respect to height and month of the year. The layers are chosen as Umkehr layers as defined as L1:0–10.3 km, L2:10.3–14.7 km, L3:14.7–19.1 km, L4:19.1–23.5 km, L5:23.5–28 km, L6:28–30 km.

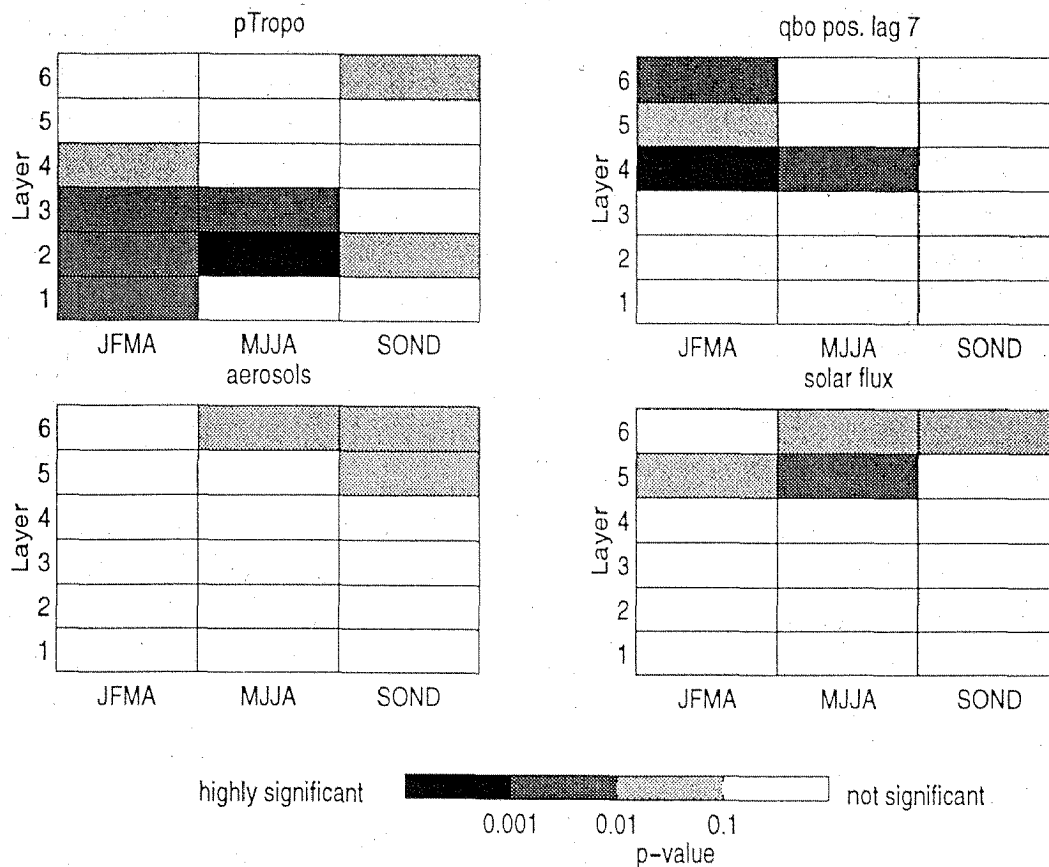


Figure 7.3: Significance of tropopause pressure ($pTropo$), positive QBO lagged 7 months, stratospheric aerosol loading and solar flux, with respect to height and season. Highly significant: black, and logarithmic scale to not significant: white. One may interpret light gray as explaining 5–10% of the variance, dark gray 10–20% and black 20–40 % with this data set. The layers are L1:0–10.3 km, L2:10.3–14.7 km, L3:14.7–19.1 km, L4:19.1–23.5 km, L5:23.5–28 km, L6:28–30 km.

Although the tropopause pressure is significant throughout the year, winter/spring stands out for the large height range which is affected. In this season, dynamic disturbances at the tropopause are larger, and can propagate higher. A barely significant contribution deserves some attention. There seems to be 8% of ozone variance explained by tropopause pressure in autumn at the suspicious high level L6. The idea it could be a pure random artifact diminishes when checking the significance of NAO (Fig. 7.4) In this height, NAO explains more (20% compared to 8%) and has strong significance. Besides the pattern which can be attributed to the NAO-influence on tropopause pressure, there is a signal in late summer and autumn which might mirror a NAO-dependent transport mechanism.

The significances of NAO are less coherent for the different months. Some information is lost when months are put together to seasons. Clearly there is a signal in spring at the lower stratosphere. Statistical uncertainty must be kept in mind when interpreting another feature in the middle stratosphere in summer/autumn. Latter even seems to propagate downward, which is repeated in the significance of solar influence. The influence of NAO in the lower stratosphere can be explained via the connection to tropopause pressure. In the upper heights, a different mechanism must be responsible and is subject of future research. Recently it has been shown (Baldwin and Dunkerton 1999) that there exist indeed pattern which propagate downwards from the higher stratosphere to the troposphere. These originate at the polar vortex, and are therefore associated with the Arctic Oscillation (AO), a climatic pattern, comparable to, but more hemispheric than the NAO.

The downward propagating pattern of Fig. 7.4, which extends from August Layer 6 to the November tropopause, cannot be explained by the phenomenon described in Baldwin and Dunkerton (1999). Their observations all identify downward propagation at a time scale of one month or shorter, whereas here about four months are involved. Further, when the AO is employed instead of NAO in the regression model, the signal wanes (Fig. 7.5). The following alternative explanation is more likely: Advection which is in different heights at different times of the year may be the cause for this curious pattern. The downward propagation in Fig. 7.4 must not be over-interpreted because of statistical uncertainty. It gives ambitious riddles for future research (Section 7.4).

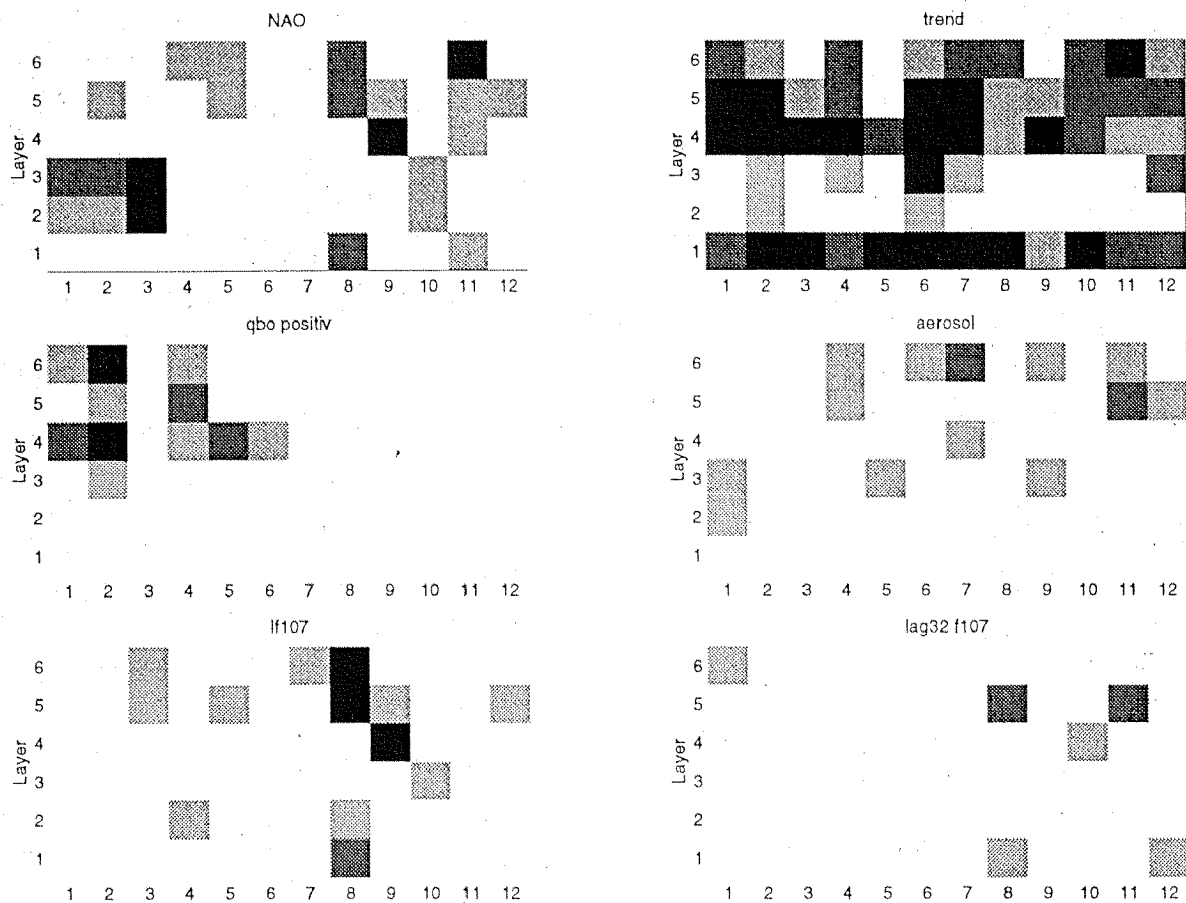


Figure 7.4: Significance of North Atlantic Oscillation for ozone trend analysis with respect to height and month of the year. Note the strong significance in spring for the lower stratosphere, which can be explained with the connection of NAO to tropopause pressure. In the upper heights, a different mechanism must be responsible. The layers are L1:0–10.3 km, L2:10.3–14.7 km, L3:14.7–19.1 km, L4:19.1–23.5 km, L5:23.5–28 km, L6:28–30 km.

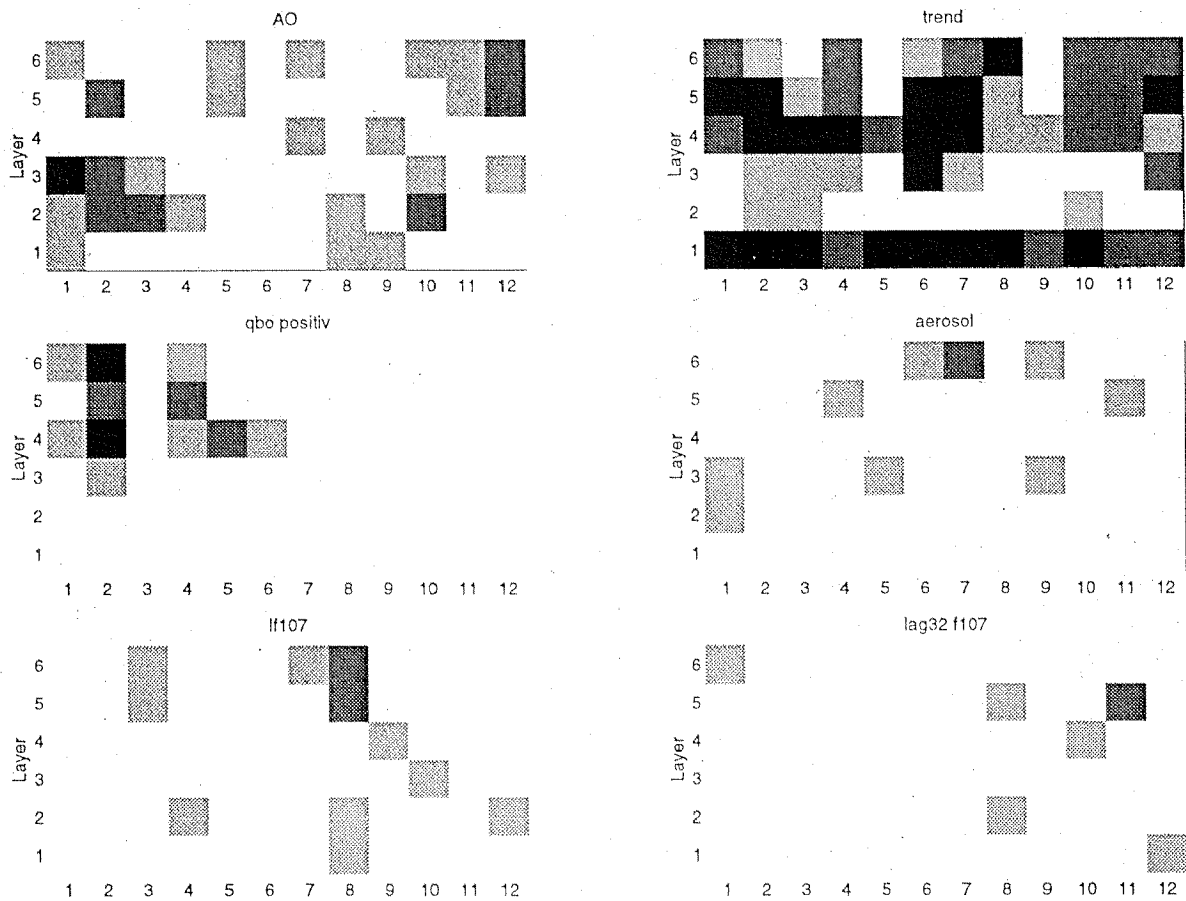


Figure 7.5: *Significance of the Arctic Oscillation for ozone trend analysis, compare to previous figure. Both show clearly the connection in spring, whereas for the higher stratosphere NAO seems to explain more.*

7.3.2 QBO, solar signal and aerosols

The QBO signal shows up in spring, in the middle stratosphere, accounting for up to 20% of ozone variability. This finding coincides well with previously reported results (Soukharev 1997).

Solar flux is weakly significant above 25 km, describing up to 15 % ozone variability above 23 km in summer. The possibility that the solar effect is an artifact cannot be ruled out. A superposition of biennial and quasi-biennial oscillations yields a frequency which is close to that of the solar cycle (Baldwin and Dunkerton 1998). However, in Fig. 7.3, solar flux seems to be significant in selected heights and seasons where the QBO does not seem to play a role. This is a motivation to search for causes of a solar influence.

The also weakly significant contribution of aerosol loading to ozone variability reaches about 10% for summer above 28 km, and for autumn already above 23 km. One reason for this could be chemical destruction which happens at the aerosol surface. As Solomon (1999) pointed out, the aerosols serve as catalysts in mid-latitudes in a similar way polar stratospheric clouds do at the poles. Suspicious is that at these altitudes (L5 and L6, i.e., 23.5 km and above) only little aerosols reside (Thomson and Poole 1997). Aerosols of volcanic eruptions are also known to influence dynamics (Kodera 1994). This explanation could explain the relative high altitudes, but not the seasons where the aerosol influence is observed.

7.3.3 Resulting ozone profile trends

Applying the stepwise regression models (Eq. 4) reduces the estimate of chemical ozone profile trends reported for Arosa in literature (Staehelin et al. 1998b). The strongest effect is in winter and spring in the lower stratosphere, where up to half of the trend can be attributed to dynamics (see Fig. 7.6).

Whether the Arctic Oscillation (AO) or the North Atlantic Oscillation (NAO) is used, changes the trends negligibly. NAO was preferred as it is more regional. Because of the physical mechanism by which NAO (AO) influences lower stratospheric ozone via the tropopause pressure

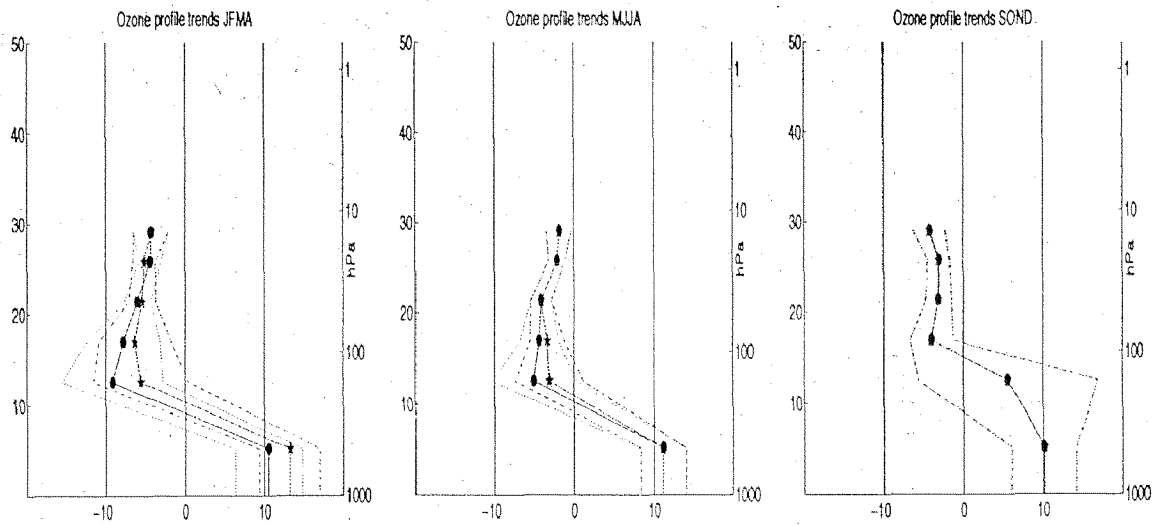


Figure 7.6: *Ozone trends per decade as observed in the Payerne sounding series (blue points) compared with ozone trends where the dynamical contribution is removed (red stars). Blue dotted lines are \pm standard deviation for the observed trends, red dashed lines for trends with the dynamical contribution removed.*

(Section 7.2), up to Layer 4 (up to 23.5 km) tropopause pressure is included in the model Eq. (4). From Layer 5 (above 23.5 km) NAO is used. This distinction is necessary because of the high correlation of both variables. It is perfectly supported by the analysis using tropopause pressure for all layers and NAO for all layers. This slightly different models do not change the trends, but improve explained variance and therefore significance. The results of this best possible estimate of ozone profile trends are compiled in Table 7.1. For comparison, the results are given when the same model is used but ignoring tropopause pressure and NAO.

The main result of Table 7.1 is that the strong trend of -9 ± 3 % per decade in layer L2 vanishes to become a not significant trend when dynamics are included. The most probable estimate is a trend half as large as previously anticipated. That means there is no trend maximum to be found in the lower stratosphere when analyzing one of the longest European profiling series. This gives rise to doubt the commonly spread Fig. 2.5. From another very long profiling series (Hohenpeissenberg, Germany), similar conclusions were drawn (Steinbrecht et al. 1999).

The explained variance measures how well the model describes the ozone

Trends with and without considering dynamics

	L1	L2	L3	L4	L5	L6
a	13.2±1.9	(-5.5±3.0)	-6.3±2.3	-5.4±0.8	-5.1±0.7	-4.3±1.1
a'	10.5±2.1	-9.1±3.2	-7.8±2.3	-6.0±0.8	-4.4±0.7	-4.3±1.1
b	11.2±1.4	(-3.1±2.1)	-3.3±1.1	-4.1±0.6	-2.1±0.5	-1.8±0.8
b'	11.2±1.4	(-5.0±2.6)	-4.3±1.2	-4.1±0.6	-2.1±0.5	-1.8±0.8
c	10.2±2.0	(5.6±5.6)	-4.0±1.3	-3.1±0.8	-3.1±0.7	-4.3±1.0
c'	10.1±2.1	(5.6±5.6)	-4.0±1.3	-3.1±0.8	-3.0±0.7	-4.2±1.0

Table 7.1: *Swiss ozone sounding trends in percent per decade calculated with the optimum model considering tropopause pressure up to L4 and NAO above (not significant trends are put in brackets). The seasons are a) JFMA, b) MJJA and c) SOND. Without considering dynamical influence: a') JFMA, b') MJJA and c') SOND. The layers are L1:0–10.3 km, L2:10.3–14.7 km, L3:14.7–19.1 km, L4:19.1–23.5 km, L5:23.5–28 km, L6:28–30 km. Note that the influence of dynamics is strongest in JFMA. The positive tropospheric trends (L1) is increasing in JFMA, and the lower stratospheric (L2 and L3) trends are decreasing in JFMA and MJJA when tropopause pressure is included in the ozone balance.*

behavior. Table 7.2 shows how much of the ozone variability is explained with the model Eq. (4). The percentage of explained variance is given for each season and layer. The variance of ozone is highest in winter and spring, and is relatively well described. In autumn, the major part of ozone variance remains unexplained. The ozone maximum is partly eroded in autumn. For this advection, no proxy is available and therefore missing in the model.

7.4 Discussion and future research

The influence of tropopause pressure and therefore NAO/AO in the lower stratosphere is explained satisfactorily. Not clear is the influence in the middle stratosphere in late summer to late autumn. Besides the small possibility, that the pattern of NAO significance (Fig. 7.4) occurred by chance, an advection process which changes height with time is conceivable. The significance of NAO (Fig. 7.4), which is somewhat stronger as that for AO (Fig. 7.5) is conjoint with the NAO index defined

Explained variance R^2 of layer ozone						
	JFMA		MJJA		SOND	
L6	59	(59)	43	(43)	66	(40)
L5	74	(69)	52	(52)	58	(57)
L4	78	(75)	72	(72)	38	(38)
L3	49	(29)	54	(32)	25	(25)
L2	44	(23)	52	(11)	20	(0)
L1	65	(48)	69	(69)	54	(49)

Table 7.2: *Explained variance R^2 [%] of models resulting from stepwise regression starting with full Eq.(4) with $pTropo$ as explanatory variable up to L4, and NAO above. Number in brackets are the R^2 obtained excluding $pTropo$ and NAO. In the lower stratosphere (L2 and L3), the model improves much when a dynamical proxy is included. Still, in autumn, there is very little variance explained in the lower stratosphere. The layers are L1:0–10.3 km, L2:10.3–14.7 km, L3:14.7–19.1 km, L4:19.1–23.5 km, L5:23.5–28 km, L6:28–30 km.*

as a more regional European phenomenon. Note that the NAO-index must not be interpreted in summer and fall season in the same way as in winter and spring, where it resembles a specific atmospheric situation commonly referred to as the North Atlantic Oscillation. In summer, the definition of the NAO-index as pressure difference between Iceland and Azores might describe partly the advection from the subtropics. This pressure difference matches by chance also the Mid-latitude Anomaly Train (MAT) (Massacand 1999) which is a measure for whether the high and deep pressure systems are adjusted more along the north-south or the east-west axis. This could affect the meridional transport. Further, the downward propagation of the solar signal similar to that of NAO is very interesting but can only be speculated about in this thesis. Including NAO in the linear ozone model increases the significance of solar influence. The solar influence occurs in summer and fall. These are seasons which are influenced by subtropical advection. The proposed coupling of solar influence and advection is consistent with the observation of Labitzke and van Loon (1997) that the solar activity influences geopotential heights in the subtropics which could affect the pole-ward transport of ozone. Studies with trajectories and ozone profile measurements from satellite will be required to resolve the riddle which

is given with the downward propagating pattern in Fig. 7.4.

7.5 Conclusions from ozone profile trend analysis

The new ozone balance includes the NAO or the tropopause pressure, the QBO and the solar cycle, and the aerosol loading as explanatory variables. The size of their contributions depends on season and height. Therefore, separate balances have to be made for at least three seasons. The profile was divided according to the Umkehr layers and each layer was investigated separately with stepwise regression.

NAO/AO and its influence on tropopause pressure have been shown to contribute to long-term ozone trends. The new estimates for anthropogenic trends over Switzerland do not have a maximum in the lower stratosphere as reported before in literature. In the lower stratosphere, about half of the winter–spring long-term ozone changes can be explained dynamically. In the middle stratosphere, the NAO-index is suggested to reflect some type of dynamical change also, but with a different mechanism, which remains to be explained.

The strongest dynamical influence is found in the lower stratosphere as expected from the proposed physical mechanism. Tropopause pressure changes are linearly connected to ozone changes. Tropopause pressure is the main cause of variability in the lower stratosphere (up to Layer 3, i.e., up to 19 km altitude) and influences ozone throughout the year.

The other natural influences on ozone are specified with respect to season and height. The quasi-biennial oscillation explains much of ozone variability in winter-spring, at the height of ozone maximum and above. The solar influence shows up more clearly when the NAO-index is included in the model, at the plausible altitude of the middle stratosphere, above the ozone maximum. There seem to be also an influence of aerosol loading, most pronounced in autumn, at this height.

It is interesting to note that aerosols do not have a discernible influence in the lower stratosphere. This give rise to the supposition that the trends observed below 30 km altitude in mid-latitudes stem mainly from

dynamical changes of the tropopause pressure and from transport of ozone depleted air originating in the polar vortex.

The reason that in summer and autumn ozone trend results seem not to be influenced so much by dynamics is because of the way tropopause pressure behaves in the time span covered by the data. One must not generalize this. If someone would choose a time span where the tropopause pressure shows a clear decline or incline, the ozone trend results would be strongly affected also in summer and autumn. This implication should be considered especially with short data series.

Chapter 8

Summary and Conclusions

The main goal of this work was to quantify anthropogenic trends in the Swiss ozone profiles and total ozone. For this purpose, the statistical trend model was developed further. A new contribution to ozone variability was found, which proved to be the most important one for interannual variability.

Changes in dynamics turned out to be of crucial importance. Changes in the North Atlantic Oscillation (NAO) and the Arctic Oscillation (AO) cause a long-term trend in tropopause pressure in winter and spring which influences ozone trends. A physical mechanism was presented and evidence for this hypothesis was found by statistical analysis.

The tropopause pressure varies in concert with NAO with a distinct geographical pattern. The sign and magnitude of the NAO/AO influence depend on latitude and longitude. This has implications also for other ozone series of the Northern mid-latitudes. It was shown that the NAO modulates the ozone such that the residual total ozone decrease, normally explained as resulting from chemical changes, is enhanced for the last 30 years over Europe (Arosa, Switzerland) whereas over the North Atlantic region (Reykjavik, Iceland) it is reduced. Including NAO in a statistical model yields a more uniform chemical winter trend by -2.4 to

-3.2 % per decade since 1970, compared to the strong variation reported earlier with -3 to -5 % over Arosa and 0 % over Iceland.

For ozone trend analysis, an improved linear regression model was developed and applied to suitable data subsets. It was found to be important to treat the different seasons separately. Tropopause pressure, the Quasi-Biennial Oscillation (QBO), solar and aerosol influence show a distinct height- and seasonal dependence. It has been demonstrated with stepwise linear regression that ozone variability due to these influences can be attributed properly to the different heights. The long term changes not explainable by natural variability are attributed to anthropogenic trends. Although the modeling of a linear anthropogenic trend starting in 1970 is the common approach, it can be improved. In this thesis, the linear relation between NAO and tropopause pressure and ozone is derived. The use of NAO/AO is justified in winter and spring. Major dynamic variability remains unexplained in late summer and autumn. This is a field of further research, possibly yielding new insights into inter-annual ozone variability.

Ozone profile trend analysis up to the middle stratosphere (30 km) was based on the Payerne balloon soundings. For higher altitudes the Umkehr measurements of Arosa were used. Up to half of the lower stratospheric trends in winter and spring can be attributed to dynamical effects. With the dynamical effect accounted for in the trend model, the following estimates for anthropogenic chemical trends (per decade) and their standard deviations have been found: In the troposphere, chosen as Umkehr layer L1 (0–10.3 km), an ozone increase of $(12 \pm 2)\%$ is found. In the lowermost stratosphere, in L2 (10.3–14.7 km) there is only a trend in winter-spring which is not significant with $(-5.5 \pm 3.0)\%$ with a 95% confidence interval. Above, the trend becomes significant in L3 (14.7–19.1 km) with $(-6.3 \pm 2.3)\%$ in winter-spring and (-3.6 ± 1.2) for the rest of the year. At the height of the ozone maximum, in L4 (19.1–23.5 km) and L5 (23.5–28 km) the trend is about (-5.3 ± 0.8) in winter-spring and about (-3.1 ± 0.7) for the rest of the year. Only half of L6 was integrated (28–30 km) because the limit of the soundings is reached. The trend there is estimated as (-4.3 ± 1.1) for winter-spring and for autumn, and (-1.8 ± 0.8) for summer.

Another aim of this study was to obtain more information on the data quality of the Swiss measurements. The long-term ozone changes as derived from the Payerne soundings and from the Arosa Umkehr dif-

fer significantly. The hypothesis was investigated whether instrumental break within the series cause this contradiction. Numerous changes were found in the difference between soundings and Umkehr employing cumulative differences for break detection. It could also be some slow changes instead of numerous events. A drift of individual Umkehr instruments is excluded by detailed comparisons with the supplementary Umkehr instruments. Satellite (SBUV and SAGE) overpass data were invoked but cannot distinguish which of both series is the more stable one. The explanation for the inconsistency between sounding and Umkehr can only be speculated about at this stage. Probably it is inherent to the Umkehr algorithm. The response of the Umkehr retrieval to the changes of the ozone profile needs further investigation.

The Payerne soundings were found to be suitable for ozone profile trend analysis. For the entire series, the clear signal of the dynamical influence was found. The independent information on tropopause pressure is mirrored in the Payerne sounding data. It cannot be ruled out that there are also instrumental problems, but they are much smaller than the dynamical ones.

The behavior of NAO/AO is not understood at the present time. Therefore, predictions of future behavior are precarious. It could be an internal vacillation of the atmosphere which switches between quasi-periodic and chaotic behavior (Christiansen 2000). There exists also the possibility that the change in NAO/AO could be determined by greenhouse gas forcing (Paeth and Hense 1999) and stratospheric ozone depletion (Shindell et al. 1999).

The turnaround in ozone depletion is expected from the retrograding chlorine loading at the turn of the millennium. To discern this ozone recovery, it is strongly recommended to take dynamical variability into account.

Seite Leer /
Blank leaf

Acronyms and Abbreviations

a.s.l.	above sea level
AO	Arctic Oscillation
BM	Brewer-Mast sonde
CFC	chlorofluorocarbon
CF	correction factor
DU	Dobson Units
ERB	Earth Radiation Budget Satellite
EOF	Empirical orthogonal function
F107	solar radio flux at the wavelength of 10.7 cm
GAW	Global Atmosphere Watch
Lidar	Light Detection And Ranging
NAO	North Atlantic Oscillation
NASA	National Aeronautics and Space Administration, USA
NOAA	National Oceanic and Atmospheric Administration, USA
PSC	Polar stratospheric cloud
QBO	Quasi-Biennial Oscillation
std	standard deviation
SAGE	Stratospheric Aerosol and Gas Experiment
SBUV	Solar Backscatter Ultraviolet Instrument
SMI	Swiss Meteorological Institute
SLP	Sea level pressure
SPARC	Stratospheric Processes and their Role in Climate
TOMS	Total Ozone Monitoring Spectrometer
UARS	Upper Atmosphere Research Satellite
WOUDC	World Ozone and Ultraviolet Radiation Data Centre

Seite Leer /
Blank leaf

Appendix A

Daily Ozone Variability

Total Ozone Variability		
month	mean	std (daily)
1	331.6	40.4
2	358.2	47.6
3	364.4	41.6
4	370.2	35.3
5	358.4	27.4
6	341.3	21.3
7	322.8	17.8
8	310.1	16.2
9	292.4	19.0
10	281.7	20.9
11	285.3	24.3
12	305.2	30.3

Table A.1: *Variability of daily total ozone depends on the season. The homogenized series 1969-1996 used.*

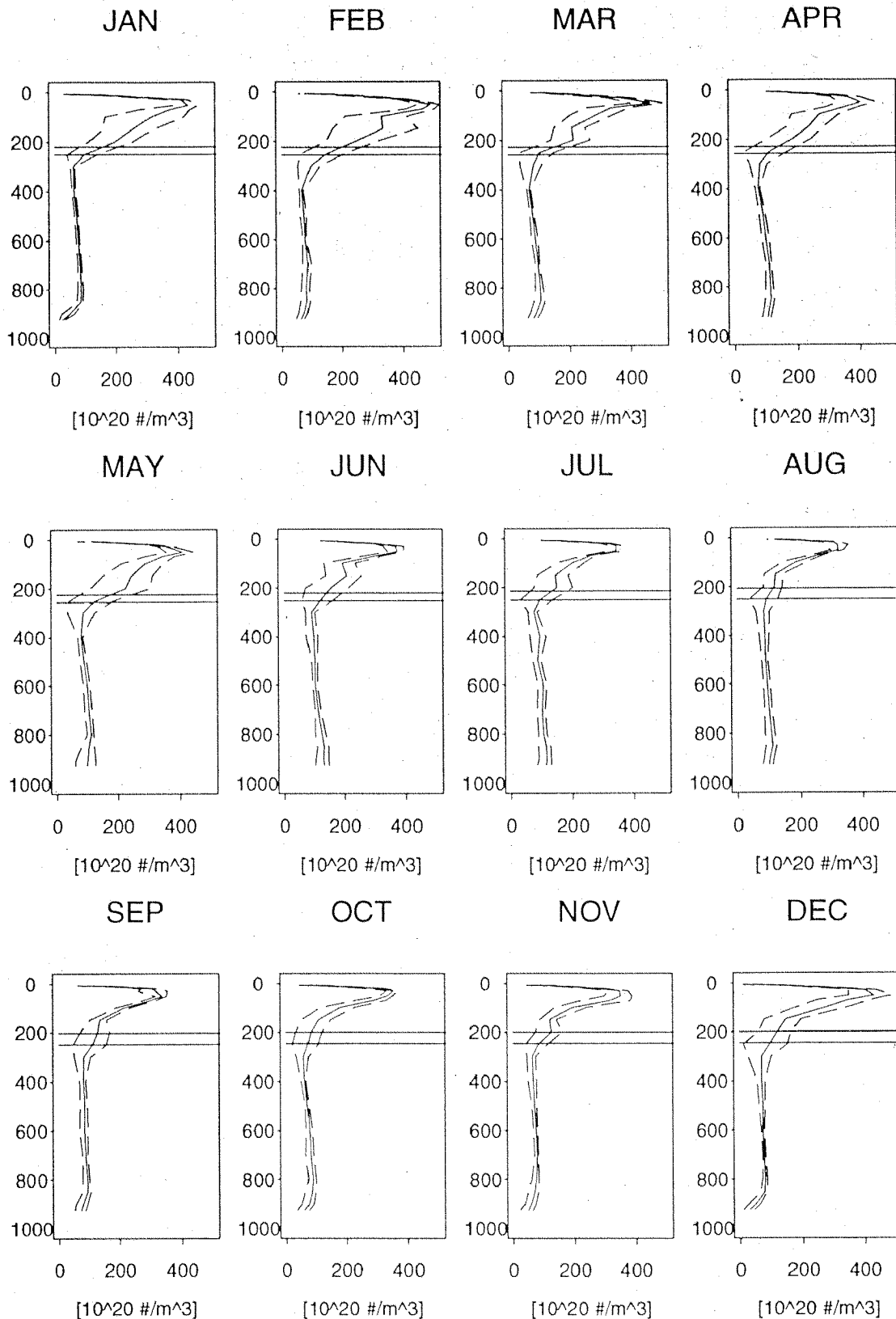


Figure A.1: Ozone profile variability in nbar and with linear pressure as ordinate. The ozone is approximately linear in the pressure range of tropopause standard deviation, supporting the assumption in Section 7.2. Compare to Fig. 2.3 for other units.

Appendix B

Conversion of units

Number density ($\#/cm^3$) \rightarrow Dobson units (DU)

The SAGE ozone profiles x are given in $\#/cm^3$, which must be integrated over the layer Li to get X , the ozone layer content in DU:

$$X[\text{DU}] = k \frac{T_1}{p_1} 10^{12} \sum_{Li} x[\#/cm^3] \quad (1)$$

with $T_1=273.15$ K and $p_1=1013$ hPa and k is Boltzmann number $k=1.3807 \cdot 10^{-23}$. This is a strait-forward conversion which does not require additional information.

Dobson units (DU) \rightarrow partial pressure (nbar)

Ozone in DU measures how many thousandstal cm height the column ozone of the atmosphere would accompany. For a certain layer of the height H the ozone X in [DU] measures how much ozone is in a column of this layer.

$$x[\text{nbar}] = p_1 * \frac{T}{T_1} \frac{X[\text{DU}]}{H} * 10 \quad (2)$$

With the required temperature T of this layer, $T_1=273.15$ K and $p_1=1013$ hPa and H the layer height in m , ozone x in [nbar] is can

be assigned to this layer.

Partial pressure (nbar) \rightarrow Dobson units (DU)

As the transferring from DU to nbar requires the stratospheric temperature which is not available for the historical data sets, it is better to transfer the balloon soundings to DU and compare then with the other ozone profiling methods. The soundings yield for each ozone measurement $oz(i)$ also the temperature $T(i)$ and the height $h(i)$. To determine the ozone content X in DU for a certain layer, all measurements which are between the layer boundaries are summed:

$$X[\text{DU}] = \sum_i \frac{oz(i) + oz(i+1)}{T(i) + T(i+1)} (h(i+1) - h(i)) \quad (3)$$

At the layer boundary, a weighted average is assigned which is calculated from the measurements before and after.

Appendix C

Used Software

Unix

Fortran 77

C

Oracle - SQLplus

matlab

Splus

L^AT_EX

Umkehr program: mk2v4.NEWCUMK

Seite Leer /
Blank leaf

Appendix D

www Data Sources

Standard Atmosphere from 1976

<http://aero.stanford.edu/StdAtm.html>

Solar flux

ftp://ftp.ngdc.noaa.gov/STP/SOLAR_DATA/

AOD

<ftp://nasagiss.giss.nasa.gov>

<http://www-arb.larc.nasa.gov/sage2/g2dd.aerosol.html>

QBO

<http://nic.fb4.noaa.gov/data/cddb>

Arosa (Switzerland) total ozone

<http://www.lapeth.ethz.ch/doc/totozon.html>

Reykjavik (Iceland) total ozone

<http://www.tor.ec.gc.ca/woudc/woudc.html>

Tropopause pressure from NCEP-reanalysis

http://www.cdc.noaa.gov/ncep_reanalysis

North Atlantic Oscillation index

from NCEP-reanalysis: http://www.cdc.noaa.gov/ncep_reanalysis

measured: http://www.cgd.ucar.edu/cas/climind/nao_monthly.html

Arctic Oscillation (AO) index

<http://tao.atmos.washington.edu/data/ao/>

Seite Leer /
Blank leaf

Bibliography

AGU 1999. *Fall Meeting 13-17 Dec. 1999 San Francisco*. Special session on the Arctic Oscillation.

Appenzeller, C., A. K. Weiss, and J. Staehelin. 2000. North Atlantic Oscillation modulates total ozone winter trends. *Geophys. Res. Lett.* **27**, 1131–1134.

Appenzeller, C., H. C. Davies, and W. A. Norton. 1996a. Fragmentation of stratospheric intrusions. *J. Geophys. Res.* **101**, 1435–1456.

Appenzeller, C., J. R. Holton, and K. H. Rosenlof. 1996b. Seasonal variation of mass transport across the tropopause. *J. Geophys. Res.* **101**, 15071–15078.

Appenzeller, C., T. F. Stocker, and M. Anklin. 1998. North Atlantic Oscillation dynamics recorded in Greenland ice cores. *Science* **282**, 446–449.

Baldwin, M. P., and T. J. Dunkerton. 1998. Biennial, quasi-biennial, and decadal oscillations of potential vorticity in the northern stratosphere. *J. Geophys. Res.* **103**, 3919–3928.

Baldwin, M. P., and T. J. Dunkerton. 1999. Downward propagation of the AO during stratospheric warmings. *J. Geophys. Res.* **104**, 30937–30946.

Bhartia, P., R. McPeters, C. L. Mateer, L. E. Flynn, and C. Wellemeyer. 1996. Algorithm for the estimation of vertical ozone profile from the backscattered ultraviolet (buv) technique. *J. Geophys. Res.* **101**, 18793–18806.

- Bintaja, R., J. P. F. Fortuin, and H. Kelder. 1997. Simulation of the meridionally and seasonally varying climate response caused by changes in ozone concentration. *J. of Climate* **10**, 1288–1311.
- Bojkov, R., L. Bishop, W. J. Hill, G. C. Reinsel, and G. C. Tiao. 1990. A statistical trend analysis of revised dobson total ozone sata over the northern hemisphere. *J. Geophys. Res.* **95**, 9785–9807.
- Brewer, A., and J. R. Milford. 1960. The oxford-kew ozone sonde. *Proc. Roy. Soc.* **256**, 470–495.
- Brewer, A. W. 1949. Evidence for a world circulation provided by the measurements of helium and water vapour distribution in the stratosphere. *Quart. J. Roy. Meteor. Soc.* **75**, 351–363.
- Bronstein, I., and K. A. Semendjajew. 1991. *Taschenbuch der Mathematik*. Teubner Verlagsgesellschaft, Leipzig.
- Chapman, S. 1930. A theory of upper atmospheric ozone. *Memoirs of the Roy. Meteo. Soc* **3**, 103–125.
- Charney, J., and P. Drazin. 1961. Propagation of planetary-scale disturbances from the lower into the upper stratosphere. *J. Geophys. Res.* **66**, 83–109.
- Chipperfield, M. P. 1999. Multiannual simulations with a three-dimensional chemical transport model. *J. Geophys. Res.* **104**, 1781–1805.
- Christiansen, B. 2000. Chaos, quasi-periodicity and interannual variability: studies of a stratospheric vacillation model, in press. *J. Atmos. Sci.*
- Chu, W., M. McCormick, J. Lenoble, B. C., and P. Pruvost. 1989. SAGE-II inversion algorithm. *J. Geophys. Res.* **94**, 8339–8351.
- Claude, H., R. Hartmannsgruber, and U. Köhler. 1987. Measurement of atmospheric ozone profiles using the Brewer/Mast sonde. preparation. procedure. evaluation. Global research and monitoring project. World Meteorological Organization, Geneva, Switzerland. Rep. 17.
- Cochrane, D., and G. Orcutt. 1949. Applications of least squares regression to relationships containing autocorrelated errors. *J. Amer. Stat. Assoc.* **44**, 32–61.

- Crutzen, P. 1970. The influence of nitrogen oxides on the atmospheric ozone content. *Quart. J. Roy. Meteor. Soc.* **103**, 320–327.
- Crutzen, P. 1974. Estimates of possible future ozone reductions from continued use of fluoro-chloro-methanes (CF_2Cl_2 , $CFCl_3$). *Geophys. Res. Lett.* **1**, 205–208.
- Cunnold, D., W. Chu, R. Barnes, M. McCormick, and R. Veiga. 1989. Validation of SAGE-II ozone measurements. *J. Geophys. Res.* **94**, 8447–8460.
- De Backer, H., D. De Muer, E. Schoubs, and M. Allaart. 1998. A new pump correction profile for Brewer-Mast ozonesondes. In *Proceedings of the XVIII Quadrennial Ozone Symposium L'Aquila, Italy*. R. Bojkov, and G. Visconti. (Eds.). Pp. 891–894.
- DeLuisi, J. J. 1979. Umkehr vertical ozon profile errors caused by the presence of stratospheric aerosols.. *J. Geophys. Res.* **84**, 1766–1770.
- DeLuisi, J. J., D. U. Longenecker, C. L. Mateer, and D. J. Wuebbles. 1989. An analysis of northern middle-latitude Umkehr measurements corrected for stratospheric aerosols for 1979–1986. *J. Geophys. Res.* **94**, 9837–9846.
- Dobson, G. 1931. A photoelectric spectrometer for measuring the amount of atmospheric ozone. *Proc. Phys. Soc* **43**, 324–339.
- Dobson, G. M. B. 1956. Origin and distribution of polyatomic molecules in the atmosphere. *Proceed. Roy. Soc.* **236**, 187–193.
- Dobson, G. M. B., D. N. Harrison, and L. Lawrence. 1929. Measurements of the amount of ozone in the earth's atmosphere and its reaction to other geophysical conditions. *Proc. Roy. Soc.* **110**, 660–693.
- Duetsch, H. U. 1979. The search for solar cycle-ozon relationships. *Atmospheric and Terrestrial Physics* **41**, 771–785.
- Ertel, H. 1942. Ein neuer hydrodynamischer Wirbelsatz. *Meteor. Z.* **59**, 277–281.
- Fahey, D., S. Kawa, E. Woodbridge, P. Tin, J. Wilson, H. Jonsson, J. Due, D. Baumgardner, S. Borrmann, D. Toohey, J. Avallone,

- M. Proffitt, J. Margitan, M. Loewenstein, J. Podolske, R. J. Salawitch, S. Wofsy, M. Ko, D. E. Anderson, M. R. Schoeberl, and K. Chan. 1993. In situ measurements constraining the role of sulphate aerosols in mid-latitude ozone depletion. *Nature* **363**, 509–514.
- Farman, J. C., B. G. Gardiner, and J. D. Shanklin. 1985. Large losses of total ozone in Antarctica reveal seasonal ClO_x/NO_x interaction. *Nature* **315**, 207–210.
- Forster, P. M. D., and K. P. Shine. 1997. Radiative forcing and temperature trends from stratospheric ozone changes. *J. Geophys. Res.* **102**, 10841–10855.
- Frederick, J., R. Cebula, and D. Heath. 1986. Instrument characterization for the detection of long-term changes in stratospheric ozone: An analysis of the SBUV/2 radiometer. *J Atmos. Oceanic Technol.* **3**, 472–480.
- Fusco, A. C., and M. L. Salby. 1999. Interannual variations of total ozone and their relationship to variations of planetary wave activity. *J. of Climate* **12**, 1619–1629.
- Giroud, M. 1996. Historique des sondages d'ozone á Payerne. *Internal report of the Swiss Meteorological Office (SMA)*. Station Aérologique Payerne.
- Götz, F., A. Meetham, and G. M. B. Dobson. 1934. The vertical distribution of ozone in the atmosphere. *Proceed. Roy. Soc.* **145**, 416–446.
- Graedel, T. E., and P. Crutzen. 1994. *Chemie der Atmosphäre, Bedeutung für Klima und Umwelt*. Spektrum Akademischer Verlag, Heidelberg.
- Graf, H., I. Kirchner, and J. Perlwitz. 1998. Changing lower stratosphere circulation: The role of ozone and greenhouse gases. *J. Geophys. Res.* **103**, 11251–11261.
- Hadjinicolaou, P., J. Pyle, M. P. Chipperfield, and J. A. Kettleborough. 1997. Effect of interannual meteorological variability on mid-latitude o₃. *Geophys. Res. Let.* **24**, 2993–2996.

- Haigh, J. D. 1996. The impact of solar variability on climate. *Science* **272**, 981–984.
- Hansen, J., M. Sato, and R. Ruedy. 1997. Radiative forcing and climate response. *J. Geophys. Res.* **102**, 6831–6864.
- Harris, N. R. P., G. Ancellet, L. Bishop, H. Hofmann, J. B. Kerr, R. D. McPeters, M. Prendez, W. J. Randel, J. Staehelin, S. B.H., A. Volz-Thomas, J. Zawodny, and C. C.S. Zerefos. 1997. Trend in stratospheric and free tropospheric ozone. *J. Geophys. Res.* **102**, 1571–1590.
- Haynes, P., C. J. Marks, M. E. McIntyre, T. G. Shepherd, and K. P. Shine. 1991. On the 'downward control' of extratropical diabatic circulations by eddy-induced mean zonal forces. *J. Atmos. Sci.* **48**, 651–678.
- Hilsenrath, E., R. Cebula, M. Deland, K. Laamann, and S. Taylor. 1995. Ultraviolet (SBUV/2) ozone data set from 1989 to 1993 using in-flight calibration data and SSBUV. *J. Geophys. Res.* **100**, 1351–1366.
- Hoegger, B., G. Levrat, J. Staehelin, H. Schill, and P. Ribordy. 1992. Recent development of the Light Climatic Observatory - ozon measuring station of the Swiss Meteorological Institut [LKO] at Arosa. *J. Atmos. Terrest. Physics* **54**, 497–505.
- Hofmann, D. J., and S. Solomon. 1989. Ozone destruction through heterogeneous chemistry following the eruption of El Chichón. *J. Geophys. Res.* **94**, 5029–5041.
- Hogrefe, C. 1996. *Seasonal Variations, Biases and Trends in Ozonesonde Data*. PhD thesis. University of Albany.
- Holton, J. R., and D. A. Tan. 1980. The influence of the equatorial quasi-biennial oscillation on the global circulation at 50 mbar. *J. Atmos. Sci.* **37**, 2200–2208.
- Holton, J. R., P. Haynes, M. E. McIntyre, A. Douglass, R. B. Rood, and L. Pfister. 1995. Stratosphere-troposphere exchange. *Rev. Geophys.* **33**, 403–439.
- Hood, L. L., and D. A. Zaff. 1995. Lower stratospheric stationary waves and the longitude dependence of ozone trends in winter. *J. Geophys. Res.* **100**, 25791–25800.

- Hood, L. L., S. Rossi, and M. Beulen. 2000. Trends in lower stratospheric zonal winds, Rossby wave breaking behavior, and column ozone at northern mid-latitudes, in press. *J. Geophys. Res.*
- Hoskins, B. J. 1991. Towards a p - θ view of the general circulation. *Tellus* **43AB**, 27–35.
- Hoskins, B. J., M. E. McIntyre, and A. Robertson. 1985. On the use and significance of isentropic potential vorticity maps. *Quart. J. Roy. Meteorol. Soc.* **111**, 877–946.
- Hurrell, J. W. 1995. Decadal trends in the North Atlantic Oscillation regional temperatures and precipitation. *Science* **269**, 676–679.
- Hurrell, J. W. 1996. Influence of variations in extratropical wintertime teleconnections on northern hemisphere temperature. *Geophys. Res. Lett.* **23**, 665–668.
- Jackman, C., E. Fleming, S. Chandra, D. B. Considine, and J. E. Rosenfield. 1996. Past, present, and future modeled ozone trends with comparisons to observed trends. *J. Geophys. Res.* **101**, 28'753–28'767.
- Johnston, H. S. 1971. Reduction of stratospheric ozone by nitrogen oxide catalysts from supersonic transport exhaust. *Science* **173**, 517–522.
- Kalnay, E., and et al.. 1996. The NCEP/NCAR 40 year reanalysis project. *Bull. Amer. Meteor. Soc.* **77**, 437–471.
- Kegel, R. U. 1995. Reevaluierung der Ozon-Ballonsondierungsreihe von Payerne (Bruch im Frühjahr 1990) und Trendanalyse (1984-1992). Diploma thesis ETH Zurich.
- Knudsen, B. M., W. A. Lahoz, A. O'Neill, and J. J. Morcrette. 1998. Evidence for a substantial role for dilution in northern mid-latitude ozone depletion. *Geophys. Res. Lett.* **25**, 4501–4504.
- Kodera, K. 1994. Influence of volcanic eruptions on the troposphere through stratospheric dynamical processes in the northern-hemisphere winter. *J. Geophys. Res.* **99**, 1273–1282.
- Komhyr, W. D. 1980. *Operations handbook - ozone observations with a Dobson spectrophotometer*. WMO Global Ozone Research and Monitoring Project. Rept. 6.

- Komhyr, W. D., S. Oltmans, R. Grass, and R. Leonard. 1991. Possible influence of long-term sea-surface temperature anomalies in the tropical pacific on global ozone. *Canadian J. of Physics* **9**, 1093–1102.
- Kosmitis, E. e. a. 1999. Re-evaluation of raw Umkehr data. *Abstracts of the Fifth European Workshop on Stratospheric Ozone, St. Jean de Luz, France, 1999*.
- Labitzke, K., and H. van Loon. 1988. Associations between the 11-year solar-cycle, the qbo and the troposphere and stratosphere in the northern hemisphere in winter. *J. of atmospheric and terrestrial physics* **50**, 197–206.
- Labitzke, K., and H. van Loon. 1997. Total ozone and the 11-yr sunspot cycle. *Journal of Atmospheric and Solar-Terrestrial Physics* **59**, 9–19.
- Langford, A. O., T. O'Leary, C. D. Masters, K. C. Aikin, and M. H. Proffitt. 1998. Modulation of middle and upper tropospheric ozone at northern midlatitudes by the El Niño/ Southern Oscillation. *Geophys. Res. Let.* **25**, 2667–2670.
- Liljequist, G. H., and K. Cihak. 1984. *Allgemeine Meteorologie*. Vieweg.
- Logan, J. A. 1994. Trends in the vertical distribution of ozone: An analysis of ozonesonde data. *J. Geophys. Res.* **99**, 25553–25585.
- Logan, J. A., I. A. Megretskaja, A. J. Miller, G. C. Tiao, D. Choi, L. Zhang, R. S. Stolarski, G. Labow, H. S. M., G. E. Bodeker, H. Claude, D. De Muer, J. Kerr, D. W. Tarasick, S. Oltmans, B. Johnson, F. Schmidlin, J. Staehelin, P. Viatte, and O. Uchino. 1999. Trends in the vertical distribution of ozone: A comparison of two analyses of ozonesonde data. *J. Geophys. Res.* **104**, 26373–26399.
- Marquardt, C. 1997. *Die tropische QBO und dynamische Prozesse in der Stratosphäre*. PhD thesis. Freie Univ. Berlin.
- Marshall, J., Y. Kushnir, D. Battisti, P. Chang, J. Hurrell, M. McCarney, and M. Visbeck. 1997. A white paper on Atlantic Climate Variability. <http://geoid.mit.edu/accp/avehtml.html>.

- Massacand, A. 1999. *Linkages between Upper-tropospheric Flow and European seasonal weather*. PhD thesis. ETH Zurich.
- Mateer, C. L. 1965. On the information content of Umkehr observations. *J. Atmos. Sci.* **22**, 370–381.
- Mateer, C. L., and J. J. DeLuisi. 1992. A new Umkehr inversion algorithm. *J Atmospheric and Terrestrial Physics* **54**, 537–556.
- Mateer, C. L., H. Dütsch, J. Staehelin, and DeLuisi J.J.. 1996. Influence of a priori profiles on trend calculations from Umkehr data. *J. Geophys. Res.* **101**, 16779–16787.
- McIntyre, M. E., and T. N. Palmer. 1983. Breaking planetary waves in the stratosphere. *Nature* **305**, 593–600.
- Miller, A. J., G. C. Tiao, G. C. Reinsel, D. Wuebbles, L. Bishop, J. Kerr, R. M. Nagatani, D. J.J., and C. L. Mateer. 1995. Comparisons of observed ozone trends in the stratosphere through examination of Umkehr and balloon ozonsonde data.. *J. Geophys. Res.* **100**, 209–11217.
- Molina, L., and M. Molina. 1987. Production of Cl_2O_2 from the self-reaction of the ClO radical. *J. Phys. Chem.* **91**, 433–436.
- Molina, M. J., and F. S. Rowland. 1974. Stratospheric sink for chlorofluoromethanes: chlorine atom catalyzed destruction of ozone. *Nature* **249**, 810–814.
- Myhre, G., F. Stordal, B. Rognerud, and I. S. A. Isaksen. 1998. Radiative forcing due to stratospheric ozone. *Proc. Qad. Ozone Symposium, Aquilla*. Pp. 813–816.
- Mysak, L., and S. A. Venegas. 1998. Decadal climate oscillations in the Arctic: a new feedback loop for atmospheric-ice-ocean interactions. *Geophys. Res. Let.* **25**, 3607–3610.
- Neuhaus, K. 1997. Contributions to the homogenization of the Payerne ozone soundings (1966-1996). *CABO technical report 8*. University of Berne, Switzerland.
- Newchurch, M., D. Cunnold, and J. Cao. 1998. Intercomparison of stratospheric aerosol and gas experiment (SAGE) with the Umkehr[64] and Umkehr[92] ozone profiles and time series: 1979-1991. *J. Geophys. Res.* **103**, 31277–31292.

- Newchurch, M., E.-S. Yang, S. Staehelin, H. Jäger, and A. Weiss. 1999. A multivariate auto-regressive combined-harmonics time-series analysis of the Dobson Umkehr and total ozone trends at Arosa 1979-1996, submitted. *J. Geophys. Res.*
- Ohhashi, Y., and K. Yamazaki. 1999. Variability of the eurasian pattern and its interpretation by wave activity flux. *J. Meteo. Soc. Japan.*
- Paeth, H., and A. Hense. 1999. CO₂ induced signals in the North Atlantic Oscillation and regional climate change. *Fall Meeting 13-17 Dec. 1999 San Francisco. AGU.*
- Perlwitz, J., and H. F. Graf. 1995. The statistical connection between tropospheric and stratospheric circulation of the northern hemisphere in winter. *Journal of Climate* **8**, 2281-2295.
- Poole, L. R. 1999. Stratospheric aerosol and gas experiment II (SAGE II) - Introduction. <http://www-sage2.larc.nasa.gov/introduction/>.
- Ramanathan, V., and R. E. Dickinson. 1979. The role of stratospheric ozone in the zonal and seasonal energy balance of the earth-troposphere system. *J. Atmos. Res.* **36**, 1084-1104.
- Randel, W., R. Stolarski, D. Cunnold, J. Logan, M. Newchurch, and J. Zawodny. 1999. Trends in the vertical distribution of ozone. *Science* **285**, 1689-1692.
- Reinsel, G. C., G. C. Tiao, A. J. Miller, R. M. Nagatani, D. Wuebbles, E. Weatherhead, W. Cheang, L. Zhang, L. E. Flynn, and J. B. Kerr. 1999. Update of Umkehr ozone profile data trend analysis through 1997. *J. Geophys. Res.* **104**, 23'881-32'898.
- Reinsel, G. C., G. C. Tiao, J. DeLuisi, S. Basu, and K. Carriere. 1989. Trend analysis of aerosol-corrected Umkehr ozon profile data through 1987. *J. Geophys. Res.* **94**, 16373-16386.
- Rodgers, C. D. 1976. Retrieval of atmospheric temperature and composition from remote measurements or thermal radiation. *Reviews of Geophysics and Space Physics* **14**, 609-624.
- Roelofs, G. J., J. Lelieveld, and R. van Dorland. 1997. A three-dimensional chemistry/general circulation model simulation of anthropogenically derived ozone in the troposphere and its radiative climat forcing. *J. Geophys. Res.* **102**, 23389-23401.

- Sato, M., J. E. Hansen, M. P. McCormick, and J. B. Pollak. 1993. Stratospheric aerosol optical depth, 1850 - 1990. *J. Geophys. Res.* **98**, 22987-22994.
- Schill, H. 1994. *Stationsbeschreibung Lichtklimatisches Observatorium Arosa*. GeoSol. available from the Swiss Meteorological Office (SMA).
- Schubert, S. D., and M.-J. Munteanu. 1988. An analysis of tropopause pressure and total ozone correlations. *Monthly Weather Review* **116**, 569-582.
- Selten, F. M., R. J. Haarsma, and J. Opsteegh. 1999. On the mechanisms of North Atlantic decadal variability. *J. of Climate* **12**, 1956-1973.
- Shindell, D. T., D. Rind, N. Balachandran, J. Lean, and P. Lonergan. 1999. Solar cycle variability, ozone, and climate. *Science* **284**, 305-308.
- Shine, K. P., and P. M. D. Forster. 1999. The effect of human activity on radiative forcing of climate change: a review of recent developments. *Global and Planetary Change* **20**, 205-225.
- Solomon, S. 1999. Stratospheric ozone depletion: a review of concepts and history. *Reviews of Geophysics* **37**, 275-316.
- Solomon, S., R. R. Garcia, F. S. Rowland, and D. Wuebbles. 1986. On the ozone depletion of Antarctic ozone. *Nature* **321**, 755-758.
- Solomon, S., R. W. Portmann, L. W. Garcia, F. Randel, F. Wu, R. Nagatani, J. Gleason, L. Thomason, L. R. Poole, and M. P. McCormick. 1998. Ozone depletion at mid-latitudes: Coupling of volcanic aerosols and temperature variability to anthropogenic chlorine. *Geophys. Res. Lett.* **25**, 1871-1874.
- Solomon, S., R. W. Portmann, W. Garcia, L. Thomason, L. R. Poole, and M. P. McCormick. 1996. The role of aerosol variations in anthropogenic ozone depletion at northern midlatitudes. *J. Geophys. Res.* **101**, 6713-6727.
- Soukharev, B. 1997. The sunspot cycle, the QBO, and the total ozone over northeastern Europe: a connection through the dynamics of stratospheric circulation. *Ann. Geophysicae* **15**, 1595-1603.

- Soukharev, B. 2000. On the solar/QBO effect on the interannual variability of total ozone and the stratospheric circulation over northern Europe. *J. Atmos. Solar-Terrest. Physics* **61**, 1093–1109.
- SPARC 1998. Assessment of trends in the vertical distribution of ozone. In *WMO Ozone Research and Monitoring Project Report Nr. 43*. N. Harris, R. Hudson, and C. Phillips. (Eds.).
- Staehelin, J., and A. K. Weiss. 1998. Homogenisation and trend analysis of the long-term Swiss ozone data sets. In *Preprints of the abstracts of the Conference Global Atmosphere Watch (GAW) Zurich*. F. Swiss Agency for the Environment, Landscape, and the Swiss Meteorological Institute. (Eds.). Pp. 45–48.
- Staehelin, J., and H. U. Duetsch. 1989. Zeigen die schweizerischen Messungen eine Gefährdung der Ozon-Schicht?. *Chimia* **43**, 338–348.
- Staehelin, J., and W. Schmid. 1991. Trend analysis of tropospheric ozone concentrations utilizing the 20-year data set of ozone balloon soundings over Payerne (Switzerland). *Atmospheric Environment* **25A**, 1739–1749.
- Staehelin, J., H. Schill, B. Hoegger, P. Viatte, G. Levrat, and A. Gamma. 1995. Total ozone observations by sun photometry at Arosa, Switzerland. *Optical Engineering* **34**, 1977–1986.
- Staehelin, J., J. Renaud, R. McPeters, P. Viatte, B. Hoegger, V. Bugnion, M. Giroud, and H. Schill. 1998a. Total ozone series at Arosa (CH): Homogenization and data comparison. *J. Geophys. Res.* **103**, 5827–5841.
- Staehelin, J., N. Harris, C. Appenzeller, and J. Eberhard. 2000. Observations of ozone trends, submitted. *Rev. Geophysics*.
- Staehelin, J., R. Kegel, and N. R. P. Harris. 1998b. Trend analysis of homogenized total ozone series of Arosa (CH), 1926–1996. *J. Geophys. Res.* **103**, 8389–8399.
- Stahel, W. A. 1995. *Statistische Datenanalyse. Eine Einführung für Naturwissenschaftler*. Vieweg Verlag Braunschweig.
- Steinbrecht, W., H. Claude, U. Köhler, and K. P. Hoinka. 1998. Correlation between tropopause height and total ozone: Implications for long-term trends. *J. Geophys. Res.* **103**, 19183–19192.

- Steinbrecht, W., H. Claude, U. Köhler, and P. Winkler. 1999. High total ozone over Central Europe in early spring of 1999: a link to the circulation of the Northern Hemisphere. *Abstracts of the Fifth European Workshop on Stratospheric Ozone, St. Jean de Luz, France, 1999*.
- Steinbrecht, W., R. Schwartz, and H. Claude. 1997. New pump correction for the Brewer-Mast ozone sonde: determination from experiment and instrument comparisons. *J. Atmos. Oceanic Technol.* **15**, 144–156.
- Stephenson, D., V. Pavan, and R. Bojariu. 2000. Is the North Atlantic Oscillation a random walk ?. *Int. J. of Climatol.* **20**, 1–18.
- Stolarski, R., R. Bojkov, L. Bishop, C. Zerefos, J. Staehelin, and J. Zawodny. 1992. Measured trends in stratospheric ozone. *Science* **256**, 342–349.
- Stuebi, R., P. Mettraux, P. Jeannet, and P. Viatte. 1998a. Sensitivity analysis of data corrections: A contribution to the re-evaluation of the Payerne ozone sounding series. In *Preprints of the abstracts of the Conference Global Atmosphere Watch (GAW) Zurich*. F. Swiss Agency for the Environment, Landscape, and the Swiss Meteorological Institute. (Eds.). Pp. 57–61.
- Stuebi, R., V. Bugnion, M. Giroud, P. Jeannet, P. Viatte, B. Hoegger, and J. Staehelin. 1998b. Long term ozone balloon sounding series at Payerne: Homogenization methods and problems. In *Proceedings of the XVIII Quadrennial Ozone Symposium L'Aquila, Italy*. R. Bojkov, and G. Visconti. (Eds.). Pp. 179–182.
- Thielmann, A. 2000. *Sensitivity of ozone production derived from field measurements in the Po basin*. PhD thesis. ETH Zurich.
- Thomason, L. W., and L. R. Poole. 1997. A global climatology of stratospheric aerosol surface area density deduced from stratospheric aerosol and gas experiment ii measurements:1984-1994. *J. Geophys. Res.* Pp. 8967–8976.
- Thompson, D. W. J., and J. M. Wallace. 1998. The Arctic Oscillation signature in the winter time geopotential height and temperature fields. *Geophys. Res. Lett.* **25**, 1297–1300.

- Thompson, D. W. J., J. M. Wallace, and G. C. Hegerl. 1999. Annual modes in the extratropical circulation, part ii: Trends. *Journal of Climate* **13**, 1018–1036.
- Uppenbrink, J. 1999. The North Atlantic Oscillation. *Science* **283**, 948–949.
- van Loon, H., and J. C. Rogers. 1978. The seesaw in winter temperatures between greenland and northern europe. part i: General description. *Mon. Wea. Rev.* **106**, 296–310.
- Vaughan, G., and J. D. Price. 1991. On the relation between total ozone and meteorology. *Quart. J. Roy. Meteor. Soc.* **117**, 1281–1298.
- Waibel, A. E., T. Peter, K. Carslaw, H. Oelhaf, G. Wetzal, P. Crutzen, U. Pöschel, A. Tsias, E. Reimer, and H. Fischer. 1999. Arctic ozone loss due to denitrification. *Science* **283**, 2064–2069.
- Wallace, J. M., and D. S. Gutzler. 1981. Teleconnections in the geopotential height field during the northern hemisphere winter. *Monthly Weather Review* **109**, 784–812.
- Weiss, A. K., J. Staehelin, and H. Schill. 1999. Ozon in unserer Atmosphäre. *Bulletin des Schweizerischen Elektrotechnischen Vereins und des Verbandes Schweizerischer Elektrizitätswerke* **11**, 33–37.
- Weiss, A. K., J. Staehelin, R. Stuebi, P. Viatte, B. Hoegger, and H. Schill. 2000. Quality of Umkehr series of Arosa (Switzerland). <http://www.lapeth.ethz.ch/>.
- WMO 1986. Atmospheric ozone 1985: Global ozone research and monitoring project. World Meteorological Organization, Geneva, Switzerland. Rep. 16.
- WMO 1988. Report of the international ozone trends panel, Global ozone research and monitoring project. World Meteorological Organization, Geneva, Switzerland. Rep. 18.
- WMO 1995. Scientific assessment of ozone depletion: 1994. World Meteorological Organization, Geneva, Switzerland. Rep. 37.
- WMO 1999. Scientific assessment of ozone depletion: 1998. World Meteorological Organization, Geneva, Switzerland. Report 44.

Ziemke, J. R., S. Chandra, R. D. McPeters, and P. A. Newman. 1997. Dynamical proxies of column ozone with applications to global trend models. *J. Geophys. Res.* **102**, 6117–6129.

Acknowledgments

This thesis was supported by the SMI (Swiss Meteorological institute) under the GAW (Global Atmosphere Watch) program. I would like to express my gratitude to all the people whose help allowed the realization of this PhD work (and made it fun).

In particular I would like to thank:

my co-examiner, Johannes Staehelin for the continuous support and scientific advice. His lively interest and his readiness to send me to conferences was greatly stimulating

my co-examiner, Neil Harris for his critical review and helpful comments on the thesis

my examiner, Prof. Thomas Peter for accepting me as his PhD student and for his kind interest and detailed hints

Christof Appenzeller (University of Bern, SMI) for the insights into dynamics, for his ideas and for the shared joy at research.

Many persons and institutions provided data and advice, thanks to:

Herbert Schill and **Kurt Aeschbacher** from the LKO (Lichtklimatisches Observatorium) Arosa for the Umkehr data and discussions.

René Stübi, Dominique Ruffieux, Pierre Alain Mettraux, Bertrand Henchoz, Bruno Hoegger, Pierre Viatte, Pierre Jeannet (all SMI) for their readiness to explain everything about balloon soundings and for fruitful discussions

Yasmine Calisesi (University of Bern) for providing the microwave data.

Richard McPeters (NASA) for kindly making the SBUV over-pass data available

Joseph Zawodny, Jim Craft, Anju Shah and Ray Wang from NASA for the help with the SAGE data

Mike Newchurch for helpful emails concerning SAGE and Umkehr and for providing essential documents

Werner Stahel of the Seminar for Statistics (ETH Zürich) for the helpful discussion regarding statistics. **Christian Keller** for letting me use his script for linear regression with autocorrelated errors.

The members of the Institute for Atmospheric Science (LAPETH), maintained the exceptional infrastructure and created pleasant working conditions and last but not least were great colleagues. I enjoyed sharing the ups and downs of being a young scientist with **Axel, Dominique** and **Franca** who were permanently ready to help.

Special thanks go to:

Sabine von Hünenbein for proof-reading.

Johannes Kaiser (University of Bremen) for his expertise review on the Umkehr retrieval problems, and so much more.

Curriculum vitae

ANDREA K. WEISS

born on 28 February 1972 in Dresden, Germany

Education:

- 09/86-07/90 Special School math.-nat.-techn. Riesa
Abitur
- 10/90-07/92 Bergakademie Freiberg (TU)
Vordiplom Geophysics
- 10/92-06/93 University of Southampton (Great Britain)
graduate student
- 10/93-02/97 Technical University Karlsruhe (Germany)
Diploma in Geophysics
- 05/97-04/00 Federal Institute of Technology (ETH) Zurich
PhD student

Professional training:

- 07/93-09/93 Practical course at Mobil Erdöl-Erdgas GmbH Celle
- 10/91-07/92 Field campaigns at Bergakademie Freiberg
- 11/93-02/95 Teaching and research assistant at the
Geophysical Institute Karlsruhe
- 02/97-04/97 Scientific collaborator at the
Geophysical Institute Karlsruhe
- 05/97-04/00 Teaching and research assistant at the ETH Zurich

Conferences:

DGG Freiberg 1996, EAGE Amsterdam 1996, GAW Zurich 1998, IUGG Birmingham 1999, Workshop on Stratospheric Ozone at St. Jean de Luz 1999, AGU San Francisco 1999.